Keratin Microparticles for Drug and Cell Delivery

Marc Aaron Thompson

Dissertation submitted to the Faculty of

Virginia Polytechnic Institute and State University

in partial fulfillment of the requirements for the degree of

Doctor of Philosophy

in

Biomedical Engineering

Mark Van Dyke, Chair

Aaron S. Goldstein

Robert Gourdie

Jia-Qiang He

Yong Woo Lee

March 21, 2019
Blacksburg, VA

Keywords: Keratin, Biomaterial, Microparticle, Mesenchymal Stromal cell, Antibiotic, Skeletal Muscle

Keratin Microparticles for Drug and Cell Delivery

Marc Aaron Thompson

Abstract

Keratins are a family of proteins found within human hair, skin and nails, as well as a broad variety of animal tissue. Prior research suggests hydrogel constructs of keratin and keratin derivatives exhibit several mechanical and biological properties that support their use for tissue engineering and regenerative medicine applications. Microparticle formulations of these hydrogels are an intriguing delivery vehicle for drugs and cellular payloads for tissue engineering purposes due to the ability to exploit size, surface area, loading potential and importantly, non-invasive delivery (i.e. injection) of cells and biologics.

Here we examine the water-in-oil emulsion synthesis procedure to produce keratin microparticles using an oxidized keratin derivative, keratose (KOS). Analyses of particle size, microstructure, and other characterization techniques were performed. Drug loading characteristics, release kinetics, and feasibility of use in two different microparticles was subsequently investigated, first using a model-drug and later testing an antibiotic payload on bacterial cultures to validate antibacterial applications. A suspension culture technique was developed to load bone marrow-derived mesenchymyal stromal cells (BM-MSCs), testing the capacity to maintain viability and express key protein-based factors in cell growth and development. Finally, we tested the in vitro effects of cell-loaded microparticles on the L6 skeletal muscle cell line to determine potentially beneficial outcomes for skeletal muscle tissue regeneration.

Largely spherical particles with a porous internal structure were obtained, displaying hydrogel properties and forming viscoelastic gels with small differences between synthesis components

(solvents, crosslinkers), generating tailorable properties. The uniquely fibrous microstructure of KOS particles may lend them to applications in rapid drug release or other payload delivery wherein a high level of biocompatibility is desired. Data showed an ability to inhibit bacterial growth in the emulsion-generated system, and thereby demonstrated the potential for a keratin-based microparticle construct to be used in wound healing applications. Dense cell populations were loaded onto particles. Particles maintained cell viability, even after freeze-thaw cycling, and provided a material substrate that supported cell attachment through the formation of focal adhesions. Finally, in vitro studies show that both KOS and BM-MSCs support varying aspects of skeletal muscle development, with combinatorial treatments of cell-loaded particles conferring the greatest growth responses.

Keratin Microparticles for Drug and Cell Delivery

Marc Aaron Thompson

General Audience Abstract

Keratins and keratin hydrogels may exhibit several properties that support their use for tissue engineering and regenerative medicine applications. Microparticle formulations of these hydrogels are an intriguing delivery vehicle for payloads for tissue engineering purposes.

Here we examine the *water-in-oil emulsion* synthesis procedure to produce keratin microparticles that were analyzed based on drug loading characteristics. A suspension culture technique was developed to load bone marrow-derived mesenchymyal stromal cells (BM-MSCs). Finally, we tested these products to determine potentially beneficial outcomes for skeletal muscle tissue regeneration.

Particles with a porous structure were obtained. The microstructure of these particles may lend them to applications in drug release or other payload delivery. Data showed an ability to load and unload specific drug payloads. Dense cell populations were loaded onto particles. Finally, studies show that both keratin and BM-MSCs support skeletal muscle development, with combinatorial treatments of cell-loaded particles conferring the greatest growth responses.

Table of Contents

List of Figures.

Chapter 1.

Introduction

Chapter 2

Synthesis and Characterization of Water-in-oil Emulsion Synthesized Keratin Microparticles for Biomedical Applications

Chapter 3

The Investigation of Drug Loading and Release Potential in a Novel Keratin-based Microparticle

Chapter 4

A Novel Fibrous Keratin Microparticle for Stromal Cell Delivery

Chapter 5

In vitro Effects of a Bone Marrow Derived Mesenchymal Stromal Cell Loaded Keratin Microparticle on the L6 Skeletal Muscle Cell Line

List of Abbreviations.

AFM	Atomic Force Microscopy
ANOVA	Analysis of Variance
Arg	Arginine
Asp	Aspartic Acid
BCA	Bicinchoninic Acid
BDDE	Butane-diol Diglycidyl Ether
BM-MSC	Bone Marrow-derived Mesenchymal Stromal Cell
Cipro	Ciprofloxacin
CMAP	Compound Motor Action Potential
DAPI	4′,6-Diamidino-2-phenylindole dihydrochloride
E. coli	Escherichia Coli
EGDE	Ethylene-glycol Diglycidyl Ether
FDA	Federal Drug Administration
FITC-BSA	Fluorescein Isothiocyanate-bound Bovine Serum Albumin
FSC	Forward Scatter
Gly	Glycine
hCSC	Human Cardiac Stromal Cell
HMSC	Human Mesenchymal Stromal Cells
KOS	Keratose
KTN	Kerateine
LB	Lysogeny Broth
Leu	Leucine
MP	Microparticle
MRSA	Methicillin-resistant S. aureus
NCV	Nerve Conduction Velocity
Poly-ε-caprolactone	PCL
Poly(glycolic acid)	PGA
PGDE	(Poly)propylene Glycol Diglycidyl Ether
S. aureus	Staphylococcus Aureus
SEM	Scanning Electron Microscopy
Ser	Serine
SMC	Skeletal Muscle Cell
SSC	Side Scatter
Val	Valine
3D	3-Dimensional

Specific Aims

Introduction: To date, muscle tissue regeneration practices have yet to successfully regenerate the mass and function of severely damaged or resected tissue. Human hair keratins are a currently underutilized polymeric biomaterial for cell and biologic payload delivery as a means of bolstering tissue regeneration rather than scar formation. This study introduces a novel water-in-oil emulsion synthesized keratin derivative (KOS) based microparticle (MP) as a method of exploiting size, surface area and the intrinsic biological compatibility of the protein, to create a non-invasively delivered vehicle capable of high loading potential coupled with an ease of delivery to tissue. Here therein, I hypothesize that a novel keratin-based microparticle can be synthesized which possesses the necessary physical, chemical and ultimately biological properties to make this biomaterial suitable for applications in simultaneous cell and bioactive agent delivery for improved regeneration of muscle, compared to previous MP biomaterial constructs.

Specific Aim 1: Synthesis and Characterization of Keratin Microparticles for Biological Applications. This aim seeks to validate the water-in-oil emulsion process as it pertains to the synthesis of KOS MPs. As a concurrent factor, successful MP synthesis will also be contingent on whether the synthesized materials exhibit mechanical, physical and biological properties deemed suitable for cell and payload delivery. Product analysis will delve into key parameters such as size, shape, surface topography and mechanical properties while cell-related inspection will ensure cell viability is unperturbed in the presence of these materials. *We hypothesize that KOS MPs can be synthesized via the established water-in-oil emulsion methods with product characteristics within the confines of those required for feasible cell and payload delivery*.

Specific Aim 2: Drug and Cell Payload Assessment. 2A. The proficiency of KOS as a bioactive load-carrying vehicle will be evaluated. Water-soluble agents chosen based on efficacy in treating

the needs of and underlying complications related to muscle tissue regeneration will be integrated into MPs during synthesis procedures. Controlled sample degradation and resulting release of keratin and payload will be quantified over a period of days. *We hypothesize that the chemical mechanisms attributed to the water-in-oil emulsion procedures support localization and retention of water-soluble agents in MPs at concentrations high enough to be delivered for significant tissue regeneration on the timescale of days.* **2B.** Assess cell-loading potential of normal rat bone marrow-derived mesenchymal stromal cells (BM-MSCs) onto KOS MPs. Loading efficiency will be determined as a function of particle size, number, and live cell count as well as cellular adhesion assays, all tests being performed at specific time intervals. *Here we hypothesize that the employed BMSC line can viably be loaded at densities high enough to support tissue regeneration, per documented cell payloads.*

Specific Aim 3: In vitro Effects of Stromal Cell-loaded KOS MPs on Muscle Cell Growth. The effects of BMSCs integrated with KOS MPs and the subsequent activation of factors that promote regeneration in the wound environment will be evaluated by identifying changes in cell characteristics such as proliferation rate as well as cellular markers commonly upregulated during regeneration in the wound. *Here we hypothesize that the innate properties of keratin or cell laden MPs can induce pro-regenerative properties in cells that can then further support regeneration of the surrounding wound.*

Chapter 1. Introduction

1.1. Physiological Relevance of Skeletal Muscle

Skeletal muscle is the most dynamic and plastic tissue in the human body, consequentially forming a required structure for human motility and mobility. In humans, skeletal muscle comprises approximately 40% of total body weight and contains 50–75 % of all body proteins (Clowes Jr et al. 1983, Goodpaster et al. 2006). Generally, muscle functionality depends on the interplay between protein production and use, both of which are impacted in the case of muscle injury (Endo 2015, Yusuf and Brand-Saberi 2012). From a mechanical standpoint, skeletal muscle converts chemical energy into mechanical energy to generate forces and produce movement. From a metabolic standpoint, skeletal muscle provides contributions to basal energy metabolism, serving as storage for important amino acids and carbohydrates, producing heat and the consuming oxygen (Saltin and Gollnick 1983, Egan and Zierath 2013). Of similar or potentially greater importance in some cases is the function of a reservoir of amino acids for other tissues (heart, brain, skin etc.) for the synthesis of proteins specific to organ processes (Argilés et al. 2016). Consequently, in terms of health and quality of life, reduced muscle mass impairs the body's ability to respond to stress and chronic illness, attributing to an overall decreased quality of life.

1.2. Traumatic Muscle Injury

Skeletal muscle comprises over half of the human body weight in non-obese subjects. With such prevalence and the exigent role played in the body, the loss of muscle through primary traumatic injuries (burns, lacerations, muscle crushing) or secondary loss as seen in some disease states, impacts to bodily support, motility and metabolic functions are seen almost immediately and often with negative prognosis (Yusuf and Brand-Saberi 2012, Blau, Cosgrove, and Ho 2015). The loss

of functional muscle occurs in all patient demographics, impacting those with a predisposition for major injury, soldiers for example, all the more. The result is a diminished quality of life due to pain, inferior motile capabilities, lack of muscle contractibility or a combination of all three.

Subsequent natural regrowth of tissue after injury can vary depending on the presence of blood vessels, neuromuscular and myotendinous connections and importantly, the distance the reforming tissue needs to span to complete these connections. Regeneration of damaged muscle can also be sporadic as the tissue strata largely attempts to reform the aforementioned connections with less concern about reproducing the native architecture and contractile capabilities, in an effort to limit the eventual necrosis of the tissue due to incomplete connections. The result is seen in the form of altered patterns of contractile unit striations, unfused myotubes, “fiber splitting”, segmental necrosis and scar formation (Ciciliot and Schiaffino 2010, Goodman, Hornberger, and Robling 2015), all of which contribute to diminished tissue regeneration and an overall lack of functionality in the muscle. To date, it has been hypothesized that a biomaterial construct capable of filling and spanning a skeletal muscle wound, while also supporting the chemical and physical requisites to bolster the wound healing process, is a viable option to improving tissue regeneration compared to wounds healing without such a construct (Woo, Park, and Lee 2014, Kim et al. 2014). It is believed that a keratin-based MP filler is a potential biomaterial (Cilurzo et al. 2013, Tomblyn et al. 2016).

1.3. Current State of Biomaterial Scaffolds for Skeletal Muscle Regeneration

To date, a wide array a biomaterial scaffolds have been tested to determine efficacy in skeletal muscle regeneration. The term scaffold has been applied previously as a general indication of a

biomaterial that provides a support, whether it be mechanical, chemical or biological in nature, to improve the regeneration process. Several materials have thus far been tested, ranging from completely synthetic in poly(glycolic acid) (PGA) or poly-ε-caprolactone (PCL) to large scale decellularized organ constructs, and each has shown some promise (Choi et al. 2008, Juhas et al. 2014, Mase et al. 2010). Generally speaking, scaffolds considered to be any sort of success or eliciting potential for skeletal muscle regeneration have been shown to support cellular survival. However, many of these scaffolds exhibit notable failures in terms of complete skeletal muscle regeneration. For example, synthetic scaffolds can be exceptionally bioinert but do not produce biologic stimuli for cell growth. As a result, additional coatings, several of which have been shown to display toxicities in the body, are required (Choi et al. 2008). Decellularized scaffolds contain a number of naturally occurring proteins that support cell survival. However, in culture they often require long incubation times to become functional or not all required cell types integrate into the construct (Wolf et al. 2012, Machingal et al. 2011). Highly touted biopolymer-based scaffolds, based on materials such as collagen or fibrin, display biocompatibility and tailorable properties but currently we see consistent shortcomings in retention of mechanical properties with many of these materials failing or degrading rapidly (Kin et al. 2007, Page et al. 2011). A suitable biomaterial should therefore be identified, that displays a propensity to overcome most if not all of these current shortcomings.

1.4. Keratin as a Biomaterial

The process of muscle wound repair can be broken into three phases: i. The initial inflammatory response ii. activation, infiltration and differentiation of satellite stem cells and iii. the formation and maturation of myofibers (Ciciliot and Schiaffino 2010, Yin, Price, and Rudnicki 2013, Tidball 2017). As a result, a biomaterial of suitable characteristics must take all of these phases into

account to ensure enhancement of the regenerative process. The biopolymer keratin is one such material that has been shown to exhibit satisfactory properties, warranting further consideration (Forbes and Rosenthal 2014).

Two types of mammalian α-keratin proteins have been characterized and denoted as “soft” α-keratins, largely found in skin (epidermal keratins), and the “hard” α-keratins (trichocyte keratins) commonly found epidermal appendages such as hair, claws and quills which often serve the functional need of more durable structures. (Ferraro, Anton, and Santé-Lhoutellier 2016, Hill, Brantley, and Van Dyke 2010). Both forms of protein are stabilized by disulfide bonds between pairs of cysteine residues. The number of disulfide bonds in trichocyte keratin is greater than in epidermal keratin (8% vs 3% respectively) (Yu et al. 1993) and the relatively high cysteine content of human hair keratins, in particular, offers several opportunities for biomaterial applications by regulating the amount of binding which, when coupled with favorable chemical properties, can produce advantageous mechanical properties as well.

Electron micrographs have shown keratin exhibits a filament and matrix-like texture (Bragulla and Homberger 2009). The cores of the filaments are formed from rod domains that are approximately 40-50 nm in length. A comparable structure exists in the keratins of birds although the structural content is chiefly in the form of β-sheets (Wang et al. 2015). Coinciding with the presence of cysteine residues, a considerable difference between trichocyte and epidermal keratins is that the matrix in trichocyte keratins contains considerable amounts of sulfur-rich and glycine-tyrosine-rich proteins which can be altered to affect material properties. Also, during transition to the oxidized state of keratin, the framework of the intermediate filaments undergoes both molecular slippage and compaction, a process that is much more apparent under chemically induced

processes but can similarly alter material properties (Grune, Reinheckel, and Davies 1997, Thiele et al. 1999). This brings the cysteine residues of neighboring molecular segments into axial alignment and enables the formation of disulfide linkages (Hill, Brantley, and Van Dyke 2010). By comparison, epidermal proteins contain very little cysteine and particular regions contain none at all, which indicates that any change in the framework of epidermal intermediate filaments on oxidation will not depend on changes in free energy associated with the formation of disulfide linkages. There is a distinct functional relationship between the concentration of disulfide bonds in the two types of keratin and their respective mechanical properties (Sun and Green 1978, McLellan et al. 2019).

The natural characteristics found within keratin promote its use as a biomaterial. Found within a broad variety of tissues including skin and human hair, the toughness and hardness of these proteinacious materials is derived from the organization and extensive crosslinking of the individual proteins. The study and application of keratins pertaining to this work chiefly use the keratin derivative keratose (KOS), isolated from human hair. Keratose employs a number of attractive properties including a lack of disulfide bonds, allowing for more control over degradation rates compared to its counterpart derivative (keratein), water solubility and hygroscopicity allow for improved water absorbance and subsequent gelation. A basic chemical schematic of KOS extraction can be seen in **Figure 1.1**.

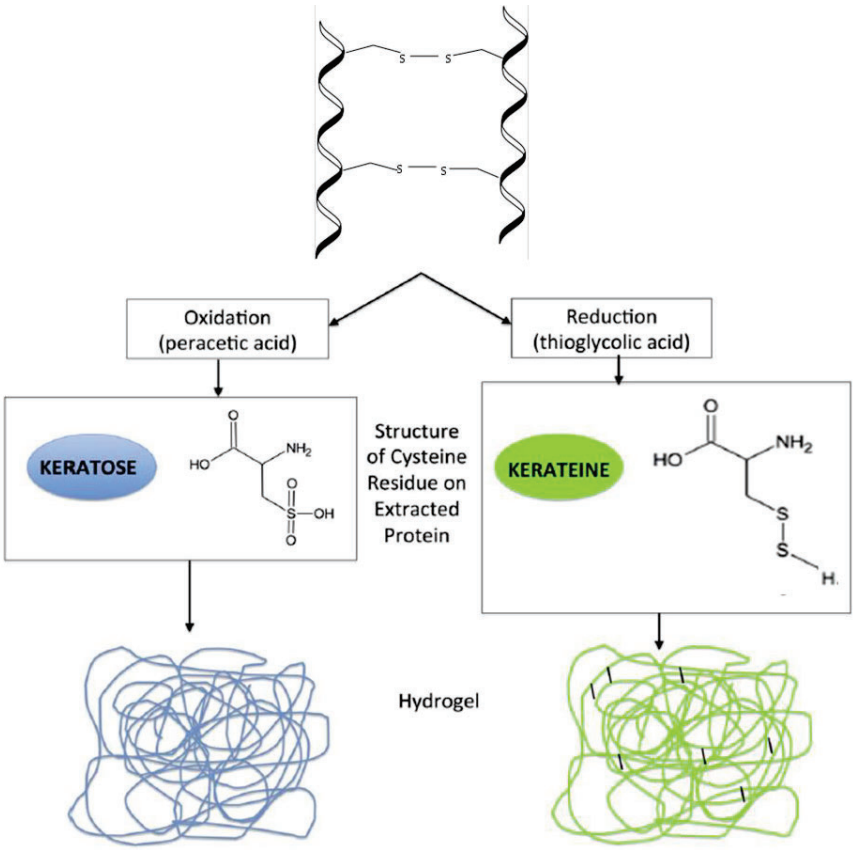

Figure 1.1. Schematic of Keratin Extraction. Schematic of oxidative (keratose) or reductive (kerateine) reactions using human hair isolates derivative keratin proteins. Successive washing of keratose produces a hygroscopic protein rich material lacking disulfide bonds.

Prior research suggests keratin and keratin derivatives exhibit several mechanical and biological properties that support their use as a cell delivery vehicle. Upon hydration, keratin hydrogels mechanically perform as a flexible viscoelastic material. The compressive modulus of keratin hydrogels ranges from 10-19 kPa with elastic moduli ranging from 0.15-12 kPa (de Guzman et al. 2011, Papir, Hsu, and Wildnauer 1975). Compared to native skeletal muscle, with compressive and elastic moduli of ~2 kPa and ~0.03 kPa respectively, keratin hydrogels are well within the mechanical scope of application in terms of matching mechanical properties. In terms of biological cues, keratin contains intrinsic amino acid binding motifs in the form of Arg-Gly-Asp (RGD), Leu-Asp-Val (LDV) and Leu-Asp-Ser (LDS) amino acid binding sites, which support cellular adhesion

specifically (Sando et al. 2010). Along with a natural propensity for cell adhesion, keratin proteins exhibit a uniquely low inflammatory response upon implantation. The mechanisms of the process are still in question, but the validity of this low response has been documented via analyses of macrophage activation when in contact with keratin, where keratin increased and decreased, anti-inflammatory and pro-inflammatory macrophage cytokines, respectively (Fearing and Van Dyke 2014, Chazaud 2014, Waters, VandeVord, and Van Dyke 2018).

Pertaining to the regeneration of muscle tissue, along with decreased inflammation and the presence of RGD, LDV and LDS amino acid binding sites, KOS is resistant to proteolytic degradation (Rouse and Van Dyke 2010) and capable of maintaining properties under cyclic loading, as would be seen during muscle contractions. Prior studies have shown that KOS supports adhesion and proliferation of muscle progenitor cells (Tomblyn et al. 2016) as well as improving compound motor action potential (CMAP) latency and the recovery of baseline nerve conduction velocity (NCV) (Hill, Brantley, and Van Dyke 2010, Pace et al. 2014), promoting increased functionality of recovered skeletal muscle. KOS also promotes angiogenesis without exacerbating inflammation (Shen et al. 2011), while also promoting myoblast differentiation of human mesenchymal stromal cells (HMSCs) (Ledford et al. 2017, Fearing and Van Dyke 2014). The assembly of these properties in one biomaterial overcomes several limitations of currently tested natural and synthetic biomaterial constructs, which includes an inability to support vascularization, myofiber alignment or to retain the biomaterial as is seen in synthetic PLA scaffolds, minced native skeletal muscle and natural collagen scaffolds, respectively (Grasman et al. 2015).

1.5. Diglycidyl Ether Crosslinkers

The chemical crosslinking of proteins has many applications in biomaterials research but are largely applied to stabilize a protein structure, modify protein properties or to allow for bound conjugates (Fingas 1995, Lu et al. 2006). Various crosslinkers with different reaction chemistries are available but ease of use, affinity for binding to the target protein and scalability concerns (such as cost) must also be considered to determine the most efficacious crosslinker. Diglycidyl ethers are a series of crosslinkers that have previously been shown to bind to nucleophiles, amino and carboxyl groups particularly, with a high affinity (Lu et al. 2006, Yamazoe et al. 2008). In this work, three diglycidyl ethers were applied in the synthesis of keratin biomaterials with the intent to stabilize the keratin construct and potentially alter (or tailor) material properties for improved use. Butane-diol diglycidyl ether (BDDE), ethylene-glycol diglycidyl ether (EGDE) and poly(propylene)-glycol diglycidyl ether (PGDE) (**Figure 1.2.**); each is a diglycidyl ether with similar binding mechanisms but with differences in chain length as a naturally occurring variant, which may become the principal factor in altering material properties. The epoxide regions on the ends of the molecules facilitate efficient binding of carboxylic acid in keratin proteins specifically. Intrinsic properties such as biocompatibility and biodegradability as well as current FDA approval make this family of diglycidyl ethers an attractive set of crosslinkers.

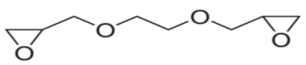

Ethylene Glycol Diglycidyl Ether (EGDE): **MW 174.19**

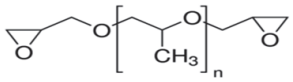

Poly(propylene) Glycol Diglycidyl Ether (PGDE): **MW ~380**

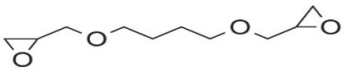

Butanediol Diglycidyl Ether (BDDE): **MW 202**

Figure 1.2. Diglycidyl Ether Crosslinkers. Chemical schematic of three diglycidyl ethers used as chemical crosslinkers capable of binding and stabilizing keratin biomaterials. Crosslinkers display similar binding mechanisms to keratin through the epoxide regions located at the ends of the molecules. These biocompatible chemicals may allow us to tailor material properties due to the dissimilarities between chain length.

1.6. Hydrogels

Hydrogels are a class of biomaterials with high water content and soft tissue-like mechanical properties (Dubbini et al. 2015) that make them attractive as scaffolds for a variety of tissue engineering applications. Moreover, highly moldable hydrogels can be injected into irregular shaped defects, enabling targeted delivery of cells for *in vivo* tissue engineering (Jeong Park et al. 2000) with limited surgical invasion (Zhang et al. 2014). Further, injectable biomaterials may be designed to crosslink in situ to facilitate integration and tissue regeneration at the region of interest (Montanari et al. 2015). In situ crosslinking is generally accomplished by chemical polymerization, photopolymerization or thermal crosslinking (Berger et al. 2004, Hennink and van Nostrum 2012, Montero-Rama et al. 2015). Chemical polymerization and photopolymerization have been applied extensively for gelation of injectable hydrogels, though the use of chemical initiators risks cytotoxicity and introduces undesired complexity to the delivery systems (Elias et al. 2015).

Thermal crosslinking is applicable for thermosensitive hydrogels that undergo phase transitions in response to temperature change, although these systems are consequently limited to temperature ranges that are well tolerated by living cells. Rapid swelling, subsequently forming a viscoelastic material, can be seen in **Figure 1.3.**

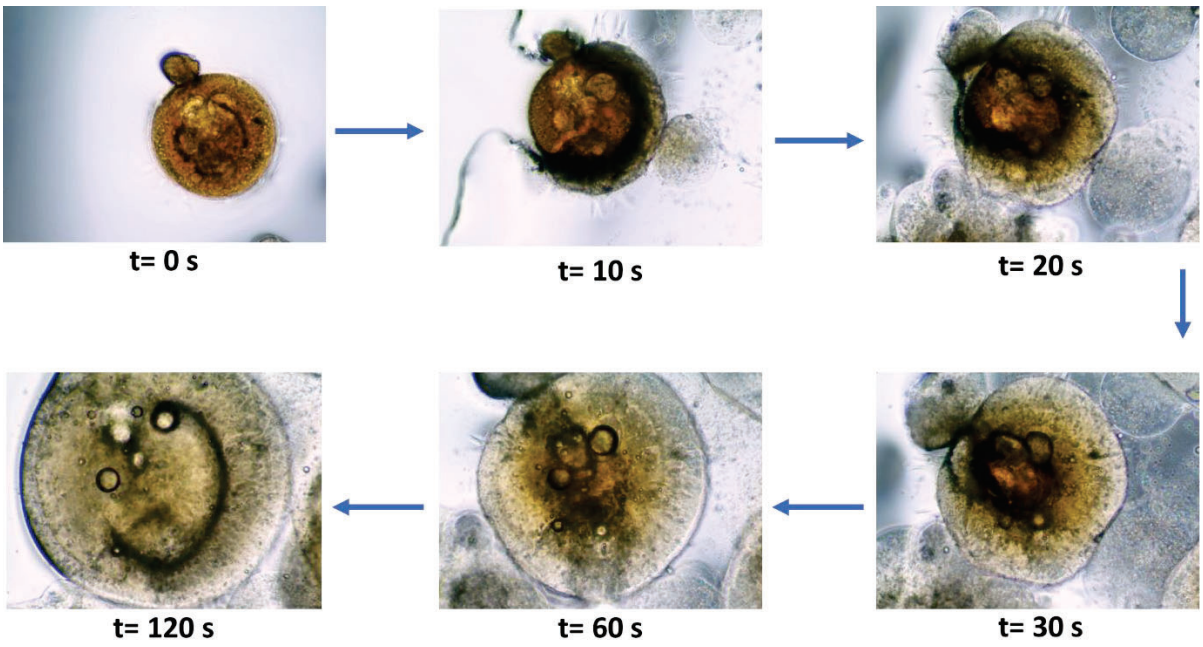

Figure 1.3. Hydrogel Rapid Water Uptake. Time course of keratin microparticles swelling during water absorption and subsequent binding. Rapid water uptake leads to a mechanically attractive biomaterial from a soft tissue standpoint. Along with intrinsic biocompatible properties, keratin-based hydrogel biomaterials serve a number of requisite properties for soft tissue regeneration.

1.7. Keratin as a Cell Loaded Scaffold

Prior research suggests keratin and keratin derivatives exhibit several attractive mechanical and biological properties that support their use as a cell delivery vehicle. Upon hydration, keratin hydrogels mechanically perform as a flexible viscoelastic material. Analysis of the compressive modulus of keratin hydrogels ranges from ~4 MPa in dry scaffolds to almost 0.01 MPa after just

five minutes of hydration (de Guzman et al. 2011). Tensile tests on keratin from various sources have shown that, once isolated, keratinized structures can display an elastic modulus anywhere between 0.01 and 9 GPa (Papir, Hsu, and Wildnauer 1975). In terms of biological cues, keratins intrinsic amino acid motifs in the form of RGD, LDV and LDS amino acid binding sites, which are integrin specific, as well as other classes of receptors which are non-integrin specific based on antibody blocking of the β2 integrin subunit, support cellular adhesion specifically (Rouse and Van Dyke 2010, Hill, Brantley, and Van Dyke 2010, Sando et al. 2010). Along with a natural propensity for cell adhesion, keratin proteins exhibit a uniquely low inflammatory response upon implantation. The mechanisms of the process are still in question but the validity of this low response has been documented via analyses of macrophage activation when in contact with keratin, where keratin increased anti-inflammatory macrophage cytokines and decreased pro-inflammatory macrophage cytokines (Fearing and Van Dyke 2014, Waters, VandeVord, and Van Dyke 2018).

1.7.1 Fabrication

Keratins are generally extracted through chemical means that first break the disulfide bonds prevalent in keratinized tissues. Initially, the alpha- and less common gamma-keratins are converted to their non-crosslinked forms via oxidation or reduction, as cystine is converted to either cysteic acid or cysteine, respectively. Next, free proteins are extracted with solvents capable of denaturing the proteins for subsequent purification (by filtration and dialysis). Here, oxidizing denaturants produce derivatives referred to as keratoses, while reducing denaturants produce cysteine-containing proteins called kerateines. While essentially homologous, the sulfur-containing cysteine groups primarily define the differences between keratoses and kerateines. Keratoses are non-disulfide crosslinkable, water soluble, and susceptible to hydrolytic degradation due to the polarized protein backbone. The higher polarized nature of keratoses causes them to

degrade relatively quickly *in vivo* (days to weeks). Kerateines are less polar and therefore slightly less soluble in water. They are more stable and can be re-crosslinked through oxidative coupling of cysteine groups. This results in biomaterials that can persist *in vivo* for weeks to months (Noishiki 1982).

1.7.2. Applications

Documented as beginning as early as the 1970's for biomedical applications, the processing of these protein solutions into derivative physical states such as gels and films began appearing in literature (Van Dyke and Nanney 2002). Early keratin biomaterials appeared in the form of a wool derivative applied as a vascular graft coating, which was successfully implanted into a canine model for nearly 6 months (Noishiki et al. 1982). Since then, keratins have been used in several *in vitro* and preclinical models for hemostasis, wound healing (Burnett et al. 2013), bone regeneration (Zhao et al. 2015) , and peripheral nerve repair (Sierpinski et al. 2008b).

Pre-clinical studies have suggested the viability of a keratin-based nerve repair biomaterial. Keratin hydrogels introduced *in vivo* have resulted in significant increases in Schwann cell proliferative and migratory ability, suggesting a potentially improved nerve regenerative response (Nakaji-Hirabayashi, Kato, and Iwata 2008, Sierpinski et al. 2008b). These materials were mechanically weaker compared to other hydrogels but maintained their structure after hydration. In other previous studies, keratin-based hydrogels carrying integrin-binding polypeptides were synthesized and evaluated as a substrate for Schwann cells (Sierpinski et al. 2008a). However, in some cases the requirement of strong denaturants to dissolve keratin molecules makes it difficult to prepare cell-seeded hydrogels for transplantation, as residual denaturants in the hydrogel can disrupt cellular processes or act in a cytotoxic manner against seeded cells.

Keratin has also been previously exploited for its ability to induce cell differentiation. Previously, human cardiac stromal cells (hCSCs) have been shifted to a smooth muscle cell lineage *in vitro* (Ledford et al. 2017). Other studies display keratins ability to induce macrophage differentiation, suggesting it be exploited as a potential wound healing therapy (Fearing and Van Dyke 2014). Results from other studies suggest that keratin biomaterials can in fact promote a greater production of anti-inflammatory cytokines and suppress production of pro-inflammatory cytokines. This is thought to be a function of keratins ability to modulate macrophage phenotype during the wound healing process, leading to decreased inflammation and an improved environment for regeneration as a whole (Fearing and Van Dyke 2014, Waters, VandeVord, and Van Dyke 2018).

1.8. Microparticles

Microparticles (MP), 1 micrometers to 1000 micrometers (μm) in diameter, have been touted as a multimodal delivery vehicle, capable of serving as a building block for 3-Dimensional (3D) constructs to fill tissue voids while simultaneously providing delivery of soluble factors and cells (Qazi et al. 2015, Moulin, Mayrand, Messier, Martinez, Lopez-Valle, et al. 2010, Huang and Fu 2010). The application of MPs provides a larger surface area for exterior cell loading while avoiding concerns about clearance commonly viewed as a potential negative side effect of similarly touted nanoparticles (Behrens et al. 2014). The benefit of a microscale protein construct lies in the interplay between the individual products size, capable of non-invasive injectable delivery, and the physical agglomeration of gel particles wherein once fully hydrated particles form a nearly contiguous hydrogel construct (Oliveira and Mano 2011, Woo, Park, and Lee 2014).

1.9. Water-in-oil Emulsion Synthesis

Emulsions are disperse systems in which two or more largely insoluble liquid phases are mixed. Except for unique cases such as high internal phase emulsions with a foam structure, the internal phase is contained in the external phase in the form of spherical droplets. This is found to be true in the case of either an oil in water (o/w) or a water in oil (w/o) emulsion (Leal-Calderon, Schmitt, and Bibette 2007). The sequestering of a material (KOS for example) that is highly preferential to one phase (water) produces concentrated droplets. Similarly, the addition of water-soluble factors like drug payloads also preferentially isolates the drug in the regions with higher water affinity.

From a synthesis standpoint, emulsion systems are highly attractive due to their simplistic mechanism of formation. The two (or more) liquid phases are innately prone to separate based on their chemical composition. The addition of rapid or even mild stirring in some formulations creates separation that eventually has a tendency to yield more monodisperse droplets (Yan and Texter 2006, Boutonnet et al. 1982). These droplets, as they are formed from a lack of affinity between the phases rather than a uniquely high affinity for self-binding, are often fragile in nature. Keratins produce an interesting solution to this problem due to the self-crosslinking capabilities found within its structure, thus producing a more stable particle. Often the addition of a chemical crosslinker with favorable chemical properties can help aid in MP stability. This work employs a series of diglycidyl-ethers which display low biological toxicity, are biodegradable, highly preferential to water-solubility and are currently approved by the Federal Drug Administration (FDA) (Nishi, Nakajima, and Ikada 1995, Zeeman et al. 1999) to produce stable MP formulations.

1.10. Biologic Payloads

Incorporation of drug or biomolecular payloads into biomaterial constructs has been a common approach in regenerative medicine (Dang et al. 2016, Martino et al. 2014, Saul, Ellenburg, de Guzman, and Van Dyke 2011). The need to control local flora has long been recognized as an imperative for wound healing. In some cases, specifically in less developed parts of the world, patient's risk to develop a nosocomial infection is as high as outside of the hospital. Delivering antibiotics in large or systemic doses carries with it the possibility of insufficient delivery of the antibiotic to the wound site, or an eventual resistance to antibiotic treatment (Saul, Ellenburg, de Guzman, and Van Dyke 2011, Park, Kim, and Suh 2004, Roy et al. 2016, Du, El-Sherbiny, and Smyth 2014). Thus, several technologies have been developed for the sustained release of antibiotic drugs from biomaterial-based topical dressings (Elsner, Berdicevsky, and Zilberman 2011). Triggered, local release has been less common (Yan et al. 1994b).

The chemistry and evolutionary biology of keratins provide a unique opportunity for a keratin biomaterial-based drug delivery system for control of microbial populations. Mammals never developed a compliment of keratinases because there was no need for a turnover mechanism directed at hard keratin-containing tissues. Horns, hair, feathers and hooves did not rely on remodeling; they were sloughed or worn off and replaced. However, microbes, particularly bacteria and fungi, developed a compliment of keratinases such that they could make use of the keratin-containing structures of mammals as a food source. As a consequence, the presence of keratinases at a wound site is a hallmark of microbial contamination in mammalian wound healing, and hence can be used as the basis of a triggered, local, keratin biomaterial-based drug delivery system.

1.11. Cellular Payloads

Often natural tissue regeneration relies on the presence of undifferentiated progenitor cells with a high proliferative potential to replace damaged and terminally differentiated cells (Hunt and Grover 2010, Man et al. 2012, Uludag, De Vos, and Tresco 2000). Characterized by the ability to self-renew and differentiate into a variety of specialized cell types, many cellular therapies for tissue regeneration employ adult progenitor cells, like mesenchymal stromal cells (MSCs). MSCs are culture-adherent, multipotent progenitor cells capable of differentiating into muscle, bone, cartilage, fat, tendon and nerve (Gao et al. 2014, Xu et al. 2015). Isolated from various sources including bone marrow, adipose tissue, muscle tissue, amniotic fluid, human placenta, periosteum, cord blood and even peripheral blood (Niemeyer et al. 2007, Cowan et al. 2004, Prigozhina et al. 2008), the efficacy and survival of MSCs have proven to be a contributor to tissue regeneration, but this also depends heavily on the method of delivery prior to transplantation (Nicodemus and Bryant 2008, Oliveira and Mano 2011).

The foregoing technologies have since provided optimism that the aforementioned characteristics can be combined into a single system, one with a keratin biomaterial as its main constituent, and in which chemistry, materials engineering, pharmacology and biology can be combined to create constructs with utility in regenerative medicine.

Chapter 2

Synthesis and Characterization of Water-in-oil Emulsion Synthesized Keratin Microparticles for Biomedical Applications

Marc Thompson[1], Aaron Guiffre[2], Andrew Vipperman[3], Dr. Mark Van Dyke[1]

1. Department of Biomedical Engineering and Mechanics, Virginia Tech, Blacksburg, VA
2. Electrical and Computer Engineering, Virginia Tech, Blacksburg, VA
3. School of Neuroscience, Virginia Tech, Blacksburg, VA

Abstract: Keratins are a family of proteins found within human hair, skin and nails, as well as a broad variety of animal tissues (Hill, Brantley, and Van Dyke 2010, Rouse and Van Dyke 2010). Prior research suggests hydrogel constructs of keratin and keratin derivatives exhibit several mechanical and biological properties that support their use for tissue engineering and regenerative medicine applications. Microparticle formulations of hydrogels are an intriguing delivery vehicle for tissue engineering purposes due to the ability to exploit size, surface area, loading potential and importantly, non-invasive delivery of cells and biologics. Here we examine the application of the well-documented water-in-oil emulsion synthesis procedure to produce keratin s using an oxidized keratin derivative, keratose (KOS). The cause and effect relationships between synthesis parameters and properties are not known for keratin s. Therefore, in this study, we conducted pilot experiments to establish a robust oil-in-water emulsion system, and investigated the use of both water and saline solutions of KOS, as well as three different crosslinkers to produce s with different properties. We examined particle size, microstructure, swelling behavior, surface topography, porosity, as well as rheological properties and enzyme-mediated degradation of -based gels. Largely spherical particles of wide size distribution were obtained, which re-hydrated readily, swelling up to 80% and forming viscoelastic gels. The strong self-assembly characteristic of KOS was evident in the rough surface and underlying fibrous nature of the particles, which caused rapid

release of a model compound payload. Small differences between crosslinker type were observed in some of the parameters tested. The unique microstructure of KOS particles may lend them to applications in rapid drug release or other payload delivery wherein a high level of biocompatibility is desired.

2.1. Introduction

The classical tissue engineering approach of using a scaffolding system can present a bulky construct that requires surgical implantation due to its size and rigidity. A minimally invasive implantation approach is often desired, provided the properties of the biomaterial lend themselves to procedures such as injection through a needle. Prior research suggests keratin and keratin derivatives exhibit several mechanical and biological properties that support their use as scaffolds for cells that can incorporate various payloads. Upon hydration, keratin hydrogels mechanically perform as a flexible viscoelastic material. Based on previous studies, compressive moduli of keratin hydrogels range from 10-19 kPa with elastic moduli ranging from 0.15-12 kPa, supporting its use in a number of tissue regeneration systems (de Guzman et al. 2011, Papir, Hsu, and Wildnauer 1975). However, most reports of keratin biomaterials in tissue engineering utilize cell-free constructs, despite keratin's intrinsic biocompatibility and apparent support of cell health and function (Konop et al. 2018, Mori and Hara 2018). This may be a consequence of the formation of keratin hydrogels being incompatible with cells, particularly in the kerateine (KTN) system where gelation is best driven by protein self-assembly at basic pH (Hill, Brantley, and Van Dyke 2010). The KOS hydrogel system is more conducive to inclusion of cells as these gels can form at physiologic pH, but the resulting constructs can be fragile and degrade rapidly. Crosslinking can be used to mitigate this, but some chemistries may compromise cell viability (Steinert et al. 1993,

Tanabe, Okitsu, and Yamauchi 2004a). Pre-formed keratin microparticle (MPs) may be a solution to these challenges.

2.2. Chemicals and Reagents

Human hair was obtained from a proprietary source. Peracetic Acid (PA), tris(hydroxymethyl)-aminomethane (Tris) base, sodium hydroxide, phosphate buffered saline (PBS) (Gibco), ethylene-glycol diglycidyl ether (EGDE) (TCI Chemicals), poly(propylene)-glycol diglycidyl ether (PGDE) (Sigma Aldrich), butane-diol diglycidyl ether (BDDE) (Alfa Aesar), light mineral oil (Thermo Fisher), hexanes (Thermo Fisher), elastase (MP Biomedicals), collagenase (Worthington) were all used as received.

2.3. Materials and Methods

2.3.1. Validation of Water-in-oil Emulsion Procedures

2.3.1.1. Keratose Extraction

Keratin proteins were extracted as previously described (de Guzman, Tsuda, et al. 2015, Hill, Brantley, and Van Dyke 2010). Briefly, human hair fibers were oxidized using a 2% peracetic acid (PA) solution (pH 2) over 18 hrs using a 20:1 ratio of PA to hair mass (20 mL PA: 1 g hair). Fibers were washed with deionized (DI) water to remove the oxidant and a Tris base (100 mM) removed the soluble keratin proteins. Extracted KOS proteins were centrifuged, filtered to remove suspended solids, and dialyzed against phosphate buffer. Sodium hydroxide neutralized the material to pH 7.4 where it was subsequently frozen and lyophilized until further use.

2.3.1.2 Water-in-oil Emulsion Microparticle Synthesis

MP synthesis via the water-in-oil emulsion process was adapted based on previous methodologies (Yan et al. 1994b, Yin Hsu, Chueh, and Jiin Wang 1999). Lyophilized KOS proteins were weighed out and dissolved in either DI water or PBS to a working concentration of 60 mg/mL. One of three diglycidyl ether-based chemical crosslinkers (EGDE, PGDE or BDDE) was added to form a 48 wt% solution (previous raman spectroscopy determined the partitioning of crosslinkers between the water and oil phases occurred in a 1:3 ratio of water and oil, therefore final crosslinking concentrations were approximately 12 wt%), which was vortexed and centrifuged at 1000 rpm for 5 min to remove air bubbles; samples were allowed to equilibrate overnight. These crosslinkers, each of which exhibits keratin binding through similar mechanisms at the epoxy region of the chain ends, were chosen for their similar structures with marginally different molecular weights due to their respective chain length. From an applicability standpoint, these particular crosslinkers are also attractive due to their documented low toxicity, biodegradability and current FDA approval for use in cosmetic fillers (Vasconcelos and Cavaco-Paulo 2013, Tanabe, Okitsu, and Yamauchi 2004b). KOS solutions were added to light mineral oil at a 1:20 volume ratio and stirred using a Caframo tabletop mixer at 2000 rpm for 24 hours. The light mineral oil was aspirated off, removing as few MPs as possible, and the resulting particles were washed with chilled hexanes at approximately -25 ^{o}C using a lab bench shaker set to a medium speed setting for 5 min. Residual hexane was aspirated and this step was repeated 2 more times to further remove any oil. MPs were stored at -25 ^{o}C. Finally, any residual hexane was aspirated from the product and MPs were lyophilized to form a stable product for subsequent analysis. A schematic of this process can be seen in **Figure 2.1.**

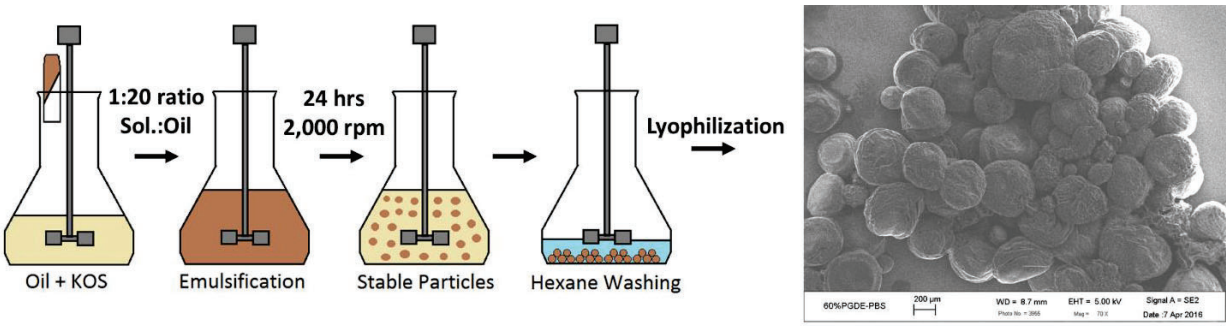

Figure 2.1. Schematic of Microparticle Formation via Water-in-oil Emulsion Synthesis. Schematic representation of synthesis procedures for KOS MPs using the developed water-in-oil emulsion methodology. The employed procedures produce stable particles with a spherical shape as expected and what appears to be relative monodispersity in terms of particle size.

2.3.2. Scanning Electron Microscopy

Scanning electron microscopy (SEM) was employed to image particles for an observation of size, shape and surface topography. MPs were fixed on a metallic chip using adhesive carbon tape and sputter coated with a 10 nm thick layer of platinum/palladium using a Leica ACE600 sputter coater prior to imaging. Samples were imaged using a Zeiss field-emission scanning electron microscope. The resulting SEM images were used largely for contextual purposes but were also utilized for size measurements.

2.3.3. Size Analysis (SEM/Particle Size Analyzer)

The average size of the synthesized MPs was determined using two methods. In the first method, the previously mentioned SEM images were processed using the *ImageJ (Schneider, Rasband, and Eliceiri 2012)* image processing software. Diameter measurements of several spherical particles (n=20) were taken based on a length to pixel ratio determined via the SEM and averaged to determine the mean and standard deviation of particle size.

The second method involved analyzing samples using a Horiba LA-950 particle size analyzer. MP samples were suspended in ethanol to prevent water absorption and swelling, consequently altering the size of the particles. Samples were agitated using a combination of stirring and sonication to prevent particle agglomeration. Samples were analyzed via laser diffraction to determine the size and variance in sizes between particles.

2.3.4. Swelling Behavior

The swelling behavior of the KOS MPs was tested to validate water absorption and determine the expected size of a hydrogel particle in vivo. The diameter of dehydrated particles was measured using light microscopy. Individual particles were hydrated using one type of a gradient combination of water and ethanol (0:4, 1:3, 2:2, 3:1, 4:0). Particles were allowed to hydrate and swell for 5 min, after which the size of the particle was measured again. Individual diameters were measured and quantified by correlating the before and after light microscopy image to the imaged length of a standard hemocytometer as a reference, at the same imaging plane.

2.3.5. Water Uptake Capacity

The capacity for water uptake and lasting water binding (thus forming the hydrogel) (Ahmed 2015, Oyen 2014) was confirmed via a simplistic water uptake experiment (Hartrianti et al. 2017). 20 mg of particles under all combinations of crosslinkers and solvents were saturated with DI water and allowed to swell for 1, 12, or 24 hours at room temperature or were immediately removed from water. After removal of the residual water, the particle mass was measured immediately after the respective incubation times as well as after a 24-hour period of air drying at ambient temperatures.

2.3.6. Surface Characterization

The topography of hydrated MPs was observed using a Veeco Multimode atomic force microscope (AFM). Particles were fixed using adhesive carbon tape prior to testing and stored in a water-tight chamber with inlet and outlet tubing to allow for water flow and hydration. Particles were hydrated for 10 minutes prior to 10 µm x 10 µm surfaces being analyzed under scanning mode with a scan speed of 3.9 μms^{-1} using a Bruker non-conductive silicon nitride probe tip ($k=0.12\ Nm^{-1}$) (n=20).

2.3.7. Structural Analysis

To analyze particle shape and internal structure we investigated the average porosity and relative pore connectivity within samples of synthesized particles using confocal microscopy. MPs were incubated with a 4′,6-Diamidino-2-phenylindole dihydrochloride (DAPI) cellular stain ($0.1\ \mu gmL^{-1}$) that was readily absorbed by the keratin protein. Particles were incubated at room temperature in the dark for 5 min, washed with PBS three times and visualized using a Zeiss confocal microscope. Z-stacks measuring between 4 µm and 5 µm in thickness were taken and compiled to create a 3-dimensional construct of an individual particle's internal structure. ImageJ image processing software, specifically the *BoneJ* plugin (Doube et al. 2010), was used to quantify both the pore fraction which pertaining to this study is defined as the volume of pore space divided by the total volume of a particle, the average pore size and the overall connectivity of the pores in three different batches of particles (n=50).

2.3.8. Elastic Properties of Hydrogels

Atomic force microscopy (AFM) was applied to measure elastic properties of individual hydrated particles under conditions that would be seen in a wound environment. Particles were fixed to the AFM chip and sealed within the air tight chamber. Inlet and outlet tubing allowed for the chamber to be filled with DI water via syringe through the inlet while the outlet tube was closed off via a

plastic clasp. Particles were allowed to hydrate for 10 min prior to testing. The Veeco Multimode AFM unit was calibrated and used a Bruker non-conductive silicon nitride probe tip (k= 0.6 N/m) in tapping mode measuring deflection upon surface contact with a forward velocity of 5.75 μm/s and a scan rate of 1 Hz. All combinations of solvents and crosslinkers were tested (n=10).

Rheological properties were tested to determine the viscoelastic properties of a bulk hydrated gel particles for a mechanical comparison to human tissues. Briefly, 60 mg of dry particles were loaded into a circular 20 mm adhesion-reducing silicone mold. Particles were hydrated with 2 mL of DI water and allowed to hydrate for 24 hours. In preparing the rheometer setup, the instrument was calibrated for rotational mapping, geometric inertia and gap width measurements. After complete sample hydration, the resulting gel was removed from the mold and placed on the Peltier plate using a plastic spatula. Frequency sweeps from 0.1-20 Hz at a constant 1% strain were performed on the gel samples. Subsequent stress sweeps from 1-500 Pa at a constant frequency of 1 Hz were similarly performed on the same gels. Elastic as well as loss moduli were quantified in each sample using Rheology Advantage, rheological analysis software.

2.3.9. Statistical Analysis

To compare experimental groups, analysis of variance (ANOVA) and/or linear regression analysis with a Tukey's post hoc test was performed in all experiments. To determine significant variances, for all tests, a p-value <0.05 was considered statistically significant. Sample sizes were determined using a power analysis where a power ($1-\beta$) of 0.9 and an alpha (α) of 0.05 was employed. All statistical analyses were performed using JMP Pro 11.

2.4. Results

2.4.1. Scanning Electron Microscopy

The resulting MPs exhibit a three dimensional and largely spherical shape when dehydrated (Figure 2.2). Particle surfaces appear rough although this roughness was later quantified via atomic force microscopy. Agglomeration is seen between some particles. No distinguishable differences between samples synthesized using either solvent or the three crosslinkers were observed.

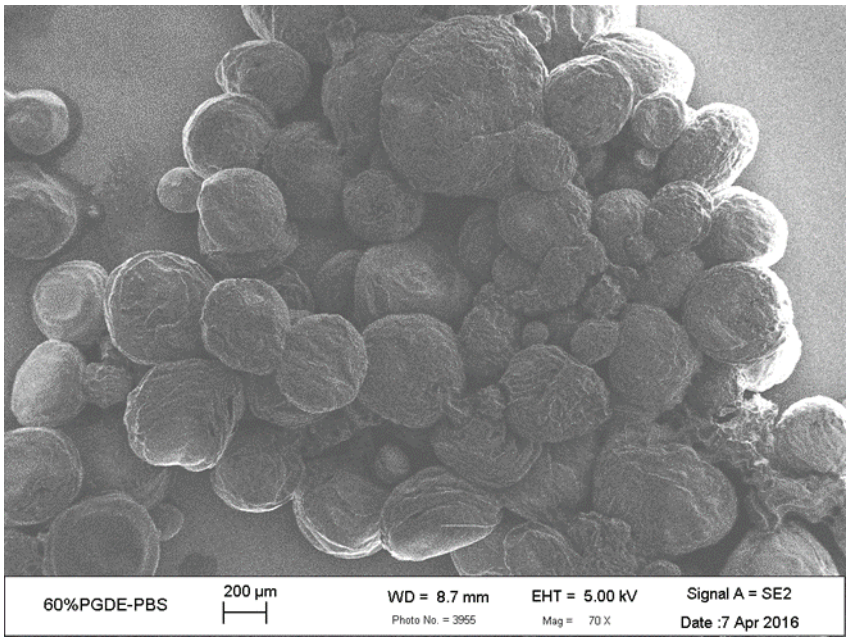

Figure 2.2. SEM of Synthesized Water-in-oil Emulsion Synthesized Microparticles. Representative scanning electron microscopy (SEM) image of the resulting KOS MPs. Particles appear largely spherical with rough surfaces. Sizes of samples also appear to vary somewhat.

2.4.2. Size Analysis (SEM/Particle Size Analyzer)

The size analysis of individual particles using ImageJ generated by scale bars provided by the SEM software suggest average particle diameters of 236 ± 80.4 µm. Based on laser diffraction analyses, mean particle diameters appear to be 366 ±59.4 µm when in an ethanol suspension (Figure 2.3). Increases in particle diameter from one method of measurement to the next may be attributed to the hygroscopic nature of these particles and associated absorption of water from the ambient air. It should also be noted that some samples initially produce particle diameters greatly outside of the normal range with diameters almost verging on the mm scale; this can be attributed to particle

aggregation. It is due to this agglomeration that the apparent large particle sizes are expected and contribute to higher average diameters, although simplistic post-processing steps such as sifting through membranes of a specific pore size are believed to circumvent issues of sample variability (Gauthier et al. 1999).

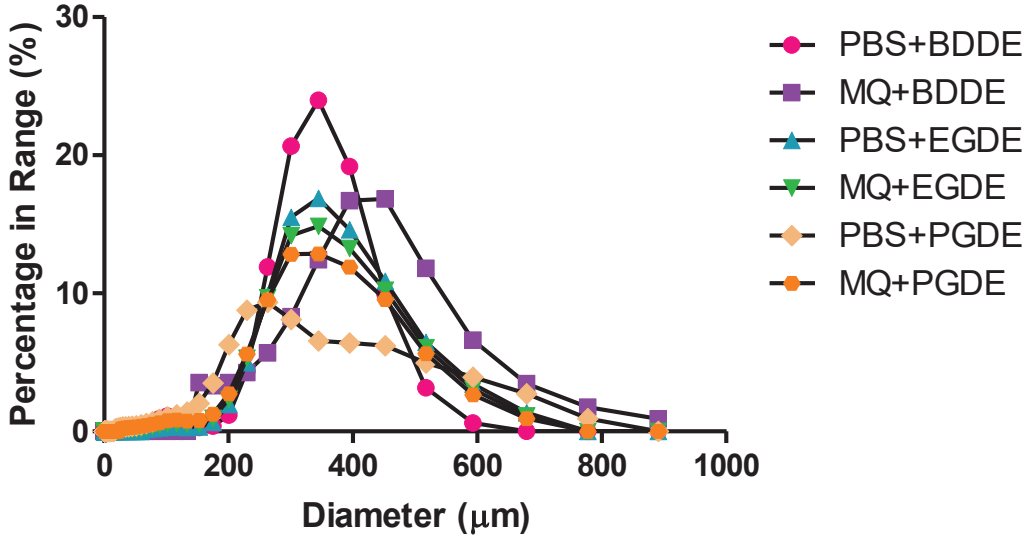

Figure 2.3. Laser Diffraction Analysis of Particle Diameters. There are no statistically significant differences between the average particle size based on crosslinkers or solvents used, primarily due to the broad distribution. Noticeable variations in the low or high end of particle sizes are attributed to particle agglomeration (high end) or residual unbound protein left in the sample (low end).

2.4.3. Swelling Behavior

The applied gradient of ethanol and water produced a relatively linear trend in particle swelling. Little to no swelling was seen in particles soaked in 100% ethanol, which was to be expected. Particles hydrated with 100% DI water produced the greatest level of swelling. Overall, there appears to be a swelling coefficient of approximately 1.6 under pure water conditions (Figure 2.4), which would be expected to be similar in vivo.

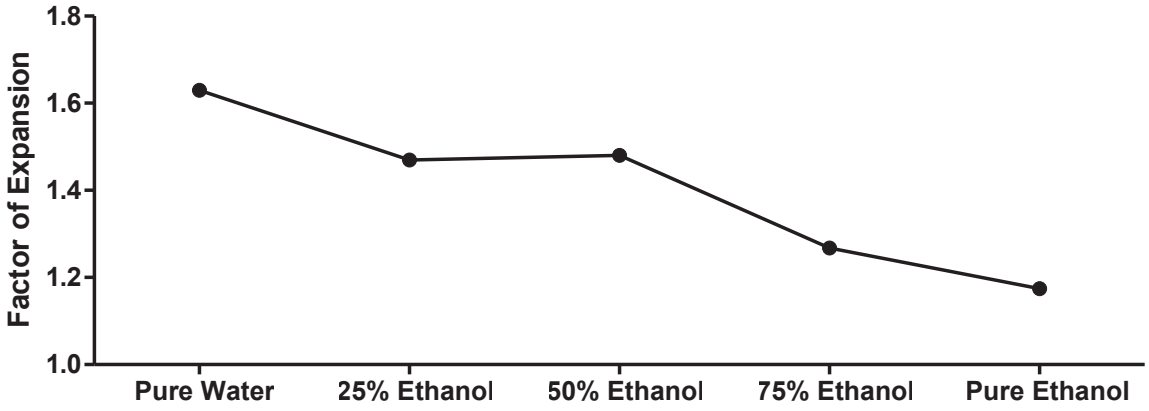

Figure 2.4. Microparticle Factor of Expansion. Factor of expansion of particles under variable solution ratios of water and ethanol. As expected, ethanol elicits little expansion. Pure water provides the most expansion in a system most similar to physiological conditions, producing a factor of expansion of ~1.6.

2.4.4. Water Uptake Capacity

Keratin hydrogels were confirmed using the water uptake experiment (Figure 2.5). No statistically significant changes were seen between either the respective crosslinker or solvent used. However, in all cases particles swelled and reached masses over 1000% of their original mass upon immediate hydration. Stable water-bound particles were achieved after 12 hours as the high water content was retained (greater than 95%) after air-drying for 24 hours. As slightly over 75% of the hydrated mass is retained after 1 hr of saturation it could be suggested that hydrogels are formed within the first few hours of hydration, rather than at 12 hrs, although further analysis must be performed to validate this aspect.

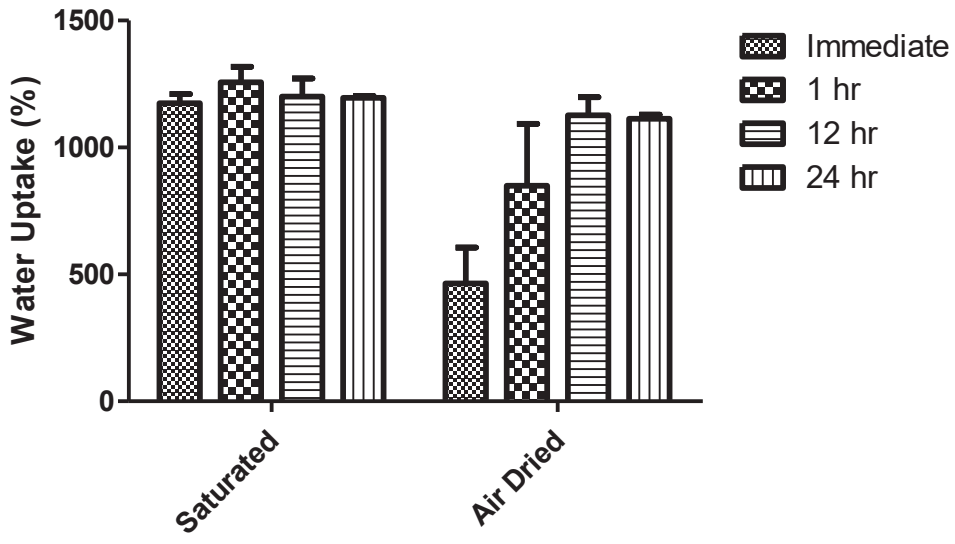

Figure 2.5. Water Uptake of Dehydrated Microparticles. Water uptake capacity and subsequent hydrogel formation was tested and confirmed by the rapid swelling, increase in mass and retention of water in particles shortly after saturation. After 24 hours of air-drying, hydrogel formation was established in the 12 hr and 24 hr hydrated samples, by a retained water uptake percentage within 95% of the original mass after hydration. No significant differences were seen between crosslinkers or solvents used.

2.4.5. Surface Characterization

Based on the 10 μm X 10 μm scans of the AFM, hydrated particle surfaces exhibit relatively rough topographies with larger ridges in some regions. Results suggest an overall average surface roughness of 264 nm with no significant variations in the topographies between particles with a given solvent or crosslinker (Figure 2.6). Surfaces of this roughness with the aforementioned intrinsic binding sites suggest the feasibility of cellular attachment (Goldmann 2016, Hallab et al. 1995).

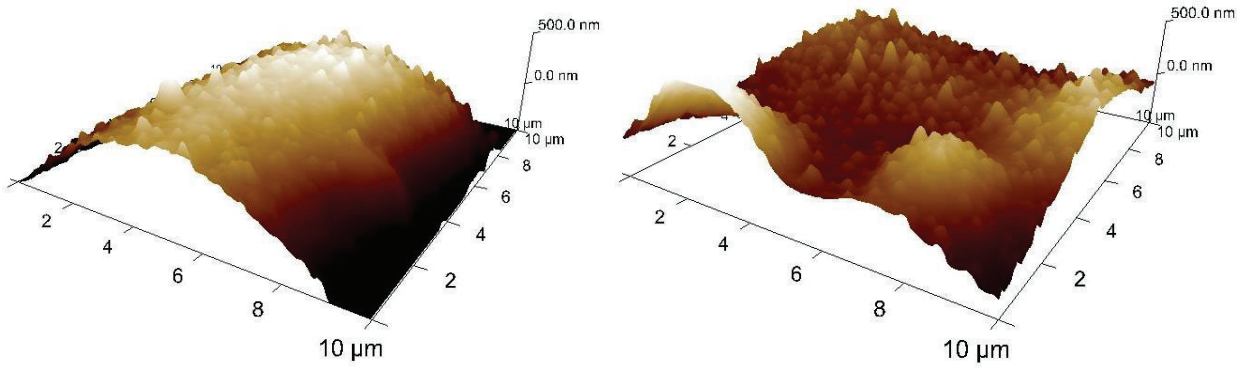

Figure 2.6. Surface Characterization of Hydrated Microparticles. Two samples of AFM scanning surface characterization of hydrated MPs. No differences can be observed between synthesis components but all particles exhibit high surface roughness (~264 nm) with ridges and peaks appearing randomly on surfaces.

2.4.6. Structural Analysis

The internal structure of the oil-in-water generated MP can be described as that of a coarsely fibrous particle with high porosity (Figure 2.7). Quantitative results indicate a protein to pore fraction of 0.58 ±0.04, suggesting that ~40% of a given particle's volume is occupied by empty space (pores) for emulsion synthesized particles. The pore size of particles was calculated to be 704 ±387 μm^2, assuming a spherical pore shape the average pore size should facilitate entry of a cellular payload (Ge et al. 2014, Zanetti et al. 2015). The pore connectivity of the structure was relatively high with a connectivity of 0.53 ±0.17, correlating to approximately half of the pores in a given particle being interconnected (Figure 2.7). Extrapolating this value from laser diffraction size analysis, the calculated average particle diameter of approximately 350 µm proposed from earlier tests (data not shown) and assuming a spherical nature suggests a number of pores ranging in the low thousands (~1,600) per particle. Based on these results, taking into consideration that a larger pore network may provide a greater surface area for cells to adhere to, keratin-based MPs synthesized via the water-in-oil emulsion procedure may support cellular loading from a physical and not merely a chemical standpoint. Similarly, mass transport of waste as well as nutrients to

and from a wound defect, which has been proven to be a significant factor in tissue regeneration (Siepmann, Faisant, and Benoit 2002), could be improved due to both the high porosity and high pore connectivity of the water-in-oil emulsion particles.

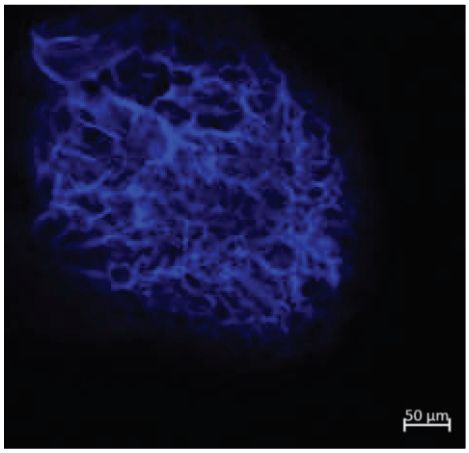

Figure 2.7. Analysis of Microparticle Internal Structure. Fluorescence microscopy image of water-in-oil emulsion synthesized MPs stained with DAPI show a relatively low solid volume fraction of 0.588 (~40% of the given volume is void space) and what appears to be a high pore interconnectivity with a connectivity value of 0.53 ±0.17. Relatively high void fractions as well as pore connectivity may contribute to both the overall surface area with which to load cells and provide improved mass transport, facilitating enhanced cellular function.

2.4.7. Elastic Behavior of Particles

Elastic moduli of individual hydrated particles (Figure 2.8) range between approximately 5 and 13 kPa. No statistically significant differences can be seen between the particles based on respective solvents, although it does appear that PBS dissolved particles produce slightly larger individual elastic properties. There is a significance difference in samples in terms of which crosslinker produces a more elastic MP, however. PGDE crosslinked particles produce significantly greater elasticities than EGDE particles and BDDE crosslinked particles produce significantly greater elasticity than either PGDE or EGDE particles. Based on this data, it is thought that the crosslinker

size or molecular weight (MW) may play a role in the variability between individual MPs elasticity (EGDE MW: 174.19, PGDE MW: ~188, BDDE MW: 202), which also warrants further examination to determine the extent of crosslinking density between individual crosslinkers. Despite the mechanism of binding being similar, it is expected that disparities between the achievable crosslinking density will similarly alter material properties.

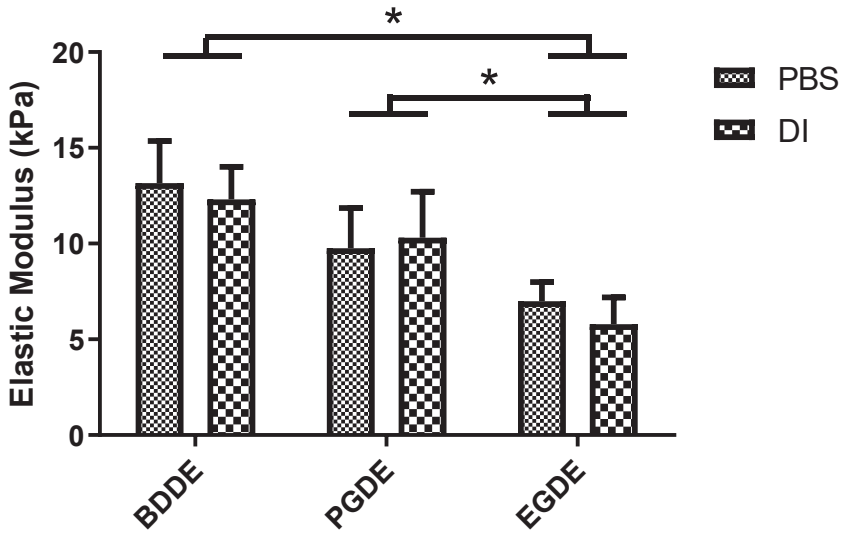

Figure 2.8. Elastic Properties of Individual Particles. AFM analysis of elastic properties of individual KOS MPs. Individual particles exhibit a range of elastic moduli. Significant differences appear to exist based on the crosslinker used during synthesis ($p<0.05$). This may be a factor of the differences in MW or binding density of respective crosslinkers. Error bars represent standard deviation (SD).

2.4.8. Rheological Properties of Microparticle-based Hydrogels

Rheological properties of bulk MP-based hydrogels do not produce a similarly significant trend determined by crosslinkers. Rather, the solvent used for a particular sample produces a more distinct difference in material characteristics. All bulk gels demonstrated elastic moduli between 0.5 and 3.5 kPa. MPs produced from KOS dissolved in DI water produced significantly more

elastic bulk gels compared to the average elastic moduli of all particles synthesized using PBS. There was no clear trend that could be gleaned from the application of crosslinkers in this analysis. Using PBS or DI water for MP synthesis may produce differences at the molecular level. The two solvents are largely similar except for the salt content. KOS is a polyanionic protein at neutral pH, and therefore may be susceptible to electrostatic repulsion induced by the salts present in PBS (Na^+, K^+, Cl^-, HPO_4^{2-}) that could interfere with crosslinking chemistry.

To investigate whether the presence of salts makes a significant difference to hydrogel rheological behavior, a 50:50 ratio of PBS to DI water was used as a solvent and MP samples including the array of all crosslinkers (in duplicates) was taken through rheological analyses, the same as previously mentioned. Result show no clear differences other than the 50:50 ratio gels are statistically stiffer than PBS gels, although the trend does suggest that 50:50 ratios of hydrogels fall in between elastic properties of gels that use one solvent or the other. Although crosslinkers elicited no clear trend in impacting elastic moduli in earlier rheological studies, it is believed that the broad variations seen in the 50:50 solvent elastic moduli can be attributed in some part to the various crosslinkers used while the global average of moduli still falls in between those of a pure DI water and pure PBS solvent solution-based bulk hydrogel.

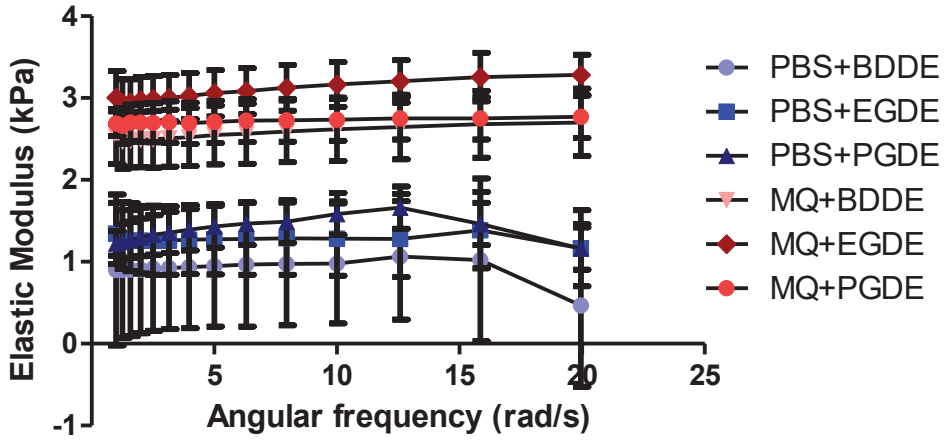

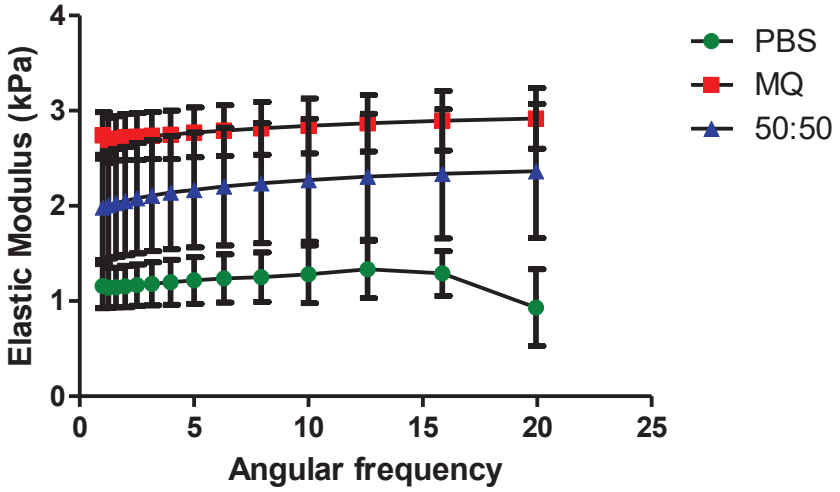

Figure 2.9. Rheological Analyses of Bulk Hydrogels. (Top) rheological analysis of elastic moduli show statistical differences between samples based on the solvent used to dissolve KOS material; error bars represent standard deviation. (Bottom) 50:50 ratio of solvents do not show a statistically significant difference between solvents, but suggest a trend towards a lower salt concentration producing more elastic bulk gels.

2.5. Discussion

The synthesis of keratin-based MPs in a water-in-oil emulsion system has been shown in the present study. The size of the MPs appear to be in the 200-400 µm diameter range with largely spherical shapes, which offers a construct that may be delivered through a needle rather than surgical implantation, although further investigation is needed to ensure this. The mechanisms surrounding the efficacy of the water-in-oil emulsion procedure, namely the phase separation between water and oil, do not necessarily mandate that the water-soluble phase (KOS protein and associated crosslinkers) remain homogenous during the stirring step. As a result, it is likely that a combination of uneven agitation due to mechanical stirring and heterogeneous protein aggregation during stirring, contribute to any non-spherical MP assembly and variations in size. Similarly, variations in protein localization within individual particles appear to contribute to varying surface

structures. Upon initial analysis by SEM, some particle surfaces appear smooth and continuous while others exhibit what appears to be significantly greater porosity. Because there is no clear mechanism to attribute to this characteristic, it is potentially a standard to expect for these particular protein-based MPs with a high self-assembly affinity. During synthesis, particles are finely dispersed and display no heavily agglomerated portions based on periodic inspection of the stirring phase by light microscopy. It was noted however, that during hexane washing some particles have a slight tendency to agglomerate. Further efforts to use particles of a specific size can rely on simplistic size exclusion techniques such as filters or sieves of a specific pore diameter to circumvent this issue.

The KOS MPs tested under hydrated conditions behave similar to classical hydrogel materials based on the elastic properties. Interestingly, the MPs take the form of a highly interconnected, porous particle, suggesting that the keratin proteins and additional chemical crosslinker are still capable of assembly back towards an equilibrium structure of intermediate filaments and not merely dispersed in the continuous oil phase.

The value of the water-in-oil emulsion synthesis technique lies in the straightforward ability to use a relatively safe material in a biopolymer such as keratin without generating potentially deleterious secondary chemical interactions upon synthesis. The resulting particles are stable, inexpensive and easy to process (Van Dyke 2009, Oh, Lee, and Park 2009). Deficiencies arise mainly in this processes reliance on random protein agglomeration and the high apparent porosity as it pertains to loading and retention of a payload *in vitro* and eventually *in vivo*, as it may be difficult to attain sustained or delayed release with such a porous construct (Yan et al. 1994b, Viswanathan et al. 1999). The tailorable properties such as elastic modulus of individual particles or bulk gel constructs are somewhat tailorable based on the results but are limited in the precision in which

these properties can be controlled when compared to other synthesis techniques such as extrusion, molding and lithographic methodologies, which produce contiguous hydrogels (Oh, Lee, and Park 2009). From a delivery standpoint, the data supports that a water-soluble compound is loadable. However, a specific concentration of a payload that is favored or acceptable in a "burst release" format would be ideal, but is limited for payloads that require sustained release.

The discussed MP formulation employed as a cell-delivery vehicle may prove more advantageous compared to other biomaterial constructs. A highly porous delivery vehicle offers improvements with regards to the total accessible surface area available for cell loading and material stability compared to solely topical loading onto similar biopolymer constructs, such as contiguous collagen-based gels, for example (Park et al. 2007, Lu et al. 2015). Similarly, cellular loading can be improved using the proposed construct through intrinsic affinities found between cells and the keratin substrate. As previously mentioned, keratin exhibits a number of properties that support cellular interactions. The surface characterization of the synthesized MPs, while yielding no indication of a difference between products based on solvents or crosslinkers, does show surfaces that could be amenable to adhesion of cells. This natural affinity may neutralize the need for added processing steps that require surface functionalization or cell encapsulation which can hinder mass transport, namely nutrient and waste transport to and away from cells respectively. Both of these can become a detriment to cell motility, functionality and survival as commonly seen in chitosan and alginate based gels (Nicodemus and Bryant 2008, Tan and Takeuchi 2007).

2.6. Conclusions

Cell therapy can be a viable approach toward tissue regeneration. Several studies have demonstrated that a primary challenge is cell retention at the site of injury. Biomaterials may aid in cell retention, integration and tissue formation, and injectable hydrogels are well-suited for this

application as they can be delivered non-invasively and conform to defect sites. Many forms of keratin biomaterials that form hydrogels are not compatible with cell incorporation. In order to circumvent this, we have proposed the approach of first creating a crosslinked keratin-based MP, with or without an optional drug or biologic payload, and then attaching cells to the outside of the particle. Toward that goal, we demonstrated the synthesis of KOS MP using a water-in-oil emulsion system. The resulting MP demonstrate tissue-like elasticity when hydrated and agglomerate to form hydrogel-like constructs. Interestingly, the microarchitecture is that of a fibrous MP with high surface roughness and porosity. While this may make the KOS MP less amenable to sustained drug or biomolecule delivery in the absence of a molecular-level binding interaction, this microarchitecture may be conducive to attaching a cellular payload to the surface.

Chapter 3

The Investigation of Drug Loading and Release Potential in a Novel Keratin-based Microparticle

Marc Thompson[1], Aaron Guiffre[2], Claire McClenny[3], Dr. Mark Van Dyke[1]

1. Department of Biomedical Engineering and Mechanics, Virginia Tech, Blacksburg, VA
2. Electrical and Computer Engineering, Virginia Tech, Blacksburg, VA
3. Biological Systems Engineering, Virginia Tech, Blacksburg, VA

Abstract: Keratin-based biomaterials present an attractive opportunity in the field of wound healing and tissue regeneration, not only for the wide array of positive chemical and physical properties they display but also for their straightforward and effective loading potential. This study employs well-established water-in-oil emulsions, as well as specific acid-precipitation methods to synthesize drug-loaded keratin microparticles. The loading characteristics, release kinetics, and feasibility of use for these two different synthesis procedures was subsequently investigated. First, a fluorescein isothiocyanate-bound bovine serum albumin (FITC-BSA) protein-based payload was tested, and later, a broad spectrum antibiotic, ciprofloxacin, was tested on bacterial cultures to demonstrate their reduction and therefore the potential for antibacterial applications. The model compound, represented by albumin, showed a burst release profile in the emulsion-generated system but the two microparticle synthesis methods demonstrated contrasting release kinetics in terms of both FITC-BSA release, ciprofloxacin payload release as well as keratin biomaterial degradation. Data showed an ability to inhibit bacterial growth in the emulsion-generated system, and thereby demonstrated the potential for a keratin-based microparticle construct to be used in wound healing applications. These two microparticle systems may therefore cover a broad variety of degradation and release kinetics, depending on the size and chemistry of the payloads.

3.1. Introduction

Prior research demonstrates that keratin and keratin derivatives exhibit several mechanical, chemical and biological properties that support their use as delivery vehicles of chemical factors in tissue regeneration applications (Hill, Brantley, and Van Dyke 2010, de Guzman et al. 2011, Van Dyke 2009). Keratin has been specifically selected in these investigations, not only for its mechanical/chemical characteristics and biocompatibility, but for its ability to bind certain classes of compounds and provide sustained release (Saul, Ellenburg, de Guzman, and Van Dyke 2011, Cilurzo et al. 2013). The binding interactions in these systems is often at the molecular level (e.g. acid-base pairing), resulting in release mechanisms that are closely tied to the degradation of the keratin matrix (Roy et al. 2016, Saul, Ellenburg, de Guzman, and Van Dyke 2011). This is an important and unique aspect as mammals, including humans, do not make keratinases – enzymes that specifically target the destruction of keratin (Brandelli 2008). Therefore, there is no targeted turnover mechanism for tissues or extracellular matrix (ECM) made primarily from trichocytic (so called "hard") keratin. As a result, keratin-based biomaterials may be better able to withstand harsh proteolytic environments such as inflamed, damaged tissue.

Incorporation of drug or biomolecular payloads into biomaterial constructs has been a common approach in regenerative medicine (Dang et al. 2016, Martino et al. 2014, Saul, Ellenburg, de Guzman, and Van Dyke 2011). The need to control local flora has long been recognized as an imperative for wound healing. In some cases, specifically in less developed parts of the world, patient's risk to develop a nosocomial infection is as high as outside of the hospital. Delivering antibiotics in large or systemic doses carries with it the possibility of insufficient delivery of the antibiotic to the wound site, or an eventual resistance to antibiotic treatment (Saul, Ellenburg, de Guzman, and Van Dyke 2011, Park, Kim, and Suh 2004, Roy et al. 2016, Du, El-Sherbiny, and

Smyth 2014). Thus, several technologies have been developed for the sustained release of antibiotic drugs from biomaterial-based topical dressings (Elsner, Berdicevsky, and Zilberman 2011). Triggered, local release has been less common (Yan et al. 1994b).

The chemistry and evolutionary biology of keratins provide a unique opportunity for a keratin biomaterial-based drug delivery system for control of microbial populations. Mammals never developed a compliment of keratinases because there was no need for a turnover mechanism directed at hard keratin-containing tissues. Horns, hair, feathers and hooves did not rely on remodeling; they were sloughed or worn off and replaced. However, microbes, particularly bacteria and fungi, developed a compliment of keratinases such that they could make use of the keratin-containing structures of mammals as a food source. As a consequence, the presence of keratinases at a wound site is a hallmark of microbial contamination in mammalian wound healing, and hence can be used as the basis of a triggered, local, keratin biomaterial-based drug delivery system.

Emulsions are disperse systems in which two or more largely insoluble liquid phases are mixed, a common example is the immiscibility of water in oil (Fingas 1995). In this study the water-soluble keratin solution is less abundant and known as the dispersed phase. The dispersed phase is mixed into a liquid oil continuous phase of greater volume. With sufficient agitation shear forces from a stirring apparatus and potentially fluid forces of the continuous phase (Adams et al. 2007) disperse the KOS solution into droplets that subsequently rely on a combination of keratin and chemical crosslinking, forming stable microparticles (MPs).

This process produces particles on the micron scale that are advantageous due to their volume (greater than nanoparticles) increasing the drug payload capacity, size scale an order of magnitude larger than cells for efficient loading, while still being small enough to deliver by non-invasive

injectable means to reduce the need for invasive surgeries that have been shown to be a detriment to wound recovery (Prow et al. 2011, Boutonnet et al. 1982).

This study investigates the synthesis of keratin-based MPs developed using two documented methods, the water-in-oil emulsion and acid-precipitation (Hsu, Chueh, and Wang 1999, van de Weert, Hennink, and Jiskoot 2000). Subsequent tests investigate the loading and unloading of the water-soluble fluoroquinolone antibiotic ciprofloxacin ("cipro"), with the expectation that the water-soluble drug is ionically bound to the keratin such that its release is tied to the degradation of the keratin, as has been shown previously (Saul, Ellenburg, de Guzman, and Van Dyke 2011). We hypothesize that bacterial metabolism, which produces proteolytic enzymes, will trigger the release of cipro, thereby creating a novel, self-extinguishing delivery system, particularly suited for contaminated skin wounds. Oxidized keratin, also known as keratose (KOS), was used in this investigation.

3.2. Materials and Methods

3.2.1 Water-in-oil Emulsion Microparticle Synthesis

MP synthesis via the water-in-oil emulsion process was adapted based on previous methodologies (Yan et al. 1994b, Yin Hsu, Chueh, and Jiin Wang 1999). Lyophilized KOS proteins were weighed out and dissolved in PBS to a working concentration of 60 mg/mL. The chemical crosslinker butanediol diglycidyl ether (BDDE) was added at 48 wt% (previous raman spectroscopy determined the partitioning of crosslinkers between the water and oil phases occurred in a 1:3 ratio of water and oil, therefore final crosslinking concentrations were approximately 12 wt%) which was vortexed and centrifuged at 1000 rpm for 5 min to remove air bubbles. Samples were allowed

to equilibrate overnight. The KOS solution was added to light mineral oil at a 1:20 volume ratio and stirred using a Caframo tabletop mixer at 2000 rpm for 24 hours. The light mineral oil was aspirated off, removing as few MPs as possible and the resulting particles were washed with chilled hexanes at approximately -25 ^{o}C using a lab bench shaker set to a medium speed setting for 5 min. Residual hexane was aspirated and this step was repeated 2 more times to further remove any oil. MPs were stored at -25 ^{o}C. Finally, any residual hexane was aspirated from the product and MPs were lyophilized to form a stable product for subsequent analysis.

3.2.2. Acid-Precipitation Microparticle Synthesis

Alternatively to the water-in-oil method of synthesis, acid-precipitation synthesis procedures were employed to produce MPs with different characteristics. 60 mg/ml of KOS was placed in PBS, stirred and allowed to dissolve for 24 hrs. 48% w/w of BDDE relative to the KOS mass was added and the solution stirred for an additional 12 hrs. For formation of acid-precipitated MP, the solution was stirred at 400 rpm using a magnetic stir bar while hydrochloric acid (HCl) was added dropwise until a fine dispersion of KOS particulate was obtained. The dispersion was washed with hexane, frozen at -25^{o}C for 24 hrs and lyophilized.

Similar to the loaded particles synthesized via water-in-oil emulsion, solutions comprised of the same materials (FITC-BSA and Ciprofloxacin), at the same concentrations, were added to the KOS solutions prior to BDDE crosslinking and MP formed by acid precipitation as described above. SEM images were taken of particles synthesized via both methods to determine initial size, shape and structure of the products.

3.2.3. FITC-BSA Loading Model

As a preliminary test of hydrophilic drug loading, a 4 mg/mL solution of FITC-BSA (5 mL) was dissolved in PBS and added to the 60 mg/mL KOS solution and BDDE crosslinked for 12 hrs. The solution was subsequently stirred for at least 24 hrs at 2000 rpm, hexane washed, frozen and lyophilized as previously described. Loaded particles were imaged using scanning electron microscopy (SEM) to ensure there were no visible structural differences between samples that may alter release outcomes.

For acid-precipitation methods a FITC-BSA solution of the same concentration and volume was added to a similar KOS solution prior to crosslinking and resuming the initial acid-precipitation methods.

3.2.4. Antibiotic Loading Model

For ciprofloxacin loaded MPs, 5 mL of a 5 mg/mL ciprofloxacin solution dissolved in sterile DI water was added to the aforementioned 60 mg/mL KOS solution, stirred, and allowed to homogenize overnight. BDDE was then added to again create a 48% w/w solution that was allowed to crosslink for 12 hrs. The solution was subsequently stirred for at least 24 hrs at 2000 rpm, hexane washed, frozen and lyophilized.

For acid-precipitation methods a cipro solution of the same concentration and volume was added to a similar KOS solution prior to crosslinking and resuming the initial acid-precipitation methods.

3.2.5. Bacterial Culture

Gram negative E. coli and gram positive S. aureus were cultured atop agar plates consisting of 1% Bacto-Tryptone, 0.5% Yeast extract, 85 mM NaCl, 1.5% Bacto Agar and cultured at 37^{o}C. Separate inoculant cultures were generated by culturing bacteria from these plates in a similar

media (without Bacto Agar) and with shaking at 500 rpm for 24 hours at 37ºC to a working concentration of ~1X10^7 CFU/mL.

3.2.6. FITC-BSA Release Kinetics

60 mg of both FITC-BSA-loaded as well as non-loaded particles were suspended in separate solutions of either 0.5 U/mL type I collagenase, 0.5 U/mL elastase or a control of PBS to investigate the degradation rate and release of KOS and the molecular payload under conditions of enzyme mediated degradation (n=3). KOS release was quantified by measuring the concentration of KOS using a bicinchonininc acid (BCA) assay (Figure 3.3.), and the concentration of the FITC was measured via plate reader at a fluorescent excitation and emission wavelengths of 490 nm and 525 nm, respectively. Concentrations were sampled for each of the first 6 hours, at 12, 24 and 48 hours.

3.2.7. Bacteria-Mediated KOS MP Degradation

The unique ability of bacteria to degrade keratin proteins (Brandelli 2008), which is atypical of enzymes produced within the human body, was tested to qualify whether, in the presence of bacterial infections, payload release may potentially be triggered during the incidence of heavily infected wounds. 5 mg of dried, non-loaded KOS MPs were saturated with 1 mL of protein rich lysogeny (LB) broth comprised of inoculum generated from ~1X10^7 CFU/mL that was centrifuged at 5000 rcf for 5 min to remove bacteria. 100 µL of the supernatant solution was sampled and replaced with fresh LB broth at varying time points and the concentration of KOS was quantified using the BCA assay. Treatment (Bact + MP) was background subtracted from the protein concentration generated from a bacterial inoculation and compared to particles degraded by base LB broth having no interaction with bacteria (Control).

3.2.8. Ciprofloxacin Release Kinetics

Using similar methods to the FITC-BSA release kinetics experiments, 60 mg of both ciprofloxacin-loaded and non-loaded particles were suspended in separate solutions of either 0.5 U/mL type I collagenase, 0.5 U/mL elastase or a control of PBS to measure the degradation rate of KOS and subsequent release of ciprofloxacin. Concentrations of KOS were determined as previously described with ciprofloxacin being quantified at excitation and emission wavelengths of 340 and 450 respectively for the first 6 hours, at 12, 24 and 48 hours. The cumulative percent of ciprofloxacin released was determined as a measure of the ciprofloxacin loaded into the initial KOS solution.

3.2.9. Bacterial Zone of Inhibition (ZOI) Assay

The zone of inhibition assay was performed to validate a ciprofloxacin loaded MPs ability to deliver the broad spectrum antibiotic to both gram negative and gram positive E. coli and S. aureus, respectively, not only to inhibit growth but to reduce colony formation. Varying masses of ciprofloxacin-loaded MPs were pelleted using a tablet press and placed atop a bacterial lawn formed by adding inoculum (~ $1X10^7$ CFU/mL) to a T100 petri dish and allowing it to incubate for 24 hrs at 37^{o}C. Ciprofloxacin-loaded MP pellets as well as controls of non-loaded pellets were hydrated with 1 mL of sterile DI water and placed atop the bacteria to incubate overnight at 37^{o}C. Zones of inhibition were calculated by measuring the area of the initial bacterial monolayer and the area of monolayer reduction after 24 hrs of incubation.

3.2.10. Statistical Analysis

To compare experimental groups, analysis of variance (ANOVA) and/or linear regression analysis with a Tukey's post hoc test was performed in all experiments. To determine significant variances,

for all tests, a p-value <0.05 was considered statistically significant. Sample sizes were determined using a power analysis where a power (1-β) of 0.9 and an alpha (α) of 0.05 was employed. All statistical analyses were performed using JMP Pro 11.

3.3. Results

3.3.1. Acid-Precipitation Microparticle Synthesis

To determine if MP synthesized using an alternative method produced similar release kinetics, a process for producing MP using acid precipitation was developed. Stable particles were formed during the acid-precipitation process (Figure 3.1), which appeared to have no common shape or size, and were quite irregular. These MP also showed rougher surface structure, and a less pronounced fibrous microarchitecture, compared to emulsion-generated MP.

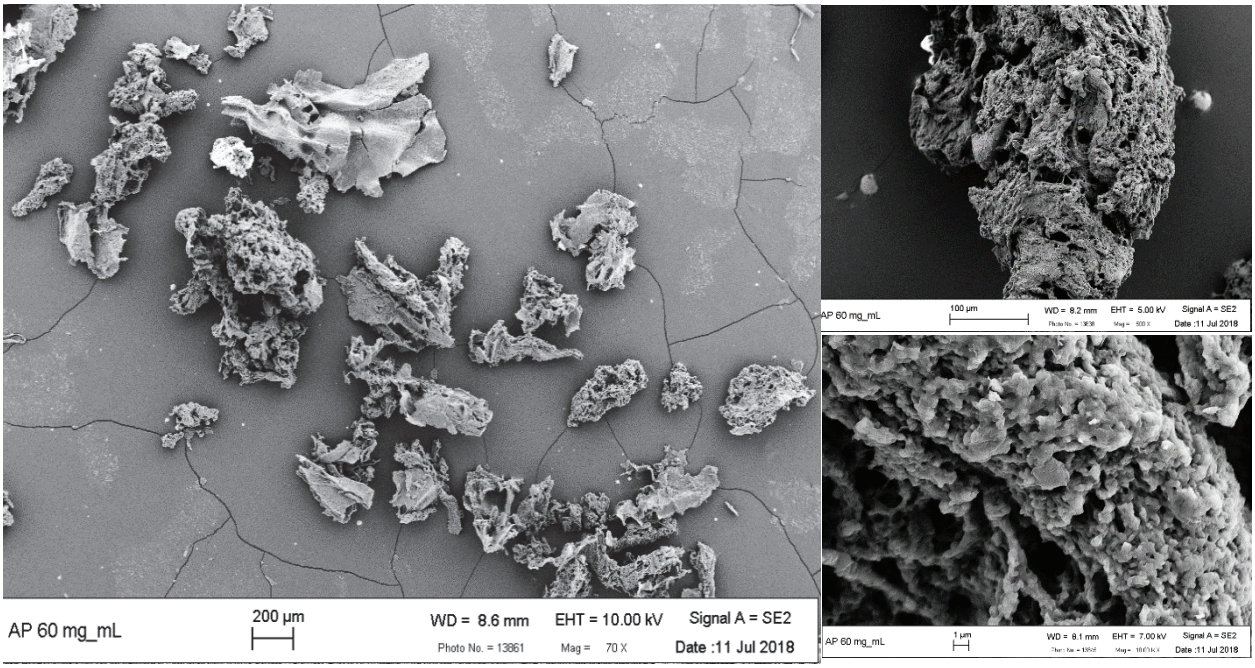

Figure 3.1. SEM Images of Acid-precipitated Microparticles. These MP share no common shape or size, which may be due to the method of synthesis. Particles exhibit what appear to be an open surface with increased roughness compared to emulsion-generated MP.

3.3.2. Particle Porosity and Pore Connectivity

The internal structure of the oil-in-water generated MP (A) can be described as that of a coarsely fibrous particle with high porosity, while the architecture of the acid-precipitated MP (B) is less coarse with relatively less porosity (Figure 3.2). Quantitative results indicate a protein to pore fraction of 0.58 ±0.035 suggesting that ~40% of a given particle's volume is occupied by empty space (pores) for emulsion synthesized particles. The pore connectivity of the structure was relatively high at 0.53 ±0.17 (Figure 3.2). Extrapolating this value, the calculated average particle diameter of approximately 366 μm proposed from earlier tests (data not shown) and assuming a spherical nature suggests a number of pores ranging in the low thousands (~1,600). The volume fraction of the acid-precipitated particles, 0.756 ±0.053, was comparably larger than the emulsion method with the average particle consisting of ~25% pore space. The quantitative value of the connectivity was calculated to be similarly smaller than that of the emulsion particles (0.24 ±0.09). Extrapolating the average size of these particles which was ~200 μm based on previous analyses (data not shown), it is reasonable to expect differing release kinetics to somewhat be a factor of particle internal structure.

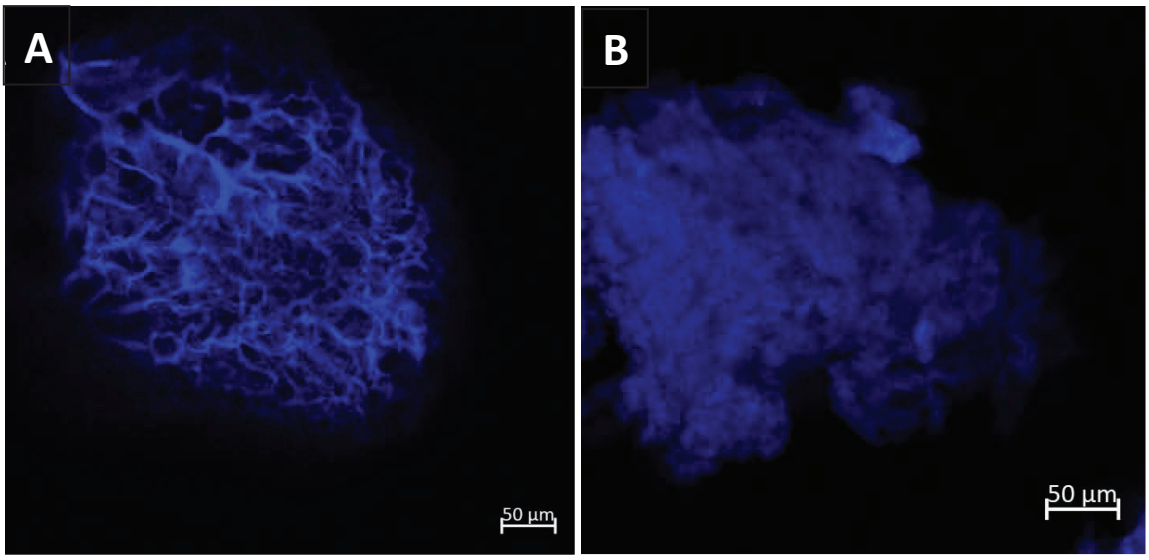

	Volume Fraction	Connectivity
Water-in-oil Emulsion	0.588 ±0.035	0.53 ±0.17
Acid Precipitation	0.756 ±0.053	0.24 ±0.09

Figure 3.2. Comparison of Particle Internal Structures. (A) Fluorescence microscopy image of water-in-oil emulsion synthesized MPs stained with DAPI show a relatively low solid volume fraction of 0.588 (~40% of the given volume is void space) and what appears to be high pore interconnectivity of 0.53 ±0.17, which suggests approximately 50% of a given particle contains interconnecting pores. (B) Acid precipitated particles display a higher solid volume fraction with approximately 25% void space and display a lower connectivity (0.24 ±0.09) as a result.

3.2.3. FITC-BSA Release Kinetics

SEM images indicate no structural differences between non-loaded or loaded particles synthesized via either method, prompting further degradation analyses. The FITC-BSA concentrations eluted into solution were quantified at each of the noted time points (Figure 3.3). Results suggest what is commonly known as a burst release profile in both methods, with a significant concentration of FITC-BSA released within the first few hours of hydration and a plateau in release after the initial

burst. Concentrations then stabilize, which may indicate that all or most of of the loaded FITC-BSA had been released. Noticeably less release was observed in acid precipitated particles as less than 10% or the calculated payload was released over the 96 hour period. This particular level of release is attributed to the density of the material and the amount of access for hydrolytic degradation, which is supported by the similarly decreased KOS release seen in the acid-precipitated particles.

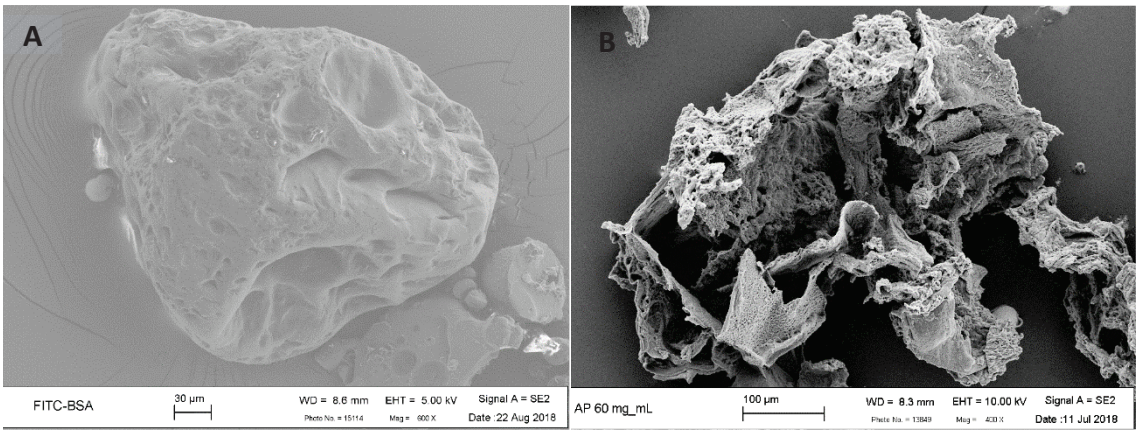

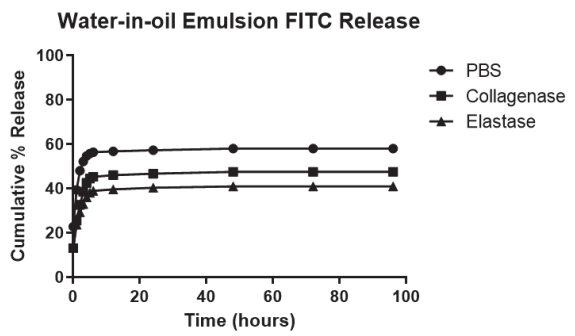

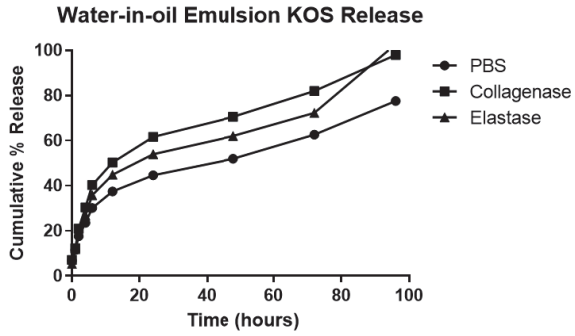

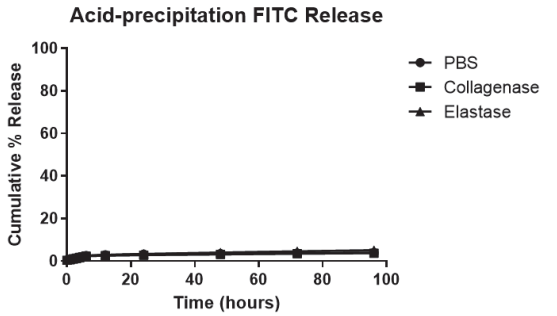

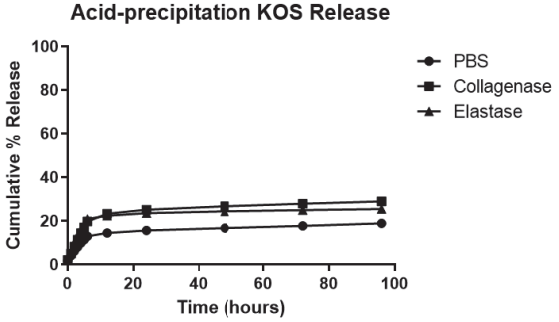

Figure 3.3. Small-molecule and KOS Release Kinetics. SEM images of FITC-BSA loaded particles synthesiszed via water-in-oil emulsion (A) and acid precipitation (B) display no noticable structural differences between un-loaded and loaded particles. Plate reader analysis of FITC-BSA concentration up to 48 hours. Results show FITC-BSA was in fact loaded into particles but exhibits a burst-release profile, releasing most of the available payload within the first 6 hours of hydration. No clear differences in the kinetics of release can be distinguished between control (PBS) samples or enzyme-mediated degradation samples. Cumulative measures of release show that between 40-60% of FITC-BSA is released in water-in-oil emulsion synthesized particles whereas 2-4% percent is released in acid-precipitation synthesized particles. These values are respective of the loaded FITC-BSA relative to the initial load concentrations released within the first 96 hours of hydration.

3.3.4. Bacteria Mediated KOS MP Degradation

Results indicate that secreted protein-rich LB broth generated from bacterial cultures does significantly increase the degradation of KOS MPs for close to 48 hours (Figure 3.4). Some residual bacterial likely remained in the broth, which, over the 48 hour period, led to further growth and the subsequent increase in protein concentration seen in the control. These results suggest that there may be potential for delivery of antibiotics to an infected wound that can be triggered by the presence of active bacteria.

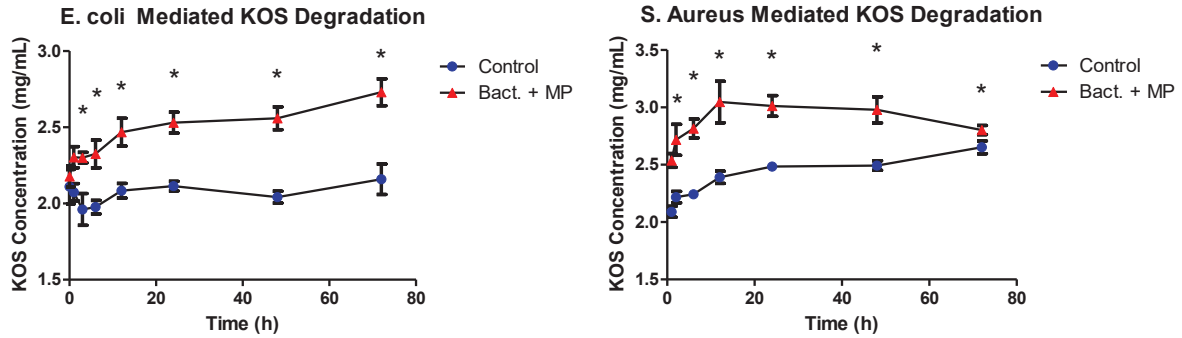

Figure 3.4. Bacteria-mediated KOS Degradation. Degradation of KOS MPs via secreted products of active bacteria E. coli and S. aureus. MPs saturated with LB broth from bacterial cultures experience greater degradation than controls of broth without inoculant bacteria. Asterisks denote statistically significant differences ($p<0.05$).

3.3.5. Ciprofloxacin Release Kinetics

The extent of KOS degradation and release of ciprofloxacin occur again in a burst pattern, with concentrations plateauing around the first 24 hours. No statistically conclusive patterns could be determined between the particular solvent used. Based on the cumulative percentages of material released (Figure 3.5), less than 5% of the ciprofloxacin is released compared to 40% of KOS after 4 days in water-in-oil emulsion synthesized particles. Conversely, cipro shows greater release in acid-precipitated particles with little KOS release over the same period of time. This, along with similar release patterns of KOS under FITC-BSA loading suggests that the acid-precipitation method may loosen the quaternanry sodium salt that comprises ciprofloxacin in its binding to keratin. Prior studies suggest that alterations made to solutions can affect the binding and/or retention of cipro. This provides a better understanding of how to efficiently load and release an antibiotic payload under desireable conditions and rates (Wischke and Borchert 2006, Buck et al. 2018).

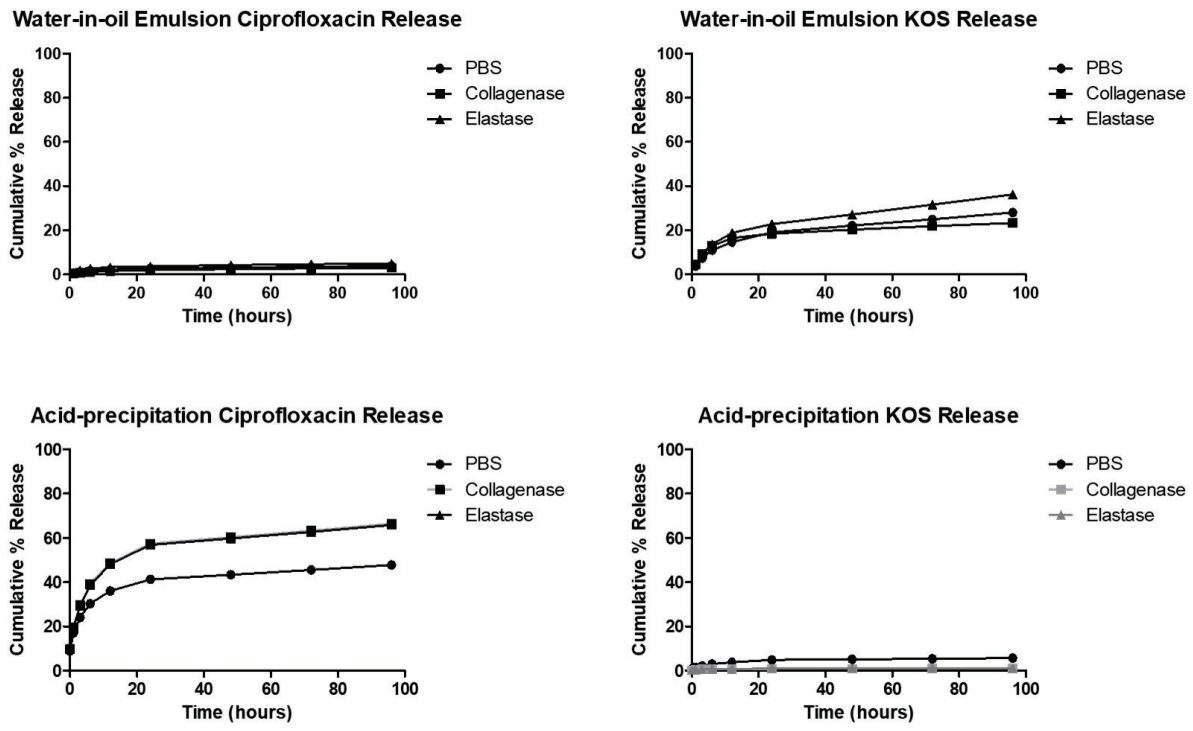

Figure 3.5. Ciprofloxacin Release Kinetics. (Top Left) Successful detection of ciprofloxacin in control and enzyme solutions suggest that ciprofloxacin is effectively loaded into water-in-oil emulsion particles and experiences burst release within the first 12 hours of hydration, which becomes more gradual thereafter. (Top Right) Cumulative percent release of KOS. The release profiles of ciprofloxacin and KOS are similar in overall shape, suggesting reproducible and therefore predictable degradation and release profiles. Ciprofloxacin release profile from acid-precipitated MP. Ciprofloxacin concentrations in solution are increased and prolonged compared to water-in-oil emulsion particles, even in PBS saturated samples. (Bottom Left) Greater cumulative ciprofloxacin percent release rates are seen in these MP in the presence of enzyme. (Bottom Right) The cumulative percent of KOS released from these particles is highest for PBS, despite the slower relative ciprofloxacin release.

3.3.6. Zone of Inhibition Assay

Ciproflaxacin-loaded MPs were visibly able to reduce the bacterial colony presence after 24 hours of incubation in water-in-oil emulsion synthesized particles (Figure 3.6). For reasons yet to be determined, release of ciprofloxacin from acid precipitated particles was non-existent or not substantial to induce significant bacterial reduction on cultured monolayers (data not shown). It is theorized that insufficient saturation may have contributed to a lack of release and ultimately less

than necessary concentrations. Bacterial reduction does occur in a concentration-dependent manner for emulsion synthesized particles, beginning at 20 mg pellet masses where introducing more particles, and consequently more ciprofloxacin, induced marked reductions in the areas coated with E. coli as well as S. aureus. S. aureus appears to be more resistant to ciprofloxacin under the same conditions. There were minor reductions to bacterial colonies in control groups, although this was attributed to physical displacement due to pipetting the bacterial monolayer.

Hydration of acid precipitated particles was performed under the same methods, yielding significantly different results. Under the same conditions, acid-precipitated particles yielded negligible bacterial reduction using all pellet masses.

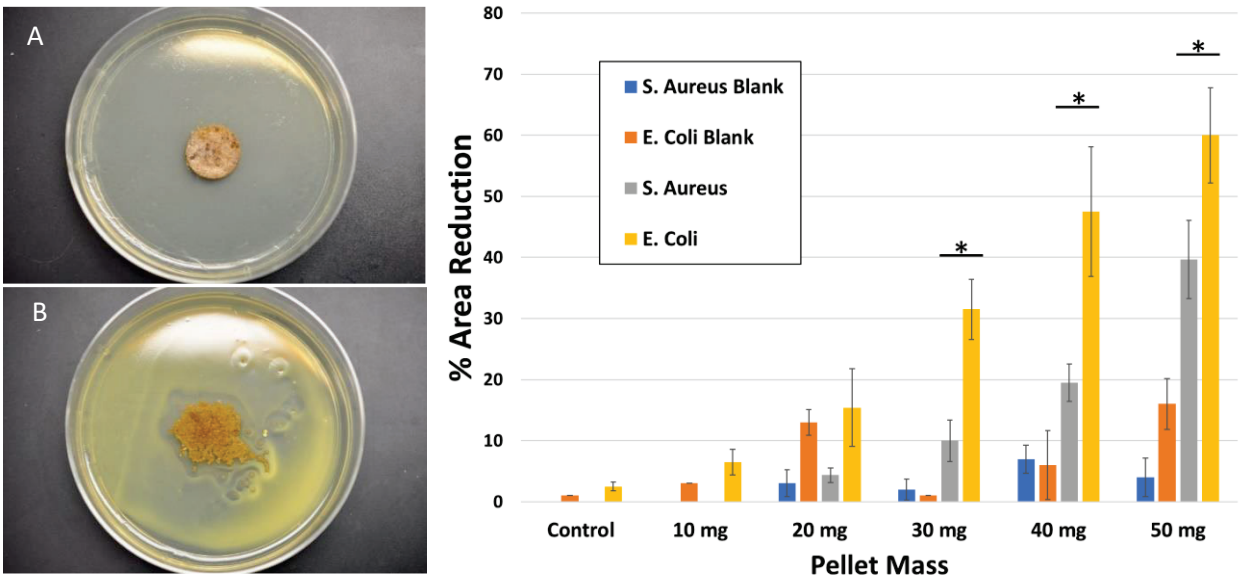

Figure 3.6. Ciprofloxacin-loaded Microparticle Bacterial Reduction. Bacterial zone of inhibition assay before (A) and after (B) 24 hrs incubation at 37°C with hydrated ciprofloaxcin loaded MPs. Results show bacterial prescence is inhibited upon ciprofloxacin release which occurs in a dose-dependent manner beginning at a pellet mass of 20 mg. Asterisks denote statistically different treatment effects compared to respective blank pellet masses ($p<0.05$).

3.4. Discussion

The aforementioned synthesis procedures for water-in-oil emulsion and acid-precipitation methods were successful in generating KOS MPs, although size, size distribution, and microarchitecture varied, not only between the two methods, but also within each method. Morphology within the MP was fibrous, suggesting that the propensity for keratin toward self-assembly was not overcome by interfacial forces of the emulsion and/or the shearing force of the vigorous mixing method employed. This created a unique microarchitecture, with loosely packed fibers in the emulsion-generated particles and more densely packed in those generated by acid-precipitation, which exerted a measurable effect on payload delivery. In the case of FITC-BSA, the high porosity and interconnectivity lead to rapid release, likely facilitated by the lack of an apparent BSA-keratin binding mechanism. Although the binding of lipids, ions, certain drugs and other proteins to serum albumin is well-known (Kraghhansen 1981, Spector 1975, Anand and Mukherjee 2013), the binding of keratin to albumin has not been studied. Absent a specific binding mechanism, the BSA, which as a molecular weight similar to that of a keratin monomer (i.e. 66 K Daltons), easily diffused out of the MP's molecular network. Indeed, FITC-BSA release was nearly identical to KOS release (i.e. 60% after 48 hours), which was only studied in the emulsion-generated MP system.

The incorporation of ciprofloxacin as a payload produced interesting and contrasting release kinetics in the two different MP systems. Incorporation into emulsion-generated MPs showed relatively slow release (i.e. approximately 4% over 4 days; Figure 3.5) of ciprofloxacin, despite the relatively large release of KOS (ca. 30%) over the same time period. This data suggests a system in which ciprofloxacin is most likely bound to the most stable portion of the KOS network structure, as these cipro-KOS interactions remain intact despite enzymatic-mediated degradation

of the network. Acid-precipitated MPs appeared to show the opposite behavior (Figure 3.5). The KOS network seemed almost impervious to enzyme-mediated degradation with only a few percent of cumulative release after 24 hours. Surprisingly, ciprofloxacin release was extensive at approximately 40% in the same time period. This suggests that the acid precipitation method may interfere with molecular interactions that would otherwise tightly bind the ciprofloxacin to the KOS. This binding mechanism was suggested in our earlier work (Saul, Ellenburg, de Guzman, and Van Dyke 2011), albeit for a hydrogel system. Obviously, the generation of MPs via an acid precipitation method forms a protein network that is highly stable toward enzyme-mediated degradation, compared to the equilibrium system represented by the emulsion-generated method, but may not offer a sustained release mechanism for certain ionic compounds, depending on their acid dissociation constant. Further experimentation may look into the effects of synthesis components, such as crosslinkers, on their respective payloads as well.

While there are numerous fibrous proteins, fibrous protein MP systems appear to be rare, with only one based on egg white protein (i.e. avian albumin) having been published (Chang et al. 2016). Many MP systems, particularly those that are protein-based, take the form of aggregated structures, formed via forces created at the oil-water interface. The fact that KOS retains its fibrous network assembly characteristics in the presence of these forces, and the apparent contrasting enzyme stability of the two systems studied here, provide a unique approach for creating KOS MP with tailored degradation and payload release characteristics. Moreover, KOS degradation appears to increase under the influence of the secreted proteome of E. coli and S. aureus (Figure 3.6), suggesting the potential for triggered release in the presence of a bacterial infection. Bacteria-triggered release of antibiotics is not a new concept, as similar systems have been envisioned for synthetic biomaterials that contain lipase-sensitive linkages, for example (Komnatnyy et al. 2014).

Conventional core-shell systems have also been developed and shown to be stable when exposed to human wound exudate, but degrade upon exposure to bacterial protease (Craig et al. 2016). Payloads using either approach to KOS MP synthesis appear to be sufficient as suggested by the bacterial zone of inhibition assay (Figure 3.6), but this system cannot be considered strictly "on" or "off" because these data show some ciprofloxacin release even in the presence of PBS. Further research may also investigate the effects of crosslinkers on the respective payloads as this may similarly effect the ability to load and eventually release a payload and prior studies did little to determine the effects of varying crosslinker concentrations (Saul, Ellenburg, de Guzman, and Van Dyke 2011, Roy et al. 2015a).

Previous application of ciprofloxacin-loaded keratin hydrogels includes two published burn studies in swine (Roy et al. 2016, Roy et al. 2015a). Oxidized keratin (i.e. KOS) was also used in these studies but was in a less pure form than the current study as it had 5 weight percent of so-called "gamma-keratose" added back into the hydrogel; it was also not crosslinked. As a consequence, approximately 50% of the payload was delivered in four days, which was sufficient to significantly reduce, but not eliminate, P. aeruginosa in the first study. However, re-epithelialization was reduced in the ciprofloxacin groups at early time points, perhaps due to a combination of the known cytotoxicity of ciprofloxacin and burst release in this hydrogel system (Tsai, Chen, and Hu 2010, Gurbay et al. 2002). In the second study, the ciprofloxacin-loaded KOS hydrogel was able to reduce, but not eliminate, both P. aeruginosa and, to a lesser extent, methicillin-resistant S. aureus (MRSA) in burns; re-epithelialization was not reported at early time points. These reports demonstrate the feasibility of topical delivery of an antibiotic using keratin biomaterial but underscore the necessity of attaining an inhibitory dose that avoids cytotoxicity of

the drug, which may be attainable through the use of different keratin biomaterials (i.e. higher purity), crosslinking chemistry, formulation processing techniques, and/or combinations thereof.

3.5. Conclusions

The intrinsic properties of keratin and keratin derivatives make them an attractive choice for tissue engineering. An ability to add various drug payloads and deliver them in efficacious amounts over time is a desirable characteristic in many systems. Leveraging molecular interactions for payload binding can be advantageous when sustained release, and/or avoidance of burst release, is desired. In this study, a non-interacting model compound, represented by BSA, showed burst release from a fibrous, highly porous and interconnected, oxidized keratin MP. Conversely, when strong acid-base pairing was facilitated, burst release was reduced and sustained delivery achieved. Different methods of production not only resulted in different microarchitecture of the particles, but completely changed the KOS degradation and drug release kinetics. These results suggest that keratin-based MP systems can be tuned within a range of delivery characteristics.

Chapter 4

A Novel Keratin MP for Stromal Cell Delivery

Marc Thompson[1], Alex Gibson[2], Claire McClenny[2], Dr. Mark Van Dyke[1]

1. Department of Biomedical Engineering and Mechanics, Virginia Tech, Blacksburg, VA
2. Department of Biological Systems Engineering, Virginia Tech, Blacksburg VA

Abstract: Keratin-based biomaterials present an attractive opportunity in the field of wound healing and tissue regeneration, not only for the chemical and physical properties they display but also for their straightforward and effective loading potential. This study employs well-established water-in-oil emulsion procedures as well as a suspension culture method to load keratin-based MPs with bone marrow-derived mesenchymal stromal cells. Fabricated MPs were characterized for size, porosity and surface structure, and further analyzed to determine whether or not they exhibit favorable hydrogel properties. The suspension culture technique was validated based on the ability for loaded cells to maintain their viability and express actin and vinculin proteins, which are key factors for cell adhesion and growth. Maintenance of cell plasticity was also a determinant for success. As a comparative model, cells were taken through similar procedures with a collagen-coated MP as a control.

Key Terms: Keratin, MP, Stromal Cell, Tissue Engineering

4.1. Introduction

Current tissue engineering approaches rely on the use of naturally- and synthetically-derived materials as platforms for regenerating tissue (Kanbe et al. 2007, Endres et al. 2010). Incomplete or insufficient regrowth of the native tissue in traumatic scenarios, a lack of autologous tissue with

which to replace the damaged tissue, or a lack of endogenous cells and factors to supply the necessary stimuli that produce further regeneration are documented as impeding tissue regeneration (Naderi, Matin, and Bahrami 2011, Endres et al. 2010). Naturally derived biomaterials in particular display several advantages including inherent biocompatibility, comparable mechanical properties to native tissue and biological cues that support cellular adhesion and growth (Kretlow and Mikos 2007, Wang et al. 2015).

Often, natural tissue regeneration relies on the presence of undifferentiated stromal cells with a high proliferative potential to replace damaged and terminally differentiated cells (Hunt and Grover 2010, Man et al. 2012, Uludag, De Vos, and Tresco 2000). Characterized by the ability to self-renew and differentiate into a variety of specialized cell types, many cellular therapies for tissue regeneration employ adult stromal cells, isolated from the mesenchyme (MSCs). MSCs are culture-adherent, multipotent progenitor cells capable of differentiating into muscle, bone, cartilage, fat, tendon and nerve (Gao et al. 2014, Xu et al. 2015). Isolated from various sources including bone marrow, adipose tissue, muscle tissue, amniotic fluid, human placenta, periosteum, cord blood and even peripheral blood (Niemeyer et al. 2007, Cowan et al. 2004, Prigozhina et al. 2008), the efficacy and survival of MSCs have proven to be a contributor to tissue regeneration, but this also depends heavily on the method of delivery (Nicodemus and Bryant 2008, Oliveira and Mano 2011).

Microparticles (MPs), 1 micrometer to 1000 micrometers (μm) in diameter, have been touted as a multimodal delivery vehicle, capable of serving as a building block for 3D constructs to fill tissue voids while simultaneously providing delivery of soluble factors and cells (Qazi et al. 2015, Moulin, Mayrand, Messier, Martinez, Lopez-Vallé, et al. 2010, Huang and Fu 2010). The application of MPs provides a larger surface area for exterior cell loading while avoiding concerns

about clearance, commonly viewed as a potential negative side effect of similarly touted nanoparticles (Behrens et al. 2014). The benefit of a microscale protein construct lies in the interplay between the individual products size, capable of non-invasive injectable delivery, and the physical agglomeration of gel particles wherein once fully hydrated particles form a nearly contiguous hydrogel construct of varying sizes and shapes (Oliveira and Mano 2011, Woo, Park, and Lee 2014).

Prior research suggests keratin and keratin derivatives from human hair exhibit several mechanical and biological properties that support their use as scaffolds for cells that can incorporate various payloads including cells and growth factors (Ledford et al. 2017, Rouse and Van Dyke 2010, Hill, Brantley, and Van Dyke 2010, Saul, Ellenburg, de Guzman, and Dyke 2011, Kowalczewski et al. 2014, Han et al. 2015, Roy et al. 2015b, Ham et al. 2015, Baker et al. 2017, Cohen et al. 2018). Upon hydration, keratin hydrogels mechanically perform as a flexible viscoelastic material. However, most reports of keratin biomaterials in tissue engineering utilize cell-free constructs, despite keratin's intrinsic biocompatibility and apparent support of cell health and function (Konop et al. 2018, Mori and Hara 2018). This may be a consequence of the formation of keratin hydrogels that are incompatible with cells, particularly in the kerateine (KTN) system where gelation is best driven by protein self-assembly at basic pH (Hill, Brantley, and Van Dyke 2010). The keratose (KOS) hydrogel system is more conducive to the inclusion of cells as these gels can form at physiologic pH, but the resulting constructs can be fragile and degrade rapidly. Crosslinking can be used to mitigate this, but some chemistries may compromise cell viability (Steinert et al. 1993, Tanabe, Okitsu, and Yamauchi 2004a).

This study employs a KOS MP synthesized via the documented water-in-oil emulsion synthesis procedure (Yan et al. 1994a, Viswanathan et al. 1999) as a potential delivery vehicle for bone

marrow-derived mesenchymal stromal cells (BM-MSCs). Initial experiments characterize the product particles and validate their potential as a hydrogel vehicle. Later experiments validate a cell loading methodology in terms of cellular response to the KOS substrate as well as cell adhesion compared to a collagen-coated MP control (Schlapp and Friess 2003, Batorsky et al. 2005).

4.2. Materials and Methods

4.2.1. Cell Culture and Loading Procedure

Primary BM-MSCs (ATCC) were isolated from the femurs of male rats and cultured in growth medium consisting of MEM-α media supplemented with 10% Fetal bovine Serum and 1% Penicillin-streptomycin. Cultures were stored in a sterile incubator at 37 ^{o}C with 5% CO_2. To integrate cells with particles, a sterile P100 petri dish was pre-wetted with growth medium. 60 mg of MPs, formed from KOS dissolved in PBS and crosslinked at 12% w/v with butanediol diglycidyl ether (BDDE), were previously sterilized using a 100 Gy dose of x-ray irradiation, and were added to the wetted petri dish to allow for swelling and media absorption. 5×10^{6} cultured BM-MSCs were added to the MP/media mixture. A magnetic stir bar was added and the suspension was stirred at 200 rpm for 3 hrs to induce integration, after which the petri dish was returned to the previously mentioned cell culture conditions. As a control, BM-MSCs were taken through the same loading procedure with commercially procured Type-I collagen MPs (Sigma) to determine the efficacy of a keratin based MP compared to another well-documented biomaterial substrate (Batorsky et al. 2005, Yin Hsu, Chueh, and Jiin Wang 1999). Step-by-step methods for cell loading can be seen in Figure 4.1.

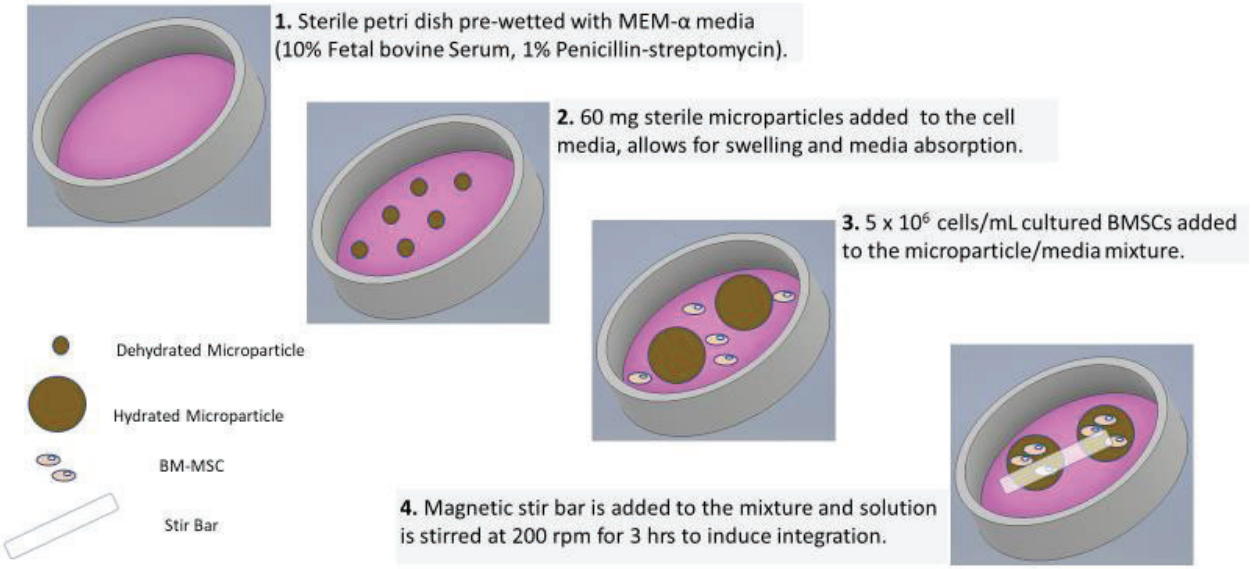

Figure 4.1. Schematic of BM-MSC Loading onto KOS MPs. Procedure for stromal cell loading onto KOS MPs. Due to intrinsic biocompatibility of KOS and mechanical properties of hydrogels, loading can be performed with a short series of basic laboratory techniques.

4.2.2. Scanning Electron Microscopy

Scanning electron microscopy (SEM) was employed to image particles and observe size, shape and surface topography. MPs were fixed on a metallic chip using adhesive carbon tape and sputter coated with a 10 nm thick layer of platinum/palladium using a Leica ACE600 sputter coater prior to imaging. Samples were imaged using a Zeiss field-emission scanning electron microscope. The resulting SEM images were used for descriptive purposes and size measurements.

4.2.3. Size (SEM/Particle Size Analyzer) and Structure Analysis

The average size of the synthesized MPs was determined using two methods. In the first method, the previously mentioned SEM images were processed using the *ImageJ (Schneider, Rasband, and Eliceiri 2012)* image processing software. Diameter measurements of spherical particles (n=20)

were taken based on a length to pixel ratio determined via the SEM and averaged to determine the mean and standard deviation of particle size.

The second method involved measurements using a Horiba LA-950 particle size analyzer. MP samples were suspended in ethanol to prevent water absorption and swelling. Samples were agitated using a combination of stirring and sonication to prevent further particle agglomeration. Samples were analyzed in triplicate via laser diffraction using refractive indices of 1.54 and 1.36 for the keratin particles and ethanol, respectively (Leertouwer, Wilts, and Stavenga 2011).

To analyze particle shape and internal structure, we investigated the average porosity and relative pore connectivity within samples using confocal microscopy. MPs were incubated with a 4′,6-Diamidino-2-phenylindole dihydrochloride (DAPI) cellular stain (0.1 μgmL^{-1}) that was readily absorbed by the keratin protein. Particles were incubated at room temperature in the dark for 5 min, washed with PBS three times and visualized using a Zeiss confocal microscope. Z-stacks measuring between 4 µm and 5 µm in thickness were taken and compiled to create a 3-dimensional construct of an individual particle's internal structure. ImageJ image processing software, specifically the *BoneJ* plugin (Doube et al. 2010), was used to quantify both the pore fraction, which is defined as the volume of pore space divided by the total volume of a particle, as well as pore connectivity, which is defined as fraction of interconnectivity per unit volume (μm^{-3}), in three different batches of particles (n=50).

4.2.4. Quantifying Loaded Cell Counts

Upon loading particles with BM-MSCs, the number of cells was quantified using confocal microscopy. BM-MSCs loaded onto keratin and collagen MPs was confirmed with a DAPI nucleic

stain. Cell-loaded particles were sampled 24 h after culture and at 24 h intervals for a total of 72 hours. Particles were DAPI stained for 5 min and washed with PBS three times, after which they were suspended in PBS and imaged within 30 minutes after washing. This process was performed for both keratin and collagen MPs.

4.2.5. Validating Cell Adhesion

24 h after the initial suspension culture, loaded particles were immunofluorescently stained using the FAK100 Actin Cytoskeleton and Focal Adhesion Staining Kit (Millipore) to identify key cellular components in structural development, motility and adhesion, as these particular proteins are documented as being critical in cellular development and survival and therefore act as crucial indicators of a cells affinity for a material substrate (Wang, Taraballi, et al. 2012). Cells loaded onto particles were fixed for 20 minutes with a 4% paraformaldehyde solution, followed by wash buffer. A 0.1% Triton-X 100 solution was applied to permeabilize the cell membrane and was also removed with wash buffer. Cells were incubated initially with primary (anti-vinculin) antibody diluted in blocking buffer and then a secondary (Goat x mouse, FITC-conjugated) antibody, both at room temperature for 1 hour. Post washing, cells were kept in PBS and imaged within 30 minutes of the finished staining procedure. The same staining procedure was used on cells loaded onto collagen MPs. Cells loaded onto both substrates were imaged using confocal microscopy to compare the presence of these key proteins.

4.2.6. Maintenance of Cell Plasticity

Prior to the integration of BM-MSCs to KOS MPs, initial tests were performed to document the expression of markers associated with cell plasticity were present in the cells before any material

or chemically induced differentiation was possible. Cells were immunofluorescently stained for surface markers C90+/CD73+/CD34-, as cells of this type would be indicative of maintaining their "stem cell" nature, and analyzed with flow cytometry (Pittenger et al. 1999). Briefly, 100 μL of cell suspension (~1x10^6 cells) was used for each sample. ~1 μg of fluorochrome-conjugated antibodies were added to their respective tubes. Tubes were vortexed and incubated on ice for 20 minutes while protected from light. To wash off excess antibody following staining, 1 mL of 1X PBS was added to each tube where they were subsequently centrifuged in a tabletop microcentrifuge for 5 minutes at 2000 rpm. The supernatant was aspirated and the pellets were resuspended in 500 μL of 2% paraformaldehyde prior to flow analysis, which occurred within 2 hrs after the process was completed. Controls for flow analyses included blank (unstained) cells and cells stained with individual antibodies.

Cells loaded onto particles were cultured for 72 hours under the same conditions mentioned previously. Elastase has previously been proven effective at digesting keratin hydrogels (Ledford et al. 2017), and was employed to facilitate cell harvest. Briefly, post-integration, cells were detached by degrading the keratin protein in a 0.5 UmL^{-1} elastase solution for 5 minutes and subsequently vortexing. After pelleting by centrifugation, cells were immunofluorescently stained as previously described, with the full spectrum of stains or used as controls to compare to unstained but loaded cells or cells stained with individual fluorophores that underwent the same loading conditions.

4.2.7. Statistical Analysis

To compare experimental groups, analysis of variance (ANOVA) and/or linear regression analysis with a Tukey's post hoc test was performed in all experiments. To determine significant variances, a p-value <0.05 was considered statistically significant. Sample sizes were determined using a

power analysis where a power (1-β) of 0.9 and an alpha (α) of 0.05 was employed. All statistical analyses were performed using JMP Pro 11.

4.3. Results

4.3.1. Water-in-oil Emulsion Microparticle Synthesis

SEM images of water-in-oil emulsion particles and a cell body atop the keratin surface can be seen in Figure 4.2**.** MPs appear three dimensional and spherical with a rough surface structure as determined by AFM of hydrated particles. These results can be expected based on the mechanisms of synthesis. Relying on the random aggregation of KOS proteins and associated crosslinker, the suspension of which are naturally inclined to form spherical droplets. The mechanisms surrounding the efficacy of the water-in-oil emulsion procedure, namely the phase separation between water and oil, do not necessarily mandate that the water-soluble phase (KOS protein and associated crosslinker) remain homogenous during the stirring step, which may account for the non-spherical MP assembly, variations in size, and the uneven and rough surface. In addition, freeze drying may also contribute to particle morphology as protein re-arrangement can occur upon concentration.

MPs integrated with cells were, by necessity, hydrated and dehydrated after going through the loading and SEM imaging processes, respectively. As a result, the rapid changes in particle size and shape may have contributed to cell detachment during SEM sample preparation, and observations of intact cells on particles was sparse. Also of note, MPs imaged after hydration are visibly more porous than dehydrated particles. This is attributed to loosely bound keratin nanomaterial being removed upon particle hydration and agitation as keratin particulates were visible after the culture process. Imaged cells appear to conform to the shape of the available

keratin, flattening along the material, indicating that the substrate is amenable to cell adhesion (Sierpinski et al. 2008b). Adhesions formed along the periphery of the cell appear to bind along the keratin material, although these adhesions cannot be solely verified using SEM and rely more heavily on the results of immunofluorescent analyses.

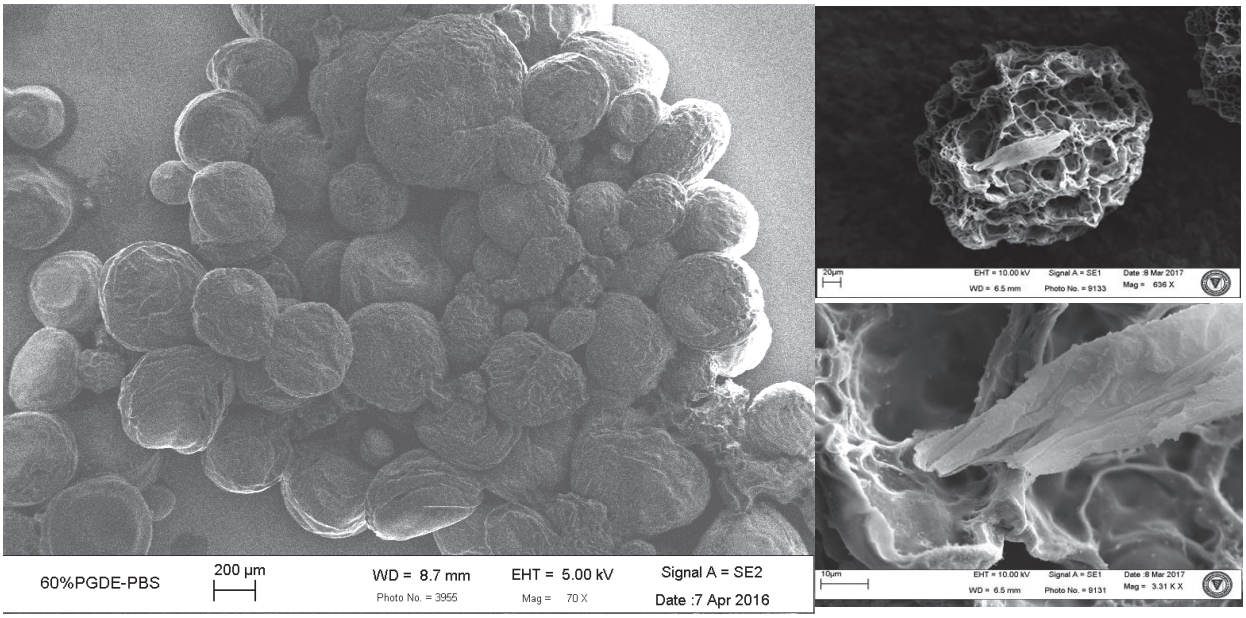

Figure 4.2. SEM of Cellular Loading. SEM image of water-in-oil emulsion synthesized KOS MPs (Left) and cell-integrated particles (Top Right, Bottom Right). Particles appear spherical in shape with variation in surface roughness. The wrinkled appearance may be due to a combination of microarchitecture and the freeze drying process. Cells are sparingly present in dried particles. Imaged cells appear to adhere to the particle surface and display noticeable adhesion at the cell-to-keratin interface.

4.3.2. Size (SEM/Particle Size Analyzer) and Structure Analysis

The size analysis of individual particles using ImageJ was translated by scale bars provided by the SEM software and indicate average particle diameters of 236 ± 80.4 µm (data not shown). Based on laser diffraction analyses, mean particle diameters appear to be 350 ±71.5 µm when in an ethanol suspension (Figure 4.3**)**. As laser diffraction was capable of processing the sizes of entire

batches (on the order of thousands) of particles, we are more inclined to rely on the results of this study to determine the average diameter of particles. It should be noted that some samples initially produce particle diameters greatly outside of the normal range, verging on the mm scale; this can be attributed to particle aggregation. Post-processing steps such as sifting through membranes of a specific pore size can be employed to circumvent issues of sample variability (Gauthier et al. 1999).

The internal structure of the oil-in-water generated MP can be described as that of a coarsely fibrous particle with high porosity (Figure 4.3). Quantitative results indicate a protein to pore fraction of 0.58 ±0.035, suggesting that ~40% of a given particle's volume is occupied by empty space (pores).

The average pore size of synthesized particles was determined to be 704 ±387 μm^2. This value may be particularly relevant in terms of both access to and invasion of BM-MSCs into this construct, which are found to have diameters ranging from 15 μm to 30 μm in suspension (Zanetti et al. 2015), suggesting successful access between the average cell and average pore of the MP construct. Spread BM-MSCs cells reach on the order of hundreds of microns in diameter (Wang, Clements, et al. 2012), which may have resulted in improved cell survival and retention on the KOS MP. Along a similar note, pore connectivity of the structure was relatively high with a connectivity of 0.53 ±0.17 (Figure 4.3), suggesting about half of a given particles' pores are connected. Based on these results, and taking into consideration that a larger pore network may provide a greater surface area for cells to adhere to, KOS MPs may support cellular loading from a physical and not merely a chemical standpoint. Similarly, mass transport of waste and nutrients to and from a wound defect, which has been proven to be a significant factor in tissue regeneration

(Siepmann, Faisant, and Benoit 2002), could be improved due to both the high porosity and high pore connectivity of the KOS MP.

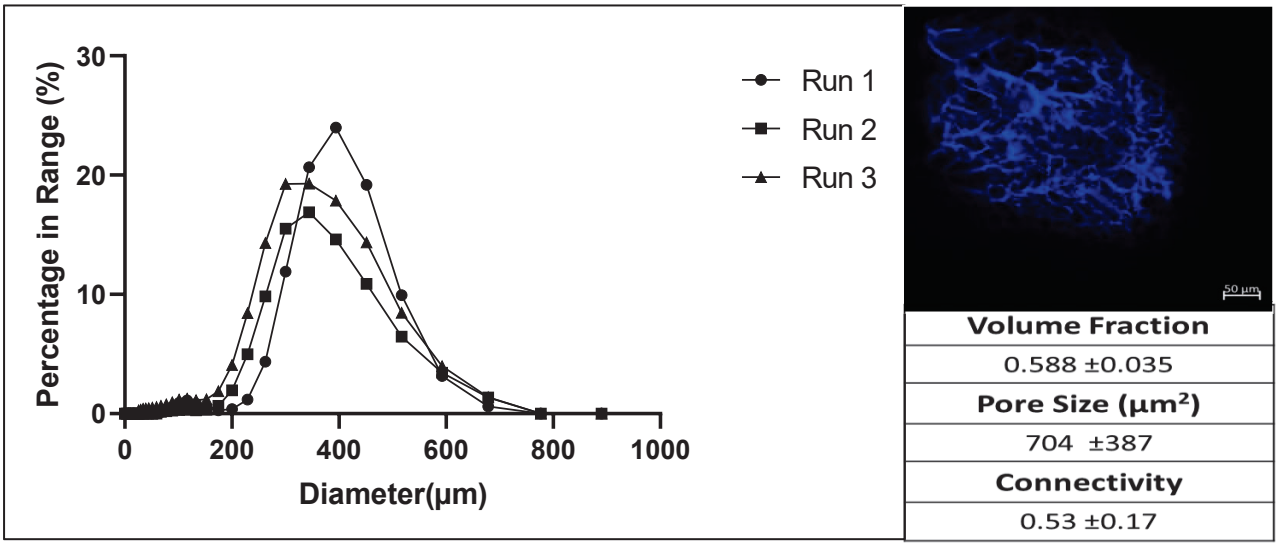

Figure 4.3. Size and Structure of MPs for Cellular Loading. Laser diffraction histogram displaying the average diameter of batches of synthesized MPs. Average particle diameters are approximately 350 ±71.5 μm with a normal distribution of diameters. Y-axis indicates the percentage of particle within that specific range of diameters. Fluorescence microscopy image of water-in-oil emulsion synthesized MPs stained with DAPI show a relatively low solid volume fraction of 0.588 (~40% of the given volume is void space) and what appears to be high pore interconnectivity with a connectivity of 0.53. Relatively high void fractions as well as pore connectivity may contribute to both the overall surface area with which to load cells and provide improved mass transport, facilitating enhanced cellular function.

4.3.3. Quantifying Loaded Cell Counts

Results show that BM-MSCs integrated with KOS MPs as part of the previously mentioned suspension culture procedure, are present at least 72 hours after integration and are attached at higher density compared to collagen-based MPs loaded using the same process (Figure 4.4).

Significant differences in the viable cell counts can be seen after 2 days and appear to increase as culture continues. High variability can be observed in the keratin-based samples and was determined to be a factor in sparse or incomplete loading observed in randomly selected particles. Confocal imaging suggests a more porous nature in the keratin-based MPs compared to that of the collagen-based control, and this likely contributes to the overall loading capacity. This characteristic of porosity coupled with enhanced surface area may be uniquely present in keratin MPs due to self-assembly, although further tests must be completed to confirm this postulate.

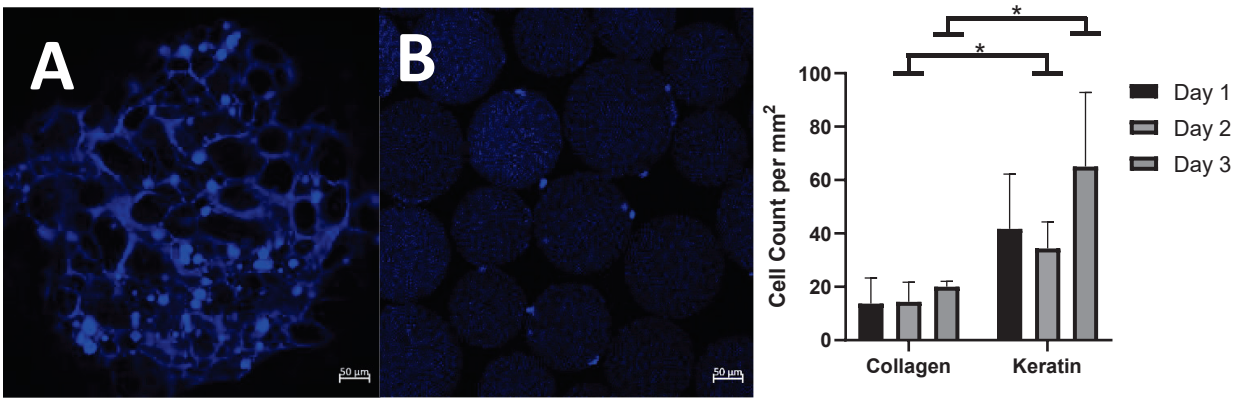

Figure 4.4. Quantifying Loaded Cell Counts. Fluorescent image of a DAPI stained BM-MSCs 24 h post suspension culture with keratin (A) and collagen-based (B) MPs. Nuclei of cells can be seen as dense, brightly fluorescent, blue regions with the MPs absorbing small amounts of dye, exhibiting a weaker blue fluorescence. KOS MPs show a greater density of cells than collagen MPs per mm^2 of surface area. This characteristic is quantified over 72 hours for each type of particle and shows statistically significant differences ($p<0.05$) after 48 h. (error bars represent standard deviation)

4.3.4. Validating Cell Adhesion

BM-MSCs suspension cultured with KOS MPs, shown in Figure 4.5, display the formation of distinct actin cytoskeletal filaments after 24 h. Similarly, vinculin membrane proteins can be identified along various cell bodies. Formation of the same protein complexes were observed in the collagen-based model, suggesting that a keratin-based MP can promote the same if not an improved cellular response compared to the commonly touted collagen-based MP substrate. Immunofluorescent images of keratin particles show the full cross section, so it is unclear whether the cells are migrating into the core of the MP or remain on the surface.

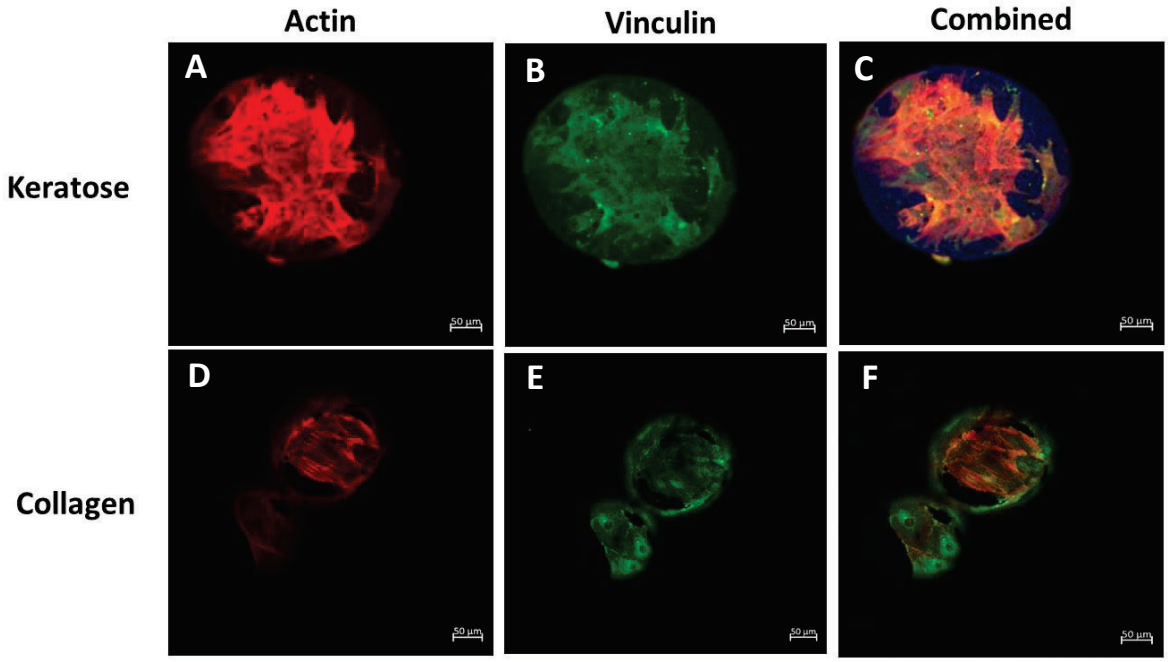

Figure 4.5 Validation of Formation of Key Cell Structures for Growth and Development. Immunofluorescently stained BM-MSCs 24h after suspension culture on keratin (A-C) and collagen (D-F) MPs. Images of individual channels show the distinct formation of cytoskeletal actin filaments in red (A) and vinculin focal adhesions in green (B). The same proteins are present in a collagen-based MP (D, E respectively) cultured under the same methods. The combined channels show the localization of these proteins around cell bodies (C, F).

4.3.5. Maintenance of Cell Plasticity

The SSC vs. FSC flow cytometry plot (Figure 4.6) of BM-MSCs prior to integration shows a homogeneous population based on cell size and intracellular content, maintaining the notion that any differentiation observed is a factor of the integration and/or detachment procedure and not from the presence of subpopulations. Prior to integration, BM-MSCs exhibit stem-like qualities with greater than 99.0% of analyzed cells testing CD90+/CD73+, and 78.0% of the analyzed population testing CD34-. 72 h after suspension culture a shift in the population was observed with only 63.1% of the detached cell population remaining CD90+/CD73+ positive while 74.9% of the cell population remained CD34-.

A number of factors may have contributed to these shifts. It was interesting to see a slight shift away from CD90+/CD73+ without a marked decrease in CD34-. This may suggest that the loaded cells are experiencing enough physical stimuli from the loading and/or unloading procedure to invoke the onset of differentiation, but a lack of other specific stimuli prevents further differentiation. However, CD34 negativity was still present, suggesting the lack of definitive differentiation. It should also be noted that the generation of a subpopulation is more unlikely rather than likely based on the fact that, post-integration, cells remained in one general population as indicated by the clustering of the flow cytometry data. Future studies will likely be necessary that track the expression of markers from these detached cell populations to determine if lineage-specific differentiation is due to the mechanisms of both loading and unloading. Moreover, alternative markers for more likely differentiation pathways should also be explored.

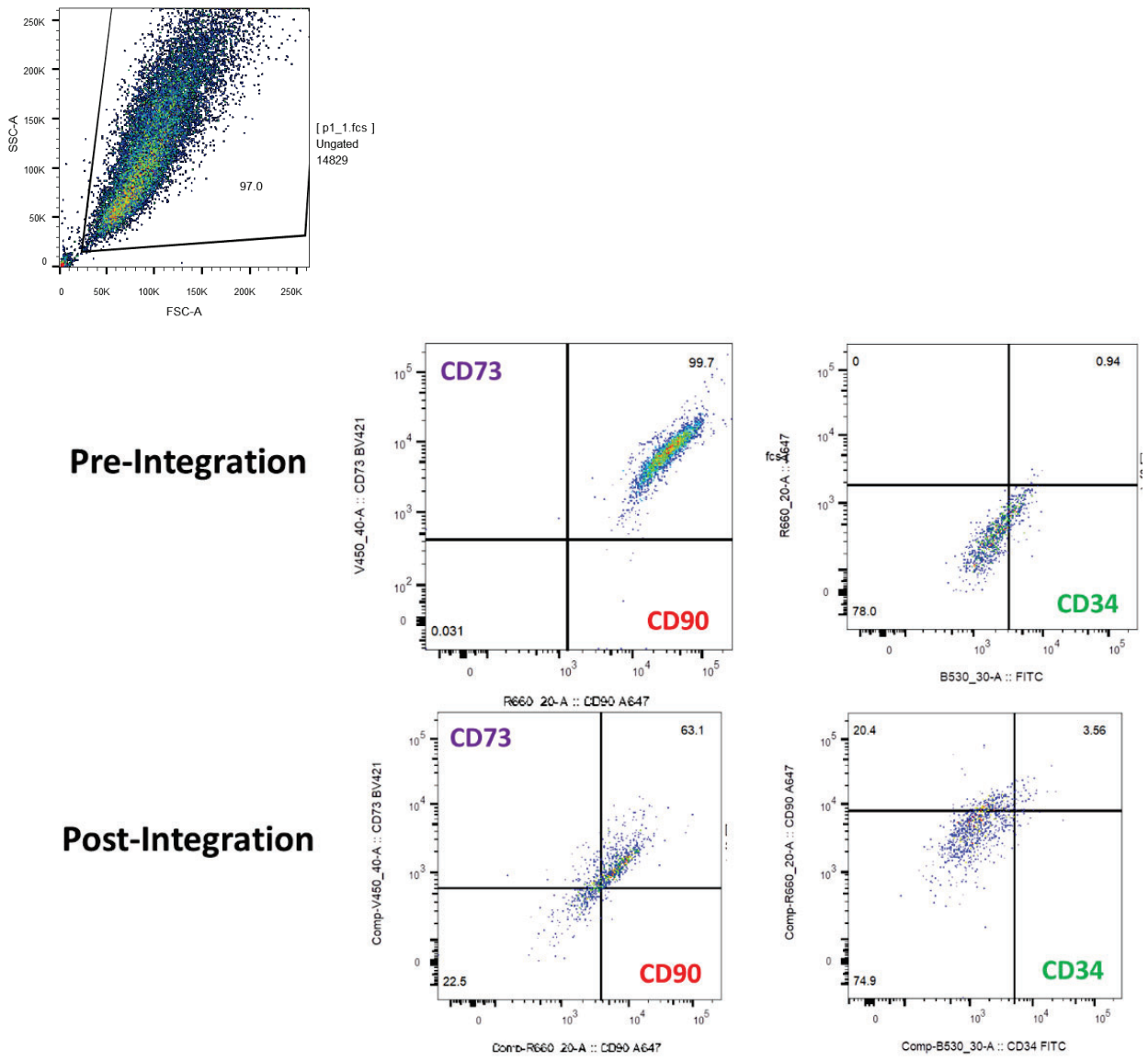

Figure 4.6. Maintenance of Cell Plasticity. (Top Left) Preliminary flow cytometry analysis for plasticity of isolated BM-MSCs. SSC vs. FSC plot show no indication of subpopulations within the stromal cell population. Based on controls, cells express positively for CD90/CD73 and negatively for CD34 (Pre-integration) which indicates plasticity. After 72 h (Post-integration), shifts in marker prevalence may be the result of the loading or unloading process or the early stages of differentiation due to the keratin biomaterial.

4.4. Discussion

The aforementioned synthesis procedure for water-in-oil emulsion synthesis was successful in generating KOS MPs, although size and size distribution varied considerably compared to initial expectations. Morphology within the MPs suggested that the propensity for keratin to self-assemble into a more homogeneous structure was not overcome by interfacial forces of the emulsion and/or the shearing force of the vigorous mixing method employed, or was introduced after emulsion during the freeze drying process. This created a unique microarchitecture, with loosely packed fibers in the emulsion-generated particles, which likely contributes greatly to the highly porous nature of the construct. Upon analysis of cell-loaded MPs by SEM, particle surfaces appear significantly more porous than unloaded particles. Loosely bound keratin was likely removed during agitation which may consequently provide a greater surface area for cells to form adhesion junctions although this has yet to be confirmed. SEM images of loaded particles display that, post-fixation, cells exhibit morphologies indicating survival upon the MP surface and an ability to conform to the protein structure to form sustainable adhesion at the cell-to-substrate interface.

Variations in protein localization within individual particles appear to contribute to rough and varying surface topography but may, overall, provide a rougher and therefore more effective substrate in terms of cellular attachment to the material (Goldmann 2016). Hydrated KOS MPs behave similarly to classical hydrogel materials based on water retention, swelling and elastic properties, allowing for several advantages in cell-loading from a materials standpoint (Hallab et al. 1995). Interestingly, MPs take the form of a highly interconnected and porous particle suggesting that, despite the high shear environment, the keratin proteins are still capable of some

level of self-assembly back toward their equilibrium structure of intermediate filaments, adding to the mechanistic simplicity with which this process is performed.

The suspension culture methodology used in this study was validated by the retention of viable cells onto the KOS MP at significantly higher levels than that of the control collagen biomaterial, beginning 48 h after culture. It is also notable that cell populations may begin to increase going into 72 h post culture. This may display a propensity not only for cell survival but improved cell proliferation on this keratin biomaterial compared to other MP biomaterial constructs.

Apart from nucleic activity acting as a representation of cell viability, as is the case with DAPI staining, loaded BM-MSCs form noticeable actin cytoskeleton filaments indicating a substrate amenable to cellular spreading and growth. Vinculin proteins were similarly present, which was expected based on keratins naturally occurring amino acid binding sites (Hill, Brantley, and Van Dyke 2010). The formation of these cytoskeletal and membranous proteins was found to be comparable to that of the collagen MP control, adding credence to the application of a similar keratin-based MP.

BM-MSCs were confirmed to be of their initial stem-like nature by a series of markers identified by flow cytometry. No significant shifts away from that stem-like nature were seen once cells were detached after 72 h of culture on KOS MPs. It was unclear whether these shifts were a product of loading or unloading, but further analysis should be performed to determine if unloading was the cause as this step is not necessary for implantation of loaded KOS MPs and cells may therefore retain their plasticity.

4.5. Conclusions

The value of the water-in-oil emulsion synthesis technique lies in the straightforward ability to use a relatively safe material such as keratin without generating potentially deleterious secondary chemical interactions upon synthesis. The resulting particles are stable, inexpensive and easy to process (Van Dyke 2009, Oh, Lee, and Park 2009). Deficiencies arise mainly in this processes reliance on random protein agglomeration and the high apparent porosity as it pertains to loading and retention of a payload *in vitro* and eventually *in vivo*, from a biomaterials standpoint (Yan et al. 1994b, Viswanathan et al. 1999).

The discussed MP formulation employed as a cell-delivery vehicle may prove more advantageous compared to other biomaterial constructs. A highly porous delivery vehicle offers improvements with regards to the total accessible surface area available for cell loading and material stability compared to solely topical loading onto similar biopolymer constructs such as contiguous collagen-based gels, for example (Park et al. 2007, Lu et al. 2015). Similarly, cellular loading can be improved using the proposed construct through intrinsic affinities found between cells and the keratin substrate. As previously mentioned, keratin exhibits a number of properties that support cellular interactions. The surface characterization of the synthesized MPs, while yielding no indication of a difference between products based on solvents or crosslinkers, does show surfaces are amenable to the adhesion of cells. This natural affinity may neutralize the need for added processing steps that require surface functionalization or cell encapsulation, which can hinder mass transport, namely nutrient and waste transport to and away from cells, respectively, both of which can become a detriment to cell functionality and survival, as commonly seen in chitosan and alginate based gel capsules (Nicodemus and Bryant 2008, Tan and Takeuchi 2007).

Chapter 5

In vitro Effects of a Bone Marrow Derived Mesenchymal Stromal Cell Loaded Keratin Microparticle on the L6 Skeletal Muscle Cell Line

Marc Thompson[1], Claire McClenny[2], Dr. Mark Van Dyke[1]

1. Department of Biomedical Engineering and Mechanics, Virginia Tech, Blacksburg, VA
2. Department of Biological Systems Engineering, Virginia Tech, Blacksburg VA

Abstract: The delivery of cells, specifically stromal cells, as a method of improving the quality of tissue engineering and regeneration under wound scenarios has become an attractive option over the past decade. Bone marrow derived mesenchymal stromal cells (BM-MSCs) are a mesenchymal cell source with properties of self-renewal and multipotential differentiation that have also been shown to improve wound healing when localized in a wound environment. 3D tissue engineering scaffolds are better able to mimic the in vivo cellular microenvironment, which benefits the localization, attachment, proliferation, and differentiation of BM-MSCs. This study investigates the potential of a keratin-based microparticle formulation synthesized via the water-in-oil emulsion method. We observe cellular loading capabilities and the in vitro effects of the L6 skeletal muscle cell line to determine potentially beneficial effects on skeletal muscle regeneration. Components of delivery, specifically stromal cell secreted factors, improved L6 cell viability beginning at 48 hours. Both keratin and stromal cells displayed an ability to activate L6 cells in terms of intracellular calcium levels. Several factors secreted by L6 cells that are correlated with improved skeletal muscle regeneration were seen in higher prevalence under keratin and stromal cell treatment groups, compared to controls.

5.1. Introduction

A prerequisite of classical tissue engineering approaches is the development of a suitable biomaterial scaffold or substrate with an architectural design, chemical, mechanical and physical makeup comparable to that of the native tissue. Early practices of delivering cell suspensions directly into a defect site have proven to be problematic—if not ineffective—due to insufficient retention within the defect and subsequent flushing into the surrounding tissue (Endres et al. 2010). Consequently, the implementation of naturally derived vehicles, composed of more durable materials found readily in the body, are an attractive option for mimicking the native host tissue in the form of 3D prefabricated scaffolds that retain the delivered cell population (Kretlow and Mikos 2007, Wang et al. 2015). Herein we focus on a keratin-based hydrogel scaffold derived from human hair that can then be processed into a beneficial size and shape for cell delivery.

Keratin and keratin derivatives from human hair exhibit several mechanical and biological properties that support their use as scaffolds for cells (Ledford et al. 2017, Rouse and Van Dyke 2010, Hill, Brantley, and Van Dyke 2010). Upon hydration, keratin hydrogels mechanically perform as a flexible viscoelastic material. However, most reports of keratin biomaterials in tissue engineering utilize cell-free constructs, despite keratin's intrinsic biocompatibility and apparent support of cell health and function (Konop et al. 2018, Mori and Hara 2018). This may be a consequence of the formation of keratin hydrogels being incompatible with cells, particularly in the kerateine (KTN) system where gelation is best driven by protein self-assembly at basic pH (Hill, Brantley, and Van Dyke 2010). The keratose (KOS) hydrogel system is more conducive to the inclusion of cells as these gels can form at physiologic pH, but the resulting constructs can be fragile and degrade rapidly. Crosslinking can be used to mitigate this, but some chemistries may compromise cell viability (Steinert et al. 1993, Tanabe, Okitsu, and Yamauchi 2004).

Microparticles (MPs) act as a building block for 3-Dimensional (3D) constructs to fill tissue voids while simultaneously providing delivery of soluble factors and cells (Qazi et al. 2015, Moulin et al. 2010, Huang and Fu 2010). The application of MPs provides a larger surface area for exterior cell loading while avoiding concerns about clearance commonly viewed as a potential negative side effect of similarly touted nanoparticles (Behrens et al. 2014). The benefit of a microscale protein construct lies in the interplay between the individual products size, capable of non-invasive injectable delivery, and the physical agglomeration of gel particles wherein once fully hydrated, particles form a nearly contiguous hydrogel construct (Oliveira and Mano 2011, Woo, Park, and Lee 2014).

This study employs a KOS MPsynthesized via the documented water-in-oil emulsion synthesis procedure (Yan et al. 1994a, Viswanathan et al. 1999) as a potential delivery vehicle for bone marrow-derived mesenchymal stromal cells (BM-MSCs). Initial studies characterize the product particles and validate their potential as a hydrogel vehicle. Later studies validate a cell loading methodology in terms of cellular response to the KOS substrate as well as loading capacity compared to other documented biomaterial constructs (Schlapp and Friess 2003, Batorsky et al. 2005). BM-MSCs from bone marrow have proven to be negative for immunologically relevant surface markers and inhibit proliferation of allogenic T-cells in vitro (Prigozhina et al. 2008). They promotes tissue regeneration by the localized retention of cells and delivery of therapeutic trophic factors over a desirable period of time.

As such, we take an early look at the effects of this cell-laden vehicle on the L6 skeletal muscle cell line as a model for skeletal regeneration. This study aims to observe effects in vitro that may later carry over to the in vivo environment.

5.2. Materials and Methods

5.2.1. Cell Culture and Loading Procedure

Primary bone marrow-derived mesenchymal stromal cells (BM-MSCs) (ATCC) were isolated from the femurs of male rats and cultured in growth medium consisting of MEM-α media supplemented with 10% Fetal bovine Serum (FBS) and 1% Penicillin-streptomycin (PS). Cultures were stored in a sterile incubator at 37 ^{o}C with 5% CO_2. L6 skeletal muscle cells (SMCs) were isolated from the thigh muscles of rats. Cells were cultured in DMEM (Gibco) supplemented with 10% FBS, 1% PS and similarly cultured in a sterile incubator at 37 ^{o}C with 5% CO_2. To integrate cells with particles, a sterile P100 petri dish was pre-wetted with growth medium. 60 mg of MPs which were previously sterilized using a 100 Gy dose of x-ray irradiation, was added to the wetted petri dish to allow for swelling and media absorption. 5 x 10^{6} cultured BM-MSCs were added to the microparticle/media mixture. A magnetic stir bar was added and the suspension was stirred at 200 rpm for 3 hrs to induce integration after which the petri dish was returned to the previously mentioned cell culture conditions. As a comparative method of study, BM-MSCs were taken through the same loading procedure with commercially procured Type-I collagen MPs (Sigma) to determine the efficacy of a keratin based MP compared to another well-documented biomaterial substrate.

5.2.2. Validating Component Effects on Cell Viability

In vitro co-cultures of SMCs and KOS MPs were cultured using a transwell culture system (Corning) consisting of a lower culture chamber and an upper culture chamber with 4 μm diameter pores allowing for interactions with the lower chamber, to determine any potential effects on cell viability. SMCs were seeded in 12-well plates at 2,000 cells/mL with SMC growth medium in the

lower well while varying masses of KOS MPs (1, 5, 10 mg) suspended in SMC growth media were deposited in the upper well to induce an interaction with the SMCs. Bicinchoninic assay (BCA) measurements of protein concentration determined the effective delivered concentrations under these conditions were approximately 2.5, 2.75 and 3 mg/mL. An alamar blue MTS assay (Hamid et al. 2004) was used to compare cell viability between the treatments. 100 µL of alamar blue was added to each of the wells and allowed to incubate for 3 hrs protected from light at culture conditions. Treatments were compared to control cultures of growth media without MPs in the upper well and analyzed over 48 hrs.

We next aimed to determine if the factors secreted by BM-MSCs could bolster the proliferative capacity of L6 cells. BM-MSCs (1,000 cells/mL) were cultured in 12-well plates for 48 hrs with SMC growth media to collect secreted factors. The resulting supernatant media was transferred to SMC cultures at varying ratios of conditioned media and untreated growth medium (0, 25, 50, 100% conditioned media) again seeded at 2,000 cells/mL in 12-well plates and were cultured for 48 hours. The MTS assay was employed as previously mentioned and in both treatment scenarios, fluorescent measurements of the wells were taken at 0, 24 and 48 hrs using a Synergy H1 plate reader (Biotek) at excitation and emission wavelengths of 560 nm and 590 nm respectively.

5.2.3. In vitro Co-culture System

The transwell culture system is an attractive technique to measure indirect cell-to-material as well as indirect cell-to-cell interactions. Using this apparatus, a well-plate consisting of two separate chambers (upper and lower) separated by a permeable and removable support membrane of varying porosity, depending on the manufacturers specifications, can effectively integrate the environments of two components (cells/cells, materials/materials, cells/materials) without the requirement of direct contact. Therefore, we can evaluate the effects of mg/mL concentrations of

KOS as well as stromal cell secreted factors on the L6 skeletal muscle cell line as it pertains to delivery from the skeletal muscle cell extracellular space, as would be seen in an in vivo setting (Figure 5.1).

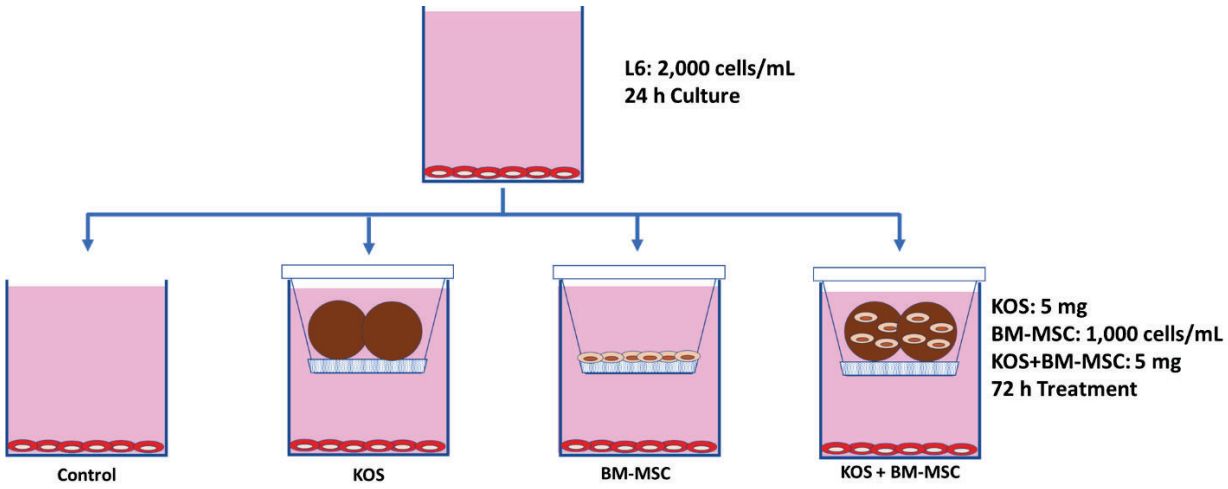

Figure 5.1. Schematic of In vitro Co-culture System. Schematic of transwell co-culture system use for determining effects of treatments on the L6 cell line. L6 cells seeded in the lower well can receive individual treatments of KOS MPs, BM-MSCs or a combination of both, measuring effects from indirect introduction of these components.

5.2.4. Intracellular Calcium Production

Intracellular calcium levels are ubiquitous with efficiency in both development and recovery from injury due to the fact that calcium is essential to muscle function (Tu et al. 2016, Ferrari, Rohrbough, and Spitzer 1996). L6 skeletal muscle cells were treated with individual treatments of BM-MSCs, KOS MPs or combinatorial treatments of BM-MSC loaded KOS MPs to determine effects on intracellular calcium production. L6 cells at a concentration of 2000 cells/mL in growth medium were seeded in the bottom well of a 12-well transwell plate (Corning). Individual treatments consisted of BM-MSCs at a concentration of 1,000 cells/mL, 5 mg of saturated

unloaded KOS MPs or 5 mg of saturated BM-MSC loaded KOS MPs; each was deposited into the upper transwell with a 4 μm pore diameter to facilitate the transport of stromal cell secreted factors and nanoscale KOS. Treatments lasted for 72 hr, after which the upper wells were removed. Fluo-4 (Thermofisher) ester for calcium specific binding was diluted in a combination of dimethyl sulfoxide (DMSO) and Pluronic F-127 (Sigma) for dispersion of the non-polar ester, to a working concentration of 5 μM. Cells were incubated with the dye for 60 min at 37 ºC and subsequently washed with Hank's buffered salt solution (Gibco). Cells were imaged using a Zeiss confocal microscope, fluorescence intensity was quantified using ImageJ and was normalized to individual cell bodies.

5.2.5. Growth Factor Production

Multiplexed detection of 14 cytokines (growth factors) documented as being important to angiogenesis, neurogenesis and skeletal muscle cell growth was performed using a high specificity biotinylated antibody growth factor array (RayBiotech). L6 cells at a concentration of 1000 cells/mL in growth medium were seeded in the bottom well of 12-well transwell plate. Individual treatments consisted of BM-MSCs at a concentration of 1,000 cells/mL, 5 mg of media-saturated non-cell-loaded KOS MPs or 5 mg of media-saturated BM-MSC-loaded KOS MPs. Controls consisted of untreated L6 cells. Treatments lasted for 72 hr, after which the upper wells were removed, cells were then allowed to grow in fresh serum-free culture media for 48 hrs, and the supernatant media sampled for testing.

Antibody array membranes were incubated in blocking buffer for 30 minutes and aspirated prior to incubating membranes in the resulting undiluted supernatant media for 3 hrs, to measure the production of secreted growth factors. Membranes were washed and immediately incubated in a biotinylated antibody cocktail for 3 hrs before subsequent washing and incubation in an HRP-

streptavidin cocktail for 3 hrs. Finally, membranes were washed, detection buffer was added and membranes were sandwiched between plastic sheets. All incubation steps were performed at room temperature under gentle shaking (~1 cycle/sec). Within 5 min, membranes were imaged by chemiluminescence using a Fujifilm LAS-3000 CCD camera to generate semiquantitative comparisons between controls. Comparisons were determined based on protein fold changes relative to controls and were considered statistically significant at a fold change greater than 1.5

5.2.6. Statistical Analysis

To compare experimental groups, analysis of variance (ANOVA) and/or linear regression analysis with a Tukey's post hoc test was performed in all experiments. To determine significant variances, for all tests, a p-value <0.05 was considered statistically significant. Sample sizes were determined using a power analysis where a power ($1-\beta$) of 0.9 and an alpha (α) of 0.05 was employed. All statistical analyses were performed using JMP Pro 11.

5.3. Results

5.3.1. Validating Component Effects on Cell Viability

Results of MTS assays (Figure 5.2) suggest that KOS MPs elicit no significantly deleterious effect on cell viability at any tested concentration but do nothing to significantly improve cell proliferation over a 48 hr period. This result was to be expected, although keratin biomaterials have been shown to significantly increase the proliferative capacity of certain cell lines (Ledford et al. 2017, Wang, Taraballi, et al. 2012), while eliciting a marginally positive effect in proliferation on others (Hill, Brantley, and Van Dyke 2010, Rouse and Van Dyke 2010). On the other hand, KOS MPs may still prove to be an efficient cell delivery vehicle due to its mechanical

properties as well as it's documented immunomodulatory effects, which may naturally counter the inflammatory stimuli generated by other materials (Burnett et al. 2013, Cilurzo et al. 2013, Rouse and Van Dyke 2010).

Media conditioned with BM-MSC-secreted factors that were used to culture L6 cells showed increased proliferation of the cell line under all treatment conditions within 12 hours of measuring. Similarly, trends appear to indicate that as more of these secreted factors were present, as indicated by the higher ratio of conditioned media to standard growth media, proliferation seemed to increase, although this is not born out with statistically significant differences. As such, the delivery of BM-MSCs for sustained regenerative stimuli is suggested to be a beneficial factor in improving the overall regenerative capacity of L6 muscle cells. The delivery of which may be improved with a KOS-based MP delivery system based on prior research, which maintains that without an appropriate delivery vehicle, delivered cells are often flushed from the system of interest (Lu et al. 2015, Park et al. 2007).

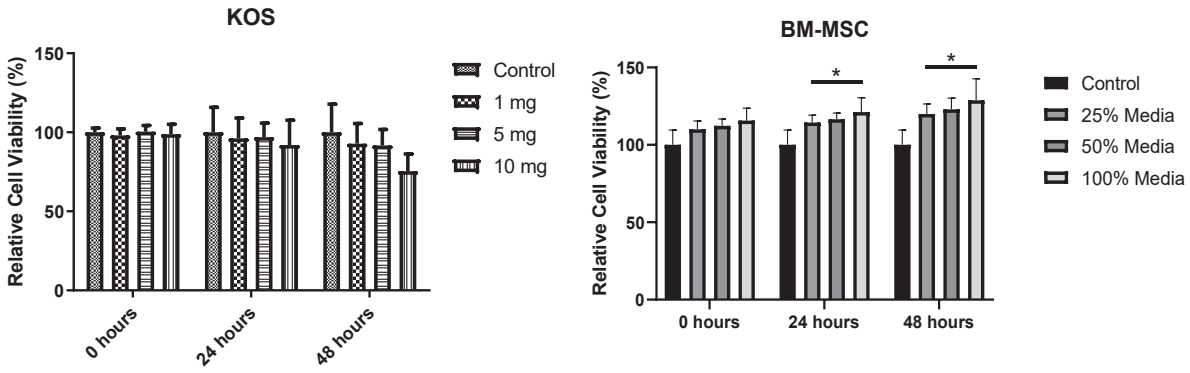

Figure 5.2. Component Effects on Cell Viability. Effects of respective components on L6 cell viability. (Left) KOS MPs at delivered masses as high as 10 mg (~3 mg/mL KOS delivered), show no significant changes in cell viability over a 48 hr period. (Right) Secreted factors from BM-MSCs produce significantly greater ($p<0.05$) cell viability using as little as 25% conditioned media. These results are present in as few as 24 hours and trend upwards as time and treatment concentration increase (error bars represent standard deviations, asterisks denote statistical significance).

5.3.2. Intracellular Calcium Production

Intracellular calcium levels of the L6 cell line after 72 hrs of treatment, seen in Figure 5.3, indicate that all potential components elicit significantly greater intracellular calcium compared to controls of no treatment. A point of note is that the calcium levels present in the BM-MSC group appear to be greater than that of the KOS group. The ability to proliferate more rapidly or simply entering a more excited state may be indicated by the increase in stores of intracellular calcium, which has been supported in altering proliferative capabilities (Stiber and Rosenberg 2011). KOS MPs did not produce significant differences in cell viability, seen in the previous MTT assays. Therefore further studies are necessary to determine by what mechanisms increases in skeletal muscle cell activity (indicated by calcium levels) may be produced. Also of importance, the combinatorial treatment of BM-MSC loaded KOS MPs appear to produce close to the greatest increase in intracellular calcium levels.

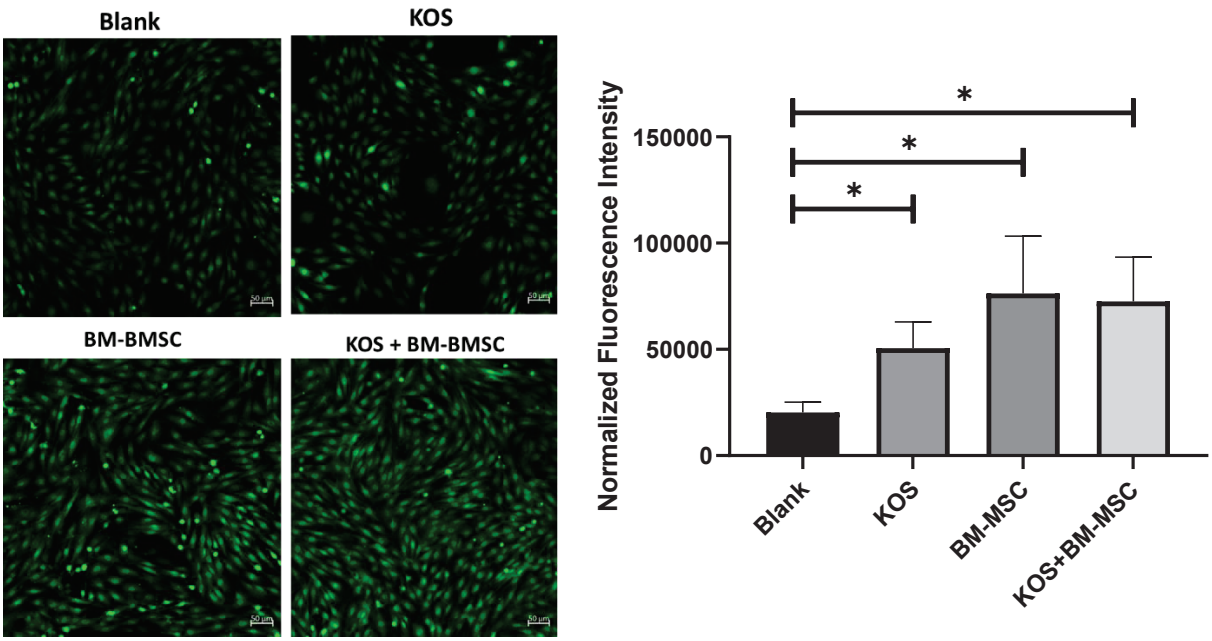

Figure 5.3. Intracellular Calcium Production as a Result of In vitro Culture Treatments. (Left) Confocal microscopy images of L6 muscle cells. Cell fluoresce green based on the levels of intracellular calcium. Cells undergo treatments of KOS MPs (KOS), BM-MSCs (BM-MSC), combinatorial treatment of cell-loaded MPs (KOS+ BM-MSC) or untreated controls (Blank). (Right) All treatments produce significantly greater intracellular calcium than the control group ($p<0.05$). The stromal cell component of treatment appears to be more of a factor than its KOS component counterpart. Of benefit is to see that the combination treatment produces the largest calcium signal of all groups (error bars represent standard deviations).

5.3.3. Growth Factor Production

Semiquantitative analysis of growth factors produced by L6 cells after respective treatments can be observed in Figure 5.4. Of the 14 cytokines measured, most display increases, albeit statistically insignificant in the KOS group (fold change<1.5 times controls) compared to that of untreated controls. The BM-MSC group shows a greater disparity of changes, with several factors (Bngf, Bfgf, EGF and FLT-3 Ligand, PDGF-AA and PDGF-BB) showing a greater than 1.5 times fold change. Similarly, several growth factors exhibit statistically singificant increases in production in

the combinatorial treatment (Activin A, bNGF, bFGF, HGF, IGF, PDGF-AA, PDGF-BB). Interestingly, factors in the combination treatment exhibited decreases in production or did not exhibit production on the same level as the BM-MSC treatment alone, EGF for example. It was thought that the delivery of factors from BM-MSC payloads may be hindered by their adsorption into the KOS MPs, which has been documented as a factor in delivery (de Guzman, M. Tsuda, et al. 2015, de Guzman et al. 2013). It was beneficial, however, that increases in these essential growth factors compared to controls samples were observed across the array of cytokines measured.

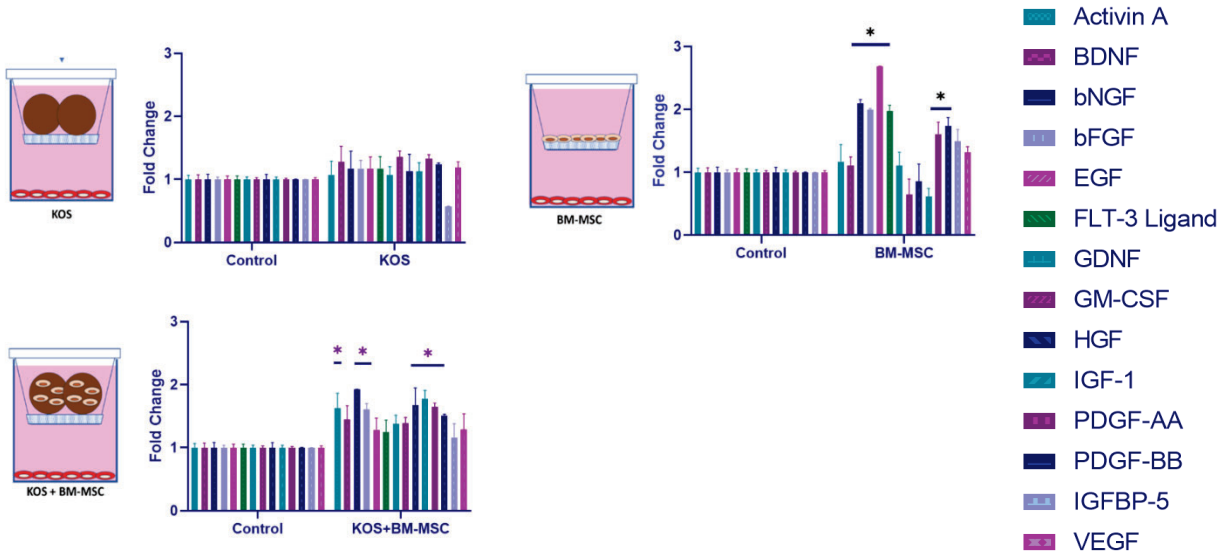

Figure 5.4. Growth Factor Expression as a Results of In vitro Treatments. Results of the multiplexed array analysis. KOS treatment groups show light increases in growth factor production although none are statistically significant. BM-MSC treatment groups show significant increases in several factors and slight down shifts in a few others. Combinatorial treatments are increased across the board, producing the most significantly increased production in factors. Several of the growth factors in the combinatorial treatment are less than their pure BM-MSC counterparts, this is thought to be an outcome of the MPs adsorbing a significant concentration of secreted factors.

5.4. Discussion

We have found that the water-in-oil emulsion procedure has been validated for producing keratin MPs with a range of size and spontaneous formation of surface topography. The size of these particles is amenable to multiple cell loading verging on the order or hundreds of cells per particle and the largely spherical nature of the particles provides ample surface area compared to other construct shapes (Oliveira and Mano 2011, Park et al. 2007). The structure and stability of this highly porous delivery vehicle may also provide a beneficial combination of access for improved cell loading and adhesion given the higher surface area and innate binding motifs found in keratin (Rouse and Van Dyke 2010, Hill, Brantley, and Van Dyke 2010).

The components of this potential biomaterial construct, namely keratin and BM-MSCs, were validated as not eliciting a statistically significant negative response in L6 skeletal muscle cell viability. The factors secreted by BM-MSCs, as noted by the use of BM-MSC conditioned culture media, produced improved cell viability and proliferation in the L6 cell line. Together, along with the documented biocompatible crosslinker in BDDE (Hermitte and Benoit 2011, Johnson and Goodman 1989), the simplicity of both the components and the synthesis procedures offers significant value from a biomaterial standpoint.

Components of this biomaterial construct promoted activity in the L6 cell line as indicated by increased intracellular calcium levels after culture with both components. Intracellular calcium levels are considered critical due to the fact that calcium is a key factor in a number of cellular processes related to skeletal muscle growth and recovery (Tu et al. 2016). As it was postulated, the combinatorial treatment produced the greatest change in calcium levels. The mechanism of this production, especially with regards to keratin, will need to be further elucidated. The same treatments produced a number of interesting increases in growth factor production. Optimization

of delivered components needs to be further reviewed considering the fact that KOS MPs may sequester some of the factors secreted by BM-MSCs, but it was beneficial to see that several growth factors that support a range of aspects of skeletal muscle regeneration including neurogenesis, angiogenesis and skeletal muscle cell proliferation (Cattaneo and McKay 1990, Yu et al. 2015), were all significantly increased compared to negative controls.

5.5. Conclusions

The intrinsic properties of keratin biomaterials, protein-to-protein self-entanglement and innate biocompatible features, makes them an attractive candidate for delivery of cellular payloads. A combination of simplistic synthesis as well as simple culture procedures allows us to generate a viable cell-loaded construct that is shown to support the viability and development of the cellular payload. The combination of keratin and BM-MSCs have been shown to excite skeletal muscle cell activity while upregulating a myriad of factors associated with the major aspects of muscle recovery and functionality (neurogenesis, angiogenesis, skeletal muscle regrowth). In all, the evaluated biomaterial construct may offer the potential for improvements to the innate skeletal muscle recovery process compared to other cell-loaded biomaterial constructs.

Chapter 6.

Conclusions and Future Directions

6.1. Conclusions

6.1.1. Specific Aim 1

Identifying that a primary challenge in cell retention at the site of traumatic skeletal muscle injury can be overcome in the presence of an applicable biomaterial construct, a non-invasively injectable hydrogel may be well-suited to conform to defect sites. Many forms of keratin biomaterials that form hydrogels are not compatible with cell incorporation. In order to circumvent this, we have proposed the approach of first creating a keratose-based crosslinked keratin microparticle (MP), with or without an optional drug or biologic payload, that possesses innate material properties that support natural regrowth of human skeletal muscle. Toward that goal, we demonstrated the synthesis of KOS MP using a water-in-oil emulsion system. The resulting MP demonstrate tissue-like elasticity when hydrated and agglomerate to form hydrogel-like constructs. Interestingly, the microarchitecture is that of a fibrous MP with high surface roughness and porosity. While this may make the KOS MP less amenable to sustained drug or biomolecule delivery in the absence of a molecular-level binding interaction, this microarchitecture may be conducive to attaching a cellular payload to the surface and the intrinsic properties of keratin may provide a more sustainable substrate than that of a bare wound defect.

6.1.2. Specific Aim 2

The intrinsic properties of keratin and keratin derivatives make them an attractive choice for tissue engineering. An ability to add various drug payloads and deliver them in efficacious amounts over time is a desirable characteristic in many systems. Leveraging molecular interactions for payload

binding can be advantageous when sustained release, and/or avoidance of burst release, is desired. In this study, a non-interacting model compound, represented by BSA, showed burst release from a fibrous, highly porous and interconnected, oxidized keratin MP. Conversely, when strong acid-base pairing was facilitated with alternative synthesis procedures, release was affected, contributing to potentially tailorable properties for release. Different methods of production not only resulted in different microarchitecture of the particles, but completely changed the KOS degradation and drug release kinetics. These results suggest that keratin-based MP systems can be tuned within a range of delivery characteristics.

The value of the water-in-oil emulsion synthesis technique lies in the straightforward ability to use a relatively safe material such as keratin without generating potentially deleterious secondary chemical interactions upon synthesis. The resulting particles are stable, inexpensive and easy to process (Van Dyke 2009, Oh, Lee, and Park 2009). Desired tailorable deficiencies arise mainly in the reliance on random protein agglomeration and the intrinsic properties of keratin as physical properties of the resulting MPs, such as the high apparent porosities in water-in-oil emulsion synthesis, may affect loading and retention of certain payloads (Yan et al. 1994b, Viswanathan et al. 1999).

The discussed MP formulation employed as a cell-delivery vehicle may prove more advantageous compared to other biomaterial constructs. A highly porous delivery vehicle offers improvements with regards to the total accessible surface area available for cell loading and material stability compared to solely topical loading onto similar biopolymer constructs such as contiguous collagen-based gels, for example (Park et al. 2007, Lu et al. 2015). Similarly, cellular loading can be improved using the proposed construct through intrinsic affinities found between cells and the keratin substrate. As previously mentioned, keratin exhibits a number of properties that support

cellular interactions. The surface characterization of the synthesized MPs, while yielding no indication of a difference between products based on solvents or crosslinkers, does show surfaces are amenable to the adhesion of cells. This natural affinity may neutralize the need for added processing steps that require surface functionalization or cell encapsulation, which can hinder mass transport, namely nutrient and waste transport to and away from cells, respectively. Both of these can become a detriment to cell functionality and survival, as commonly seen in chitosan and alginate based gels (Nicodemus and Bryant 2008, Tan and Takeuchi 2007).

6.1.3. Specific Aim 3

The intrinsic properties of keratin biomaterials, protein-to-protein self-entanglement and innate biocompatible features, makes them a considerable candidate for delivery of cellular payloads that can contribute to tissue regeneration. A combination of simplistic synthesis as well as simple culture procedures allows us to generate a viable cell-loaded material that was shown to support the viability and development of its cellular payload. The combination of keratin and BM-MSCs have been shown to excite skeletal muscle cell activity while upregulating a myriad of factors associated with the major aspects of muscle recovery and functionality (neurogenesis, angiogenesis, skeletal muscle regrowth). In all, the evaluated biomaterial construct may provide a significant improvement to the innate skeletal muscle recovery process compared to other cell-loaded biomaterial constructs.

6.2. Future Work

The water-in-oil emulsion procedure has been validated in producing stable microscale particles out of keratin and crosslinker components. The shape of particles is relatively consistent based on

synthesis procedures and mechanisms, although experimentation may be performed to synthesize particles of a more specific size. Alterations may include limiting the stirring times or alterations to crosslinker concentrations to more efficiently stabilize the particle size under specific stirring times. Further work may be pursued to tailor the properties of synthesized particles to better suit the regeneration of skeletal muscle or other tissues, if need be. The effects of the applied crosslinker as well as the salt concentration appear to have a direct effect on individual and/or bulk hydrogel properties, a fact that may better suit this biomaterial construct to additional skeletal muscle or alternate soft tissue-based biomaterial constructs, whether they be innate mechanical properties or those associated with payload loading potential.

MP drug loading has been established under two particular loading mechanisms. Assuming water solubility, isolation and loading of a number of drug payloads can be performed. Based on the current results, drug delivery efficiency will vary based on: 1) The synthesis procedures and 2) the intrinsic properties of the payload. Water-in-oil emulsion particles produce burst release whereas acid-precipitated particles retain similar drugs. However, this does appear to vary based on factors such as solution pH and affinity for hydrolytic degradation, among many other possible characteristics. An array of water-soluble payloads with known properties may allow us to determine which characteristics can effectively and reliably alter loading and release kinetics. The efficacy of an antibiotic payload in particular has shown a propensity for delivery and its application in vivo has warranted further study.

The properties of a hydrogel keratin construct have proven sufficient in loading a stromal cell-based payload. The current mechanisms of loading are based on classical suspension culture methodologies. Applicability in an in vivo environment should be the ultimate goal of this research. However, once validated, optimizing the construct should be a goal. Optimization of cell-

loading in the current construct will vary based on the overall MP construct, the cellular concentration, stirring times as well as a number of other variables. While these factors may not be optimized in the current study, the overall optimization of this suspension culture procedure will almost assuredly produce more effective results in terms of cell loading and in vitro/in vivo efficacy.

Current applications of the tested biomaterial construct, specifically BM-MSC loaded particles and the effects on skeletal muscle cells, warrants further in vitro experimentation. Further work may include the determination of whether or not treated skeletal muscle cells can efficiently form multinucleated myofibers, an experiment that can easily be employed under the current methodologies. Another interesting facet could be, upon forming myofibers, noting that these treatments have increased intracellular calcium, measuring the conduction potential of the generated myofibers to support the overall functionality of repaired muscle. The current methodology, however, can reliably be employed to further the investigation of cell-loaded keratin MPs and their effects on skeletal muscle for the purpose of improved skeletal muscle regeneration.

In closing, several questions regarding the use of keratin-based MPs for biomedical have been answered. The results do in fact warrant further investigation into the possibilities of using this construct and its constituent components (payloads) to aid in the progress of biomedical research.

References

Adams, Freddy, P Walstra, BW Brooks, HN Richmond, M Zerfa, Jerome Bibette, DJ Hibberd, MM Robins, JG Weers, and AS Kabalnov. 2007. *Modern aspects of emulsion science*: Royal Society of Chemistry.

Anand, U., and S. Mukherjee. 2013. "Binding, unfolding and refolding dynamics of serum albumins." *Biochimica Et Biophysica Acta-General Subjects* 1830 (12):5394-5404. doi: 10.1016/j.bbagen.2013.05.017.

Argilés, Josep M, Nefertiti Campos, José M Lopez-Pedrosa, Ricardo Rueda, and Leocadio %J Journal of the American Medical Directors Association Rodriguez-Mañas. 2016. "Skeletal muscle regulates metabolism via interorgan crosstalk: roles in health and disease." 17 (9):789-796.

Baker, HB, JA Passipieri, Mevan Siriwardane, Mary D Ellenburg, Manasi Vadhavkar, Christopher R Bergman, Justin M Saul, Seth Tomblyn, Luke Burnett, and George J %J Tissue Engineering Part A Christ. 2017. "Cell and growth factor-loaded keratin hydrogels for treatment of volumetric muscle loss in a mouse model." 23 (11-12):572-584.

Batorsky, Anna, Jiehong Liao, Amanda W. Lund, George E. Plopper, and Jan P. Stegemann. 2005. "Encapsulation of adult human mesenchymal stem cells within collagen-agarose microenvironments." *Biotechnology and Bioengineering* 92 (4):492-500. doi: 10.1002/bit.20614.

Behrens, Adam M., Michael J. Sikorski, Tieluo Li, Zhongjun J. Wu, Bartley P. Griffith, and Peter Kofinas. 2014. "Blood-aggregating hydrogel particles for use as a hemostatic agent." *Acta Biomaterialia* 10 (2):701-708. doi: https://doi.org/10.1016/j.actbio.2013.10.029.

Berger, J., M. Reist, J. M. Mayer, O. Felt, N. A. Peppas, and R. Gurny. 2004. "Structure and interactions in covalently and ionically crosslinked chitosan hydrogels for biomedical applications." *Eur J Pharm Biopharm* 57 (1):19-34.

Blau, H. M., B. D. Cosgrove, and A. T. V. Ho. 2015. "The central role of muscle stem cells in regenerative failure with aging." *Nature Medicine* 21 (8):854-862. doi: 10.1038/nm.3918.

Boutonnet, Magali, Jerzy Kizling, Per Stenius, Gilbert %J Colloids Maire, and Surfaces. 1982. "The preparation of monodisperse colloidal metal particles from microemulsions." 5 (3):209-225.

Bragulla, H. H., and D. G. Homberger. 2009. "Structure and functions of keratin proteins in simple, stratified, keratinized and cornified epithelia." *J Anat* 214 (4):516-59. doi: 10.1111/j.1469-7580.2009.01066.x.

Brandelli, A. 2008. "Bacterial Keratinases: Useful Enzymes for Bioprocessing Agroindustrial Wastes and Beyond." *Food and Bioprocess Technology* 1 (2):105-116. doi: 10.1007/s11947-007-0025-y.

Buck, Emily, Vimal Maisuria, Nathalie Tufenkji, and Marta Cerruti. 2018. "Antibacterial Properties of PLGA Electrospun Scaffolds Containing Ciprofloxacin Incorporated by Blending or Physisorption." *ACS Applied Bio Materials* 1 (3):627-635. doi: 10.1021/acsabm.8b00112.

Burnett, L. R., M. B. Rahmany, J. R. Richter, T. A. Aboushwareb, D. Eberli, C. L. Ward, G. Orlando, R. R. Hantgan, and M. E. Van Dyke. 2013. "Hemostatic properties and the role of cell receptor recognition in human hair keratin protein hydrogels." *Biomaterials* 34 (11):2632-40. doi: 10.1016/j.biomaterials.2012.12.022.

Cattaneo, Elena, and Ron %J Nature McKay. 1990. "Proliferation and differentiation of neuronal stem cells regulated by nerve growth factor." 347 (6295):762.

Chang, C. H., F. G. Niu, L. P. Gu, X. Li, H. Yang, B. Zhou, J. W. Wang, Y. J. Su, and Y. J. Yang. 2016. "Formation of fibrous or granular egg white protein microparticles and properties of the integrated emulsions." *Food Hydrocolloids* 61:477-486. doi: 10.1016/j.foodhyd.2016.06.002.

Chazaud, B. 2014. "Macrophages: Supportive cells for tissue repair and regeneration." *Immunobiology* 219 (3):172-178. doi: 10.1016/j.imbio.2013.09.001.

Choi, Jin San, Sang Jin Lee, George J. Christ, Anthony Atala, and James J. Yoo. 2008. "The influence of electrospun aligned poly(ε-caprolactone)/collagen nanofiber meshes on the formation of self-aligned skeletal muscle myotubes." *Biomaterials* 29 (19):2899-2906. doi: https://doi.org/10.1016/j.biomaterials.2008.03.031.

Ciciliot, Stefano, and Stefano %J Current pharmaceutical design Schiaffino. 2010. "Regeneration of mammalian skeletal muscle: basic mechanisms and clinical implications." 16 (8):906-914.

Cilurzo, F., F. Selmin, A. Aluigi, and S. Bellosta. 2013. "Regenerated keratin proteins as potential biomaterial for drug delivery." *Polymers for Advanced Technologies* 24 (11):1025-1028. doi: 10.1002/pat.3168.

Clowes Jr, George HA, Barbara C George, Claude A Villee Jr, and Calvin A %J New England Journal of Medicine Saravis. 1983. "Muscle proteolysis induced by a circulating peptide in patients with sepsis or trauma." 308 (10):545-552.

Cohen, David Joshua, Sharon L Hyzy, Salma Haque, Lucas C Olson, Barbara D Boyan, Justin M Saul, and Zvi %J Tissue Engineering Part A Schwartz. 2018. "Effects of Tunable Keratin Hydrogel Erosion on Recombinant Human Bone Morphogenetic Protein 2 Release, Bioactivity, and Bone Induction." 24 (21-22):1616-1630.

Cowan, C. M., Y. Y. Shi, O. O. Aalami, Y. F. Chou, C. Mari, R. Thomas, N. Quarto, C. H. Contag, B. Wu, and M. T. Longaker. 2004. "Adipose-derived adult stromal cells heal critical-size mouse calvarial defects." *Nat Biotechnol* 22 (5):560-7. doi: 10.1038/nbt958.

Craig, M., A. Altskar, L. Nordstierna, and K. Holmberg. 2016. "Bacteria-triggered degradation of nanofilm shells for release of antimicrobial agents." *Journal of Materials Chemistry B* 4 (4):672-682. doi: 10.1039/c5tb01274k.

Dang, P. N., N. Dwivedi, L. M. Phillips, X. H. Yu, S. Herberg, C. Bowerman, L. D. Solorio, W. L. Murphy, and E. Alsberg. 2016. "Controlled Dual Growth Factor Delivery From Microparticles Incorporated Within Human Bone Marrow-Derived Mesenchymal Stem Cell Aggregates for Enhanced Bone Tissue Engineering via Endochondral Ossification." *Stem Cells Translational Medicine* 5 (2):206-217. doi: 10.5966/sctm.2015-0115.

de Guzman, Roche C, Michelle R Merrill, Jillian R Richter, Rawad I Hamzi, Olga K Greengauz-Roberts, and Mark E Van Dyke. 2011. "Mechanical and biological properties of keratose biomaterials." *Biomaterials* 32 (32):8205-8217.

de Guzman, Roche C, Justin M Saul, Mary D Ellenburg, Michelle R Merrill, Heather B Coan, Thomas L Smith, and Mark E %J Biomaterials Van Dyke. 2013. "Bone regeneration with BMP-2 delivered from keratose scaffolds." 34 (6):1644-1656.

de Guzman, Roche C, Shanel M Tsuda, Minh-Thi N Ton, Xiao Zhang, Alan R Esker, and Mark E Van Dyke. 2015. "Binding interactions of keratin-based hair fiber extract to gold, keratin, and BMP-2." *PloS one* 10 (8):e0137233.

de Guzman, Roche, Shanel M. Tsuda, Minh-Thi N. Ton, Xiao Zhang, Alan R. Esker, and Mark E. Van Dyke. 2015. *Binding Interactions of Keratin-Based Hair Fiber Extract to Gold, Keratin, and BMP-2*. Vol. 10.

Doube, Michael, Michał M Kłosowski, Ignacio Arganda-Carreras, Fabrice P Cordelières, Robert P Dougherty, Jonathan S Jackson, Benjamin Schmid, John R Hutchinson, and Sandra J %J Bone Shefelbine. 2010. "BoneJ: free and extensible bone image analysis in ImageJ." 47 (6):1076-1079.

Du, J., I. M. El-Sherbiny, and H. D. Smyth. 2014. "Swellable Ciprofloxacin-Loaded Nano-in-Micro Hydrogel Particles for Local Lung Drug Delivery." *Aaps Pharmscitech* 15 (6):1535-1544. doi: 10.1208/s12249-014-0176-x.

Dubbini, Alessandra, Roberta Censi, Maria Eugenia Butini, Maria Giovanna Sabbieti, Dimitrios Agas, Tina Vermonden, and Piera Di Martino. 2015. "Injectable hyaluronic acid/PEG-p(HPMAm-lac)-based

hydrogels dually cross-linked by thermal gelling and Michael addition." *European Polymer Journal* 72:423-437. doi: http://dx.doi.org/10.1016/j.eurpolymj.2015.07.036.

Egan, Brendan, and Juleen R %J Cell metabolism Zierath. 2013. "Exercise metabolism and the molecular regulation of skeletal muscle adaptation." 17 (2):162-184.

Elias, P. Z., G. W. Liu, H. Wei, M. C. Jensen, P. J. Horner, and S. H. Pun. 2015. "A functionalized, injectable hydrogel for localized drug delivery with tunable thermosensitivity: synthesis and characterization of physical and toxicological properties." *J Control Release* 208:76-84. doi: 10.1016/j.jconrel.2015.03.003.

Elsner, J. J., I. Berdicevsky, and M. Zilberman. 2011. "In vitro microbial inhibition and cellular response to novel biodegradable composite wound dressings with controlled release of antibiotics." *Acta Biomaterialia* 7 (1):325-336. doi: 10.1016/j.actbio.2010.07.013.

Endo, T. 2015. "Molecular mechanisms of skeletal muscle development, regeneration, and osteogenic conversion." *Bone* 80:2-13. doi: 10.1016/j.bone.2015.02.028.

Endres, M., N. Wenda, H. Woehlecke, K. Neumann, J. Ringe, C. Erggelet, D. Lerche, and C. Kaps. 2010. "Microencapsulation and chondrogenic differentiation of human mesenchymal progenitor cells from subchondral bone marrow in Ca-alginate for cell injection." *Acta Biomater* 6 (2):436-44. doi: 10.1016/j.actbio.2009.07.022.

Fearing, B. V., and M. E. Van Dyke. 2014. "In vitro response of macrophage polarization to a keratin biomaterial." *Acta Biomater* 10 (7):3136-44. doi: 10.1016/j.actbio.2014.04.003.

Ferrari, M. B., J. Rohrbough, and N. C. Spitzer. 1996. "Spontaneous calcium transients regulate myofibrillogenesis in embryonic Xenopus myocytes." *Dev Biol* 178 (2):484-97. doi: 10.1006/dbio.1996.0233.

Ferraro, Vincenza, Marc Anton, and Véronique Santé-Lhoutellier. 2016. "The “sisters” α-helices of collagen, elastin and keratin recovered from animal by-products: Functionality, bioactivity and trends of application." *Trends in Food Science & Technology* 51:65-75. doi: https://doi.org/10.1016/j.tifs.2016.03.006.

Fingas, M. 1995. "Water-in-Oil Emulsion Formation - a Review of Physics and Mathematical-Modeling." *Spill Science & Technology Bulletin* 2 (1):55-59. doi: Doi 10.1016/1353-2561(95)94483-Z.

Forbes, S. J., and N. Rosenthal. 2014. "Preparing the ground for tissue regeneration: from mechanism to therapy." *Nature Medicine* 20 (8):857-869. doi: 10.1038/nm.3653.

Gao, X., A. Usas, Y. Tang, A. Lu, J. Tan, J. Schneppendahl, A. M. Kozemchak, B. Wang, J. H. Cummins, R. S. Tuan, and J. Huard. 2014. "A comparison of bone regeneration with human mesenchymal stem cells and muscle-derived stem cells and the critical role of BMP." *Biomaterials* 35 (25):6859-70. doi: 10.1016/j.biomaterials.2014.04.113.

Gauthier, O., J. M. Bouler, P. Weiss, J. Bosco, E. Aguado, and G. Daculsi. 1999. "Short-term effects of mineral particle sizes on cellular degradation activity after implantation of injectable calcium phosphate biomaterials and the consequences for bone substitution." *Bone* 25 (2):71s-74s. doi: Doi 10.1016/S8756-3282(99)00137-4.

Ge, J. F., L. Guo, S. Wang, Y. L. Zhang, T. Cai, R. C. H. Zhao, and Y. J. Wu. 2014. "The Size of Mesenchymal Stem Cells is a Significant Cause of Vascular Obstructions and Stroke." *Stem Cell Reviews and Reports* 10 (2):295-303. doi: 10.1007/s12015-013-9492-x.

Goldmann, W. H. 2016. "Role of vinculin in cellular mechanotransduction." *Cell Biology International* 40 (3):241-256. doi: 10.1002/cbin.10563.

Goodman, C. A., T. A. Hornberger, and A. G. Robling. 2015. "Bone and skeletal muscle: Key players in mechanotransduction and potential overlapping mechanisms." *Bone* 80:24-36. doi: 10.1016/j.bone.2015.04.014.

Goodpaster, B. H., S. W. Park, T. B. Harris, S. B. Kritchevsky, M. Nevitt, A. V. Schwartz, E. M. Simonsick, F. A. Tylavsky, M. Visser, A. B. Newman, and Hlth ABC Study. 2006. "The loss of skeletal muscle

strength, mass, and quality in older adults: The health, aging and body composition study." *Journals of Gerontology Series a-Biological Sciences and Medical Sciences* 61 (10):1059-1064. doi: DOI 10.1093/gerona/61.10.1059.

Grasman, Jonathan M, Michelle J Zayas, Raymond L Page, and George D %J Acta biomaterialia Pins. 2015. "Biomimetic scaffolds for regeneration of volumetric muscle loss in skeletal muscle injuries." 25:2-15.

Grune, T., T. Reinheckel, and K. J. Davies. 1997. "Degradation of oxidized proteins in mammalian cells." *FASEB J* 11 (7):526-34.

Gurbay, A., C. Garrel, M. Osman, M. J. Richard, A. Favier, and F. Hincal. 2002. "Cytotoxicity in ciprofloxacin-treated human fibroblast cells and protection by vitamin E." *Human & Experimental Toxicology* 21 (12):635-641. doi: 10.1191/0960327102ht305oa.

Hallab, NJ, KJ Bundy, K O'connor, R Clark, and RL Moses. 1995. "Cell adhesion to biomaterials: correlations between surface charge, surface roughness, adsorbed protein, and cell morphology." *Journal of long-term effects of medical implants* 5 (3):209-231.

Ham, Trevor R, Ryan T Lee, Sangheon Han, Salma Haque, Yael Vodovotz, Junnan Gu, Luke R Burnett, Seth Tomblyn, and Justin M %J Biomacromolecules Saul. 2015. "Tunable keratin hydrogels for controlled erosion and growth factor delivery." 17 (1):225-236.

Hamid, R., Y. Rotshteyn, L. Rabadi, R. Parikh, and P. Bullock. 2004. "Comparison of alamar blue and MTT assays for high through-put screening." *Toxicology in Vitro* 18 (5):703-710. doi: https://doi.org/10.1016/j.tiv.2004.03.012.

Han, Sangheon, Trevor R Ham, Salma Haque, Jessica L Sparks, and Justin M %J Acta biomaterialia Saul. 2015. "Alkylation of human hair keratin for tunable hydrogel erosion and drug delivery in tissue engineering applications." 23:201-213.

Hennink, W. E., and C. F. van Nostrum. 2012. "Novel crosslinking methods to design hydrogels." *Advanced Drug Delivery Reviews* 64:223-236. doi: http://dx.doi.org/10.1016/j.addr.2012.09.009.

Hermitte, Laurence, and Olivier Benoit. 2011. Biocompatible crosslinked gel. Google Patents.

Hill, Paulina, Helen Brantley, and Mark Van Dyke. 2010. "Some properties of keratin biomaterials: Kerateines." *Biomaterials* 31 (4):585-593. doi: http://dx.doi.org/10.1016/j.biomaterials.2009.09.076.

Hsu, F. Y., S. C. Chueh, and Y. J. Wang. 1999. "Microspheres of hydroxyapatite/reconstituted collagen as supports for osteoblast cell growth." *Biomaterials* 20 (20):1931-1936.

Huang, Sha, and Xiaobing Fu. 2010. "Cell behavior on microparticles with different surface morphology." *Journal of Alloys and Compounds* 493 (1):246-251. doi: https://doi.org/10.1016/j.jallcom.2009.12.065.

Hunt, Nicola C., and Liam M. Grover. 2010. "Cell encapsulation using biopolymer gels for regenerative medicine." *Biotechnology Letters* 32 (6):733-742. doi: 10.1007/s10529-010-0221-0.

Jeong Park, Yoon, Yong Moo Lee, Si Nae Park, Seung Yoon Sheen, Chong Pyoung Chung, and Seung Jin Lee. 2000. "Platelet derived growth factor releasing chitosan sponge for periodontal bone regeneration." *Biomaterials* 21 (2):153-159. doi: https://doi.org/10.1016/S0142-9612(99)00143-X.

Johnson, Susan S, and James R Goodman. 1989. Biocompatible protein or ligand immobilization system. Google Patents.

Juhas, Mark, George C. Engelmayr, Andrew N. Fontanella, Gregory M. Palmer, and Nenad Bursac. 2014. "Biomimetic engineered muscle with capacity for vascular integration and functional maturation in vivo." 111 (15):5508-5513. doi: 10.1073/pnas.1402723111 %J Proceedings of the National Academy of Sciences.

Kanbe, K., X. Yang, L. Wei, C. Sun, and Q. Chen. 2007. "Pericellular matrilins regulate activation of chondrocytes by cyclic load-induced matrix deformation." *J Bone Miner Res* 22 (2):318-28. doi: 10.1359/jbmr.061104.

Kim, T. H., S. H. Oh, S. B. Kang, and J. H. Lee. 2014. "Myoblast differentiation on growth factor-immobilized polycaprolactone microparticles: a potential bioactive bulking agent for fecal incontinence." *Pure and Applied Chemistry* 86 (8):1269-1280. doi: 10.1515/pac-2014-0209.

Kin, Shuichi, Akeo Hagiwara, Yuen Nakase, Yoshiaki Kuriu, Susumu Nakashima, Tetsuji Yoshikawa, Chohei Sakakura, Eigo Otsuji, Tatsuo Nakamura, and Hisakazu %J ASAIO journal Yamagishi. 2007. "Regeneration of skeletal muscle using in situ tissue engineering on an acellular collagen sponge scaffold in a rabbit model." 53 (4):506-513.

Komnatnyy, V. V., W. C. Chiang, T. Tolker-Nielsen, M. Givskov, and T. E. Nielsen. 2014. "Bacteria-Triggered Release of Antimicrobial Agents." *Angewandte Chemie-International Edition* 53 (2):439-441. doi: 10.1002/anie.201307975.

Konop, M., J. Czuwara, E. Klodzinska, A. K. Laskowska, U. Zielenkiewicz, I. Brzozowska, S. M. Nabavi, and L. Rudnicka. 2018. "Development of a novel keratin dressing which accelerates full-thickness skin wound healing in diabetic mice: In vitro and in vivo studies." *Journal of Biomaterials Applications* 33 (4):527-540. doi: 10.1177/0885328218801114.

Kowalczewski, Christine J, Seth Tombyln, David C Wasnick, Michael R Hughes, Mary D Ellenburg, Michael F Callahan, Thomas L Smith, Mark E Van Dyke, Luke R Burnett, and Justin M %J Biomaterials Saul. 2014. "Reduction of ectopic bone growth in critically-sized rat mandible defects by delivery of rhBMP-2 from kerateine biomaterials." 35 (10):3220-3228.

Kraghhansen, U. 1981. "Molecular Aspects of Ligand-Binding to Serum-Albumin." *Pharmacological Reviews* 33 (1):17-53.

Kretlow, J. D., and A. G. Mikos. 2007. "Review: mineralization of synthetic polymer scaffolds for bone tissue engineering." *Tissue Eng* 13 (5):927-38. doi: 10.1089/ten.2006.0394.

Leal-Calderon, Fernando, Véronique Schmitt, and Jerome Bibette. 2007. *Emulsion science: basic principles*: Springer Science & Business Media.

Ledford, B. T., J. Simmons, M. Chen, H. M. Fan, C. Barron, Z. M. Liu, M. Van Dyke, and J. Q. He. 2017. "Keratose Hydrogels Promote Vascular Smooth Muscle Differentiation from C-kit-Positive Human Cardiac Stem Cells." *Stem Cells and Development* 26 (12):888-900. doi: 10.1089/scd.2016.0351.

Leertouwer, Hein L, Bodo D Wilts, and Doekele G %J Optics Express Stavenga. 2011. "Refractive index and dispersion of butterfly chitin and bird keratin measured by polarizing interference microscopy." 19 (24):24061-24066.

Lu, Xiuling, Yuhong Xu, Chunyang Zheng, Guifeng Zhang, Zhiguo %J Journal of Chemical Technology Su, Environmental Biotechnology: International Research in Process, and Clean Technology. 2006. "Ethylene glycol diglycidyl ether as a protein cross-linker: a case study for cross-linking of hemoglobin." 81 (5):767-775.

Lu, Y. C., W. Song, D. An, B. J. Kim, R. Schwartz, M. M. Wu, and M. L. Ma. 2015. "Designing compartmentalized hydrogel microparticles for cell encapsulation and scalable 3D cell culture." *Journal of Materials Chemistry B* 3 (3):353-360. doi: 10.1039/c4tb01735h.

Machingal, Masood A, Benjamin T Corona, Thomas J Walters, Venu Kesireddy, Christine N Koval, Ashley Dannahower, Weixin Zhao, James J Yoo, and George J %J Tissue Engineering Part A Christ. 2011. "A tissue-engineered muscle repair construct for functional restoration of an irrecoverable muscle injury in a murine model." 17 (17-18):2291-2303.

Man, Y., P. Wang, Y. Guo, L. Xiang, Y. Yang, Y. Qu, P. Gong, and L. Deng. 2012. "Angiogenic and osteogenic potential of platelet-rich plasma and adipose-derived stem cell laden alginate microspheres." *Biomaterials* 33 (34):8802-11. doi: 10.1016/j.biomaterials.2012.08.054.

Martino, M. M., P. S. Briquez, E. Guc, F. Tortelli, W. W. Kilarski, S. Metzger, J. J. Rice, G. A. Kuhn, R. Muller, M. A. Swartz, and J. A. Hubbell. 2014. "Growth Factors Engineered for Super-Affinity to the Extracellular Matrix Enhance Tissue Healing." *Science* 343 (6173):885-888. doi: 10.1126/science.1247663.

Mase, Vincent J, Joseph R Hsu, Steven E Wolf, Joseph C Wenke, David G Baer, Johnny Owens, Stephen F Badylak, and Thomas J %J Orthopedics Walters. 2010. "Clinical application of an acellular biologic scaffold for surgical repair of a large, traumatic quadriceps femoris muscle defect." 33 (7).

McLellan, James, Starla G Thornhill, Spencer Shelton, and Manish Kumar. 2019. "Keratin-Based Biofilms, Hydrogels, and Biofibers." In *Keratin as a Protein Biopolymer*, 187-200. Springer.

Montanari, E., M. C. De Rugeriis, C. Di Meo, R. Censi, T. Coviello, F. Alhaique, and P. Matricardi. 2015. "One-step formation and sterilization of gellan and hyaluronan nanohydrogels using autoclave." *J Mater Sci Mater Med* 26 (1):5362. doi: 10.1007/s10856-014-5362-6.

Montero-Rama, María Pilar, Marta Liras, Olga García, and Isabel Quijada-Garrido. 2015. "Thermo- and pH-sensitive hydrogels functionalized with thiol groups." *European Polymer Journal* 63:37-44. doi: http://dx.doi.org/10.1016/j.eurpolymj.2014.11.044.

Mori, H., and M. Hara. 2018. "Transparent biocompatible wool keratin film prepared by mechanical compression of porous keratin hydrogel." *Materials Science & Engineering C-Materials for Biological Applications* 91:19-25. doi: 10.1016/j.msec.2018.05.021.

Moulin, V. J., D. Mayrand, H. Messier, M. C. Martinez, C. A. Lopez-Valle, and H. Genest. 2010. "Shedding of Microparticles by Myofibroblasts as Mediator of Cellular Cross-Talk During Normal Wound Healing." *Journal of Cellular Physiology* 225 (3):734-740. doi: 10.1002/jcp.22268.

Moulin, Véronique J., Dominique Mayrand, Hugo Messier, Maria Carmen Martinez, Carlos A. Lopez-Vallé, and Hervé Genest. 2010. "Shedding of microparticles by myofibroblasts as mediator of cellular cross-talk during normal wound healing." *Journal of Cellular Physiology* 225 (3):734-740. doi: 10.1002/jcp.22268.

Naderi, H., M. M. Matin, and A. R. Bahrami. 2011. "Review paper: critical issues in tissue engineering: biomaterials, cell sources, angiogenesis, and drug delivery systems." *J Biomater Appl* 26 (4):383-417. doi: 10.1177/0885328211408946.

Nakaji-Hirabayashi, Tadashi, Koichi Kato, and Hiroo Iwata. 2008. "Self-assembling chimeric protein for the construction of biodegradable hydrogels capable of interaction with integrins expressed on neural stem/progenitor cells." *Biomacromolecules* 9 (5):1411-1416.

Nicodemus, G. D., and S. J. Bryant. 2008. "Cell encapsulation in biodegradable hydrogels for tissue engineering applications." *Tissue Engineering Part B-Reviews* 14 (2):149-165. doi: DOI 10.1089/ten.teb.2007.0332.

Niemeyer, P., M. Kornacker, A. Mehlhorn, A. Seckinger, J. Vohrer, H. Schmal, P. Kasten, V. Eckstein, N. P. Sudkamp, and U. Krause. 2007. "Comparison of immunological properties of bone marrow stromal cells and adipose tissue-derived stem cells before and after osteogenic differentiation in vitro." *Tissue Eng* 13 (1):111-21. doi: 10.1089/ten.2006.0114.

Nishi, Chika, Naoki Nakajima, and Yoshito %J Journal of biomedical materials research Ikada. 1995. "In vitro evaluation of cytotoxicity of diepoxy compounds used for biomaterial modification." 29 (7):829-834.

Noishiki, Y, H Ito, T Miyamoto, and H Inagaki. 1982. "Application of Denatured Wool Keratin Derivatives to an Antithrombogenic Biomaterial-Vascular Graft Coated with a Heparinized Keratin Derivative." *Kobunshi Ronbunshu* 39 (4):221-227.

Noishiki, Y. 1982. "Application of immunoperoxidase method to electron microscopic observation of plasma protein on polymer surface." *J Biomed Mater Res* 16 (4):359-67. doi: 10.1002/jbm.820160405.

Oh, Jung Kwon, Do Ik Lee, and Jong Myung Park. 2009. "Biopolymer-based microgels/nanogels for drug delivery applications." *Progress in Polymer Science* 34 (12):1261-1282. doi: https://doi.org/10.1016/j.progpolymsci.2009.08.001.

Oliveira, Mariana B., and João F. Mano. 2011. "Polymer-based microparticles in tissue engineering and regenerative medicine." *Biotechnology Progress* 27 (4):897-912. doi: 10.1002/btpr.618.

Pace, L. A., J. F. Plate, S. Mannava, J. C. Barnwell, L. A. Koman, Z. Y. Li, T. L. Smith, and M. Van Dyke. 2014. "A Human Hair Keratin Hydrogel Scaffold Enhances Median Nerve Regeneration in Nonhuman Primates: An Electrophysiological and Histological Study." *Tissue Engineering Part A* 20 (3-4):507-517.

Page, Raymond L, Christopher Malcuit, Lucy Vilner, Ina Vojtic, Sharon Shaw, Emmett Hedblom, Jason Hu, George D Pins, Marsha W Rolle, and Tanja %J Tissue Engineering Part A Dominko. 2011. "Restoration of skeletal muscle defects with adult human cells delivered on fibrin microthreads." 17 (21-22):2629-2640.

Papir, Y. S., K. H. Hsu, and R. H. Wildnauer. 1975. "The mechanical properties of stratum corneum. I. The effect of water and ambient temperature on the tensile properties of newborn rat stratum corneum." *Biochim Biophys Acta* 399 (1):170-80.

Park, H., J. S. Temenoff, Y. Tabata, A. I. Caplan, and A. G. Mikos. 2007. "Injectable biodegradable hydrogel composites for rabbit marrow mesenchymal stem cell and growth factor delivery for cartilage tissue engineering." *Biomaterials* 28 (21):3217-3227. doi: 10.1016/j.biomaterials.2007.03.030.

Park, S. N., J. K. Kim, and H. Suh. 2004. "Evaluation of antibiotic-loaded collagen-hyaluronic acid matrix as a skin substitute." *Biomaterials* 25 (17):3689-3698. doi: 10.1016/j.biomaterials.2003.10.072.

Pittenger, Mark F., Alastair M. Mackay, Stephen C. Beck, Rama K. Jaiswal, Robin Douglas, Joseph D. Mosca, Mark A. Moorman, Donald W. Simonetti, Stewart Craig, and Daniel R. Marshak. 1999. "Multilineage Potential of Adult Human Mesenchymal Stem Cells." 284 (5411):143-147. doi: 10.1126/science.284.5411.143 %J Science.

Prigozhina, T. B., S. Khitrin, G. Elkin, O. Eizik, S. Morecki, and S. Slavin. 2008. "Mesenchymal stromal cells lose their immunosuppressive potential after allotransplantation." *Exp Hematol* 36 (10):1370-6. doi: 10.1016/j.exphem.2008.04.022.

Prow, T. W., J. E. Grice, L. L. Lin, R. Faye, M. Butler, W. Becker, E. M. T. Wurm, C. Yoong, T. A. Robertson, H. P. Soyer, and M. S. Roberts. 2011. "Nanoparticles and microparticles for skin drug delivery." *Advanced Drug Delivery Reviews* 63 (6):470-491. doi: 10.1016/j.addr.2011.01.012.

Qazi, Taimoor H, David J Mooney, Matthias Pumberger, Sven Geissler, and Georg N Duda. 2015. "Biomaterials based strategies for skeletal muscle tissue engineering: existing technologies and future trends." *Biomaterials* 53:502-521.

Rouse, Jillian G, and Mark E Van Dyke. 2010. "A review of keratin-based biomaterials for biomedical applications." *Materials* 3 (2):999-1014.

Roy, D. C., S. Tomblyn, D. M. Burmeister, N. L. Wrice, S. C. Becerra, L. R. Burnett, J. M. Saul, and R. J. Christy. 2015a. "Ciprofloxacin-Loaded Keratin Hydrogels Prevent Pseudomonas aeruginosa Infection and Support Healing in a Porcine Full-Thickness Excisional Wound." *Advances in Wound Care* 4 (8):457-468. doi: 10.1089/wound.2014.0576.

Roy, D. C., S. Tomblyn, K. M. Isaac, C. J. Kowalczewski, D. M. Burmeister, L. R. Burnett, and R. J. Christy. 2016. "Ciprofloxacin-loaded keratin hydrogels reduce infection and support healing in a porcine partial-thickness thermal burn." *Wound Repair and Regeneration* 24 (4):657-668. doi: 10.1111/wrr.12449.

Roy, Daniel C, Seth Tomblyn, David M Burmeister, Nicole L Wrice, Sandra C Becerra, Luke R Burnett, Justin M Saul, and Robert J %J Advances in wound care Christy. 2015b. "Ciprofloxacin-loaded

keratin hydrogels prevent Pseudomonas aeruginosa infection and support healing in a porcine full-thickness excisional wound." 4 (8):457-468.
Saltin, Bengt, and Philip D %J Handbook of Physiology. Skeletal Muscle Gollnick. 1983. "Skeletal muscle adaptability: significance for metabolism and performance." 10:555-631.
Sando, Lillian, Misook Kim, Michelle L. Colgrave, John A. M. Ramshaw, Jerome A. Werkmeister, and Christopher M. Elvin. 2010. "Photochemical crosslinking of soluble wool keratins produces a mechanically stable biomaterial that supports cell adhesion and proliferation." *Journal of Biomedical Materials Research Part A* 95A (3):901-911. doi: 10.1002/jbm.a.32913.
Saul, J. M., M. D. Ellenburg, R. C. de Guzman, and M. Van Dyke. 2011. "Keratin hydrogels support the sustained release of bioactive ciprofloxacin." *Journal of Biomedical Materials Research Part A* 98a (4):544-553. doi: 10.1002/jbm.a.33147.
Saul, Justin M, Mary D Ellenburg, Roche C de Guzman, and Mark Van %J Journal of biomedical materials research Part A Dyke. 2011. "Keratin hydrogels support the sustained release of bioactive ciprofloxacin." 98 (4):544-553.
Schlapp, M., and W. Friess. 2003. "Collagen/PLGA microparticle controlled composites for local delivery of gentamicin." *Journal of Pharmaceutical Sciences* 92 (11):2145-2151. doi: 10.1002/jps.10460.
Schneider, C. A., W. S. Rasband, and K. W. Eliceiri. 2012. "NIH Image to ImageJ: 25 years of image analysis." *Nature Methods* 9 (7):671-675. doi: 10.1038/nmeth.2089.
Shen, D. L., X. F. Wang, L. Zhang, X. Y. Zhao, J. Y. Li, K. Cheng, and J. Y. Zhang. 2011. "The amelioration of cardiac dysfunction after myocardial infarction by the injection of keratin biomaterials derived from human hair." *Biomaterials* 32 (35):9290-9299. doi: 10.1016/j.biomaterials.2011.08.057.
Sierpinski, P., J. Garrett, J. Ma, P. Apel, D. Klorig, T. Smith, L. A. Koman, A. Atala, and M. Van Dyke. 2008a. "The use of keratin biomaterials derived from human hair for the promotion of rapid regeneration of peripheral nerves." *Biomaterials* 29 (1):118-128. doi: 10.1016/j.biomaterials.2007.08.023.
Sierpinski, P., J. Garrett, J. Ma, P. Apel, D. Klorig, T. Smith, L. A. Koman, A. Atala, and M. Van Dyke. 2008b. "The use of keratin biomaterials derived from human hair for the promotion of rapid regeneration of peripheral nerves." *Biomaterials* 29 (1):118-28. doi: 10.1016/j.biomaterials.2007.08.023.
Spector, A. A. 1975. "Fatty-Acid Binding to Plasma Albumin." *Journal of Lipid Research* 16 (3):165-179.
Steinert, P. M., L. N. Marekov, R. D. B. Fraser, and D. A. D. Parry. 1993. "Keratin Intermediate Filament Structure - Cross-Linking Studies Yield Quantitative Information on Molecular Dimensions and Mechanism of Assembly." *Journal of Molecular Biology* 230 (2):436-452. doi: DOI 10.1006/jmbi.1993.1161.
Stiber, Jonathan A., and Paul B. Rosenberg. 2011. "The role of store-operated calcium influx in skeletal muscle signaling." *Cell Calcium* 49 (5):341-349. doi: https://doi.org/10.1016/j.ceca.2010.11.012.
Sun, TT, and H %J Journal of Biological Chemistry Green. 1978. "Keratin filaments of cultured human epidermal cells. Formation of intermolecular disulfide bonds during terminal differentiation." 253 (6):2053-2060.
Tan, W. H., and S. Takeuchi. 2007. "Monodisperse alginate hydrogel microbeads for cell encapsulation." *Advanced Materials* 19 (18):2696-+. doi: 10.1002/adma.200700433.
Tanabe, T., N. Okitsu, and K. Yamauchi. 2004a. "Fabrication and characterization of chemically crosslinked keratin films." *Materials Science & Engineering C-Biomimetic and Supramolecular Systems* 24 (3):441-446. doi: 10.1016/j.msec.2003.11.004.
Tanabe, Toshizumi, Naoya Okitsu, and Kiyoshi Yamauchi. 2004b. "Fabrication and characterization of chemically crosslinked keratin films." *Materials Science and Engineering: C* 24 (3):441-446. doi: https://doi.org/10.1016/j.msec.2003.11.004.

Thiele, Jens J., Sherry N. Hsieh, Karlis Briviba, and Helmut Sies. 1999. "Protein Oxidation in Human Stratum Corneum: Susceptibility of Keratins to Oxidation In Vitro and Presence of a Keratin Oxidation Gradient In Vivo." *Journal of Investigative Dermatology* 113 (3):335-339. doi: http://dx.doi.org/10.1046/j.1523-1747.1999.00693.x.

Tidball, J. G. 2017. "Regulation of muscle growth and regeneration by the immune system." *Nature Reviews Immunology* 17 (3):165-178. doi: 10.1038/nri.2016.150.

Tomblyn, S., E. L. P. Kneller, S. J. Walker, M. D. Ellenburg, C. J. Kowalczewski, M. Van Dyke, L. Burnett, and J. M. Saul. 2016. "Keratin hydrogel carrier system for simultaneous delivery of exogenous growth factors and muscle progenitor cells." *Journal of Biomedical Materials Research Part B-Applied Biomaterials* 104 (5):864-879. doi: 10.1002/jbm.b.33438.

Tsai, T. H., W. L. Chen, and F. R. Hu. 2010. "Comparison of fluoroquinolones: cytotoxicity on human corneal epithelial cells." *Eye* 24 (5):909-917. doi: 10.1038/eye.2009.179.

Tu, Michelle K., Jacqueline B. Levin, Andrew M. Hamilton, and Laura N. Borodinsky. 2016. "Calcium signaling in skeletal muscle development, maintenance and regeneration." *Cell calcium* 59 (2-3):91-97. doi: 10.1016/j.ceca.2016.02.005.

Uludag, Hasan, Paul De Vos, and Patrick A. Tresco. 2000. "Technology of mammalian cell encapsulation." *Advanced Drug Delivery Reviews* 42 (1):29-64. doi: http://dx.doi.org/10.1016/S0169-409X(00)00053-3.

van de Weert, M., W. E. Hennink, and W. Jiskoot. 2000. "Protein instability in poly(lactic-co-glycolic acid) microparticles." *Pharmaceutical Research* 17 (10):1159-1167. doi: Doi 10.1023/A:1026498209874.

Van Dyke, Mark E. 2009. Keratin biomaterials for cell culture and methods of use. Google Patents.

Van Dyke, ME, and LB Nanney. 2002. "Elastomeric biomaterials from human hair keratins as bioactive wound dressings." ABSTRACTS OF PAPERS OF THE AMERICAN CHEMICAL SOCIETY.

Vasconcelos, A., and A. Cavaco-Paulo. 2013. "The Use of Keratin in Biomedical Applications." *Current Drug Targets* 14 (5):612-619. doi: Doi 10.2174/1389450111314050010.

Viswanathan, N. Badri, P. A. Thomas, J. K. Pandit, M. G. Kulkarni, and R. A. Mashelkar. 1999. "Preparation of non-porous microspheres with high entrapment efficiency of proteins by a (water-in-oil)-in-oil emulsion technique." *Journal of Controlled Release* 58 (1):9-20. doi: https://doi.org/10.1016/S0168-3659(98)00140-0.

Wang, M. O., C. E. Vorwald, M. L. Dreher, E. J. Mott, M. H. Cheng, A. Cinar, H. Mehdizadeh, S. Somo, D. Dean, E. M. Brey, and J. P. Fisher. 2015. "Evaluating 3D-printed biomaterials as scaffolds for vascularized bone tissue engineering." *Adv Mater* 27 (1):138-44. doi: 10.1002/adma.201403943.

Wang, P. Y., L. R. Clements, H. Thissen, S. C. Hung, N. C. Cheng, W. B. Tsai, and N. H. Voelcker. 2012. "Screening the attachment and spreading of bone marrow-derived and adipose-derived mesenchymal stem cells on porous silicon gradients." *Rsc Advances* 2 (33):12857-12865. doi: 10.1039/c2ra21557h.

Wang, Shuai, Francesca Taraballi, Lay Poh Tan, Kee Woei %J Cell Ng, and tissue research. 2012. "Human keratin hydrogels support fibroblast attachment and proliferation in vitro." 347 (3):795-802.

Waters, Michele, Pamela VandeVord, and Mark Van Dyke. 2018. "Keratin biomaterials augment anti-inflammatory macrophage phenotype in vitro." *Acta Biomaterialia* 66:213-223. doi: https://doi.org/10.1016/j.actbio.2017.10.042.

Wischke, C., and H. H. Borchert. 2006. "Fluorescein isothiocyanate labelled bovine serum albumin (FITC-BSA) as a model protein drug: opportunities and drawbacks." *Pharmazie* 61 (9):770-774.

Wolf, Matthew T., Kerry A. Daly, Janet E. Reing, and Stephen F. Badylak. 2012. "Biologic scaffold composed of skeletal muscle extracellular matrix." *Biomaterials* 33 (10):2916-2925. doi: https://doi.org/10.1016/j.biomaterials.2011.12.055.

Woo, Eunkyeong, Honghyun Park, and Kuen Yong Lee. 2014. "Shear Reversible Cell/Microsphere Aggregate as an Injectable for Tissue Regeneration." *Macromolecular Bioscience* 14 (5):740-748. doi: 10.1002/mabi.201300365.

Xu, Y., Z. Li, X. Li, Z. Fan, Z. Liu, X. Xie, and J. Guan. 2015. "Regulating myogenic differentiation of mesenchymal stem cells using thermosensitive hydrogels." *Acta Biomater* 26:23-33. doi: 10.1016/j.actbio.2015.08.010.

Yamazoe, Hironori, Toshizumi %J Journal of Biomedical Materials Research Part A: An Official Journal of The Society for Biomaterials Tanabe, The Japanese Society for Biomaterials,, The Australian Society for Biomaterials, and the Korean Society for Biomaterials. 2008. "Preparation of water-insoluble albumin film possessing nonadherent surface for cells and ligand binding ability." 86 (1):228-234.

Yan, C. H., J. H. Resau, J. Hewetson, M. West, W. L. Rill, and M. Kende. 1994a. "Characterization and Morphological Analysis of Protein-Loaded Poly(Lactide-Co-Glycolide) Microparticles Prepared by Water-in Oil-in-Water Emulsion Technique." *Journal of Controlled Release* 32 (3):231-241. doi: Doi 10.1016/0168-3659(94)90233-X.

Yan, Changhong, James H. Resau, John Hewetson, Michael West, Wayne L. Rill, and Meir Kende. 1994b. "Characterization and morphological analysis of protein-loaded poly(lactide-co-glycolide) microparticles prepared by water-in-oil-in-water emulsion technique." *Journal of Controlled Release* 32 (3):231-241. doi: https://doi.org/10.1016/0168-3659(94)90233-X.

Yan, Feng, and John %J Chemical Communications Texter. 2006. "Surfactant ionic liquid-based microemulsions for polymerization." (25):2696-2698.

Yin, H., F. Price, and M. A. Rudnicki. 2013. "Satellite Cells and the Muscle Stem Cell Niche." *Physiological Reviews* 93 (1):23-67. doi: 10.1152/physrev.00043.2011.

Yin Hsu, Fu, Shan-Chang Chueh, and Yng Jiin Wang. 1999. "Microspheres of hydroxyapatite/reconstituted collagen as supports for osteoblast cell growth." *Biomaterials* 20 (20):1931-1936. doi: https://doi.org/10.1016/S0142-9612(99)00095-2.

Yu, Jialin, Da-wen Yu, Daniel M. Checkla, Irwin M. Freedberg, and Arthur P. Bertolino. 1993. "Human hair keratins." *Journal of Investigative Dermatology* 101 (1, Supplement):S56-S59. doi: https://doi.org/10.1016/0022-202X(93)90501-8.

Yu, Minli, Huan Wang, Yali Xu, Debing Yu, Dongfeng Li, Xiuhong Liu, and Wenxing %J Cell biology international Du. 2015. "Insulin-like growth factor-1 (IGF-1) promotes myoblast proliferation and skeletal muscle growth of embryonic chickens via the PI3K/Akt signalling pathway." 39 (8):910-922.

Yusuf, F., and B. Brand-Saberi. 2012. "Myogenesis and muscle regeneration." *Histochemistry and Cell Biology* 138 (2):187-199. doi: 10.1007/s00418-012-0972-x.

Zanetti, A., M. Grata, E. B. Etling, R. Panday, F. S. Villanueva, and C. Toma. 2015. "Suspension-Expansion of Bone Marrow Results in Small Mesenchymal Stem Cells Exhibiting Increased Transpulmonary Passage Following Intravenous Administration." *Tissue Engineering Part C-Methods* 21 (7):683-692. doi: 10.1089/ten.tec.2014.0344.

Zeeman, R, Pieter J Dijkstra, PB Van Wachem, MJA Van Luyn, M Hendriks, PT Cahalan, Jan %J Journal of Biomedical Materials Research: An Official Journal of The Society for Biomaterials Feijen, The Japanese Society for Biomaterials,, The Australian Society for Biomaterials, and the Korean Society for Biomaterials. 1999. "Crosslinking and modification of dermal sheep collagen using 1, 4-butanediol diglycidyl ether." 46 (3):424-433.

Zhang, Y., Y. Sun, X. Yang, J. Hilborn, A. Heerschap, and D. A. Ossipov. 2014. "Injectable in situ forming hybrid iron oxide-hyaluronic acid hydrogel for magnetic resonance imaging and drug delivery." *Macromol Biosci* 14 (9):1249-59. doi: 10.1002/mabi.201400117.

Zhao, X., Y. S. Lui, C. K. Choo, W. T. Sow, C. L. Huang, K. W. Ng, L. P. Tan, and J. S. Loo. 2015. "Calcium phosphate coated Keratin-PCL scaffolds for potential bone tissue regeneration." *Mater Sci Eng C Mater Biol Appl* 49:746-53. doi: 10.1016/j.msec.2015.01.084.